“Low-Energy” Electron Scattering for Exotic Nuclei and Nucleons

Toshimi Suda (RARIS, Tohoku Univ.)
suda@lns.tohoku.ac.jp

for SCRIT and ULQ2 collaboration

Low-energy electron-scattering facilities in Japan

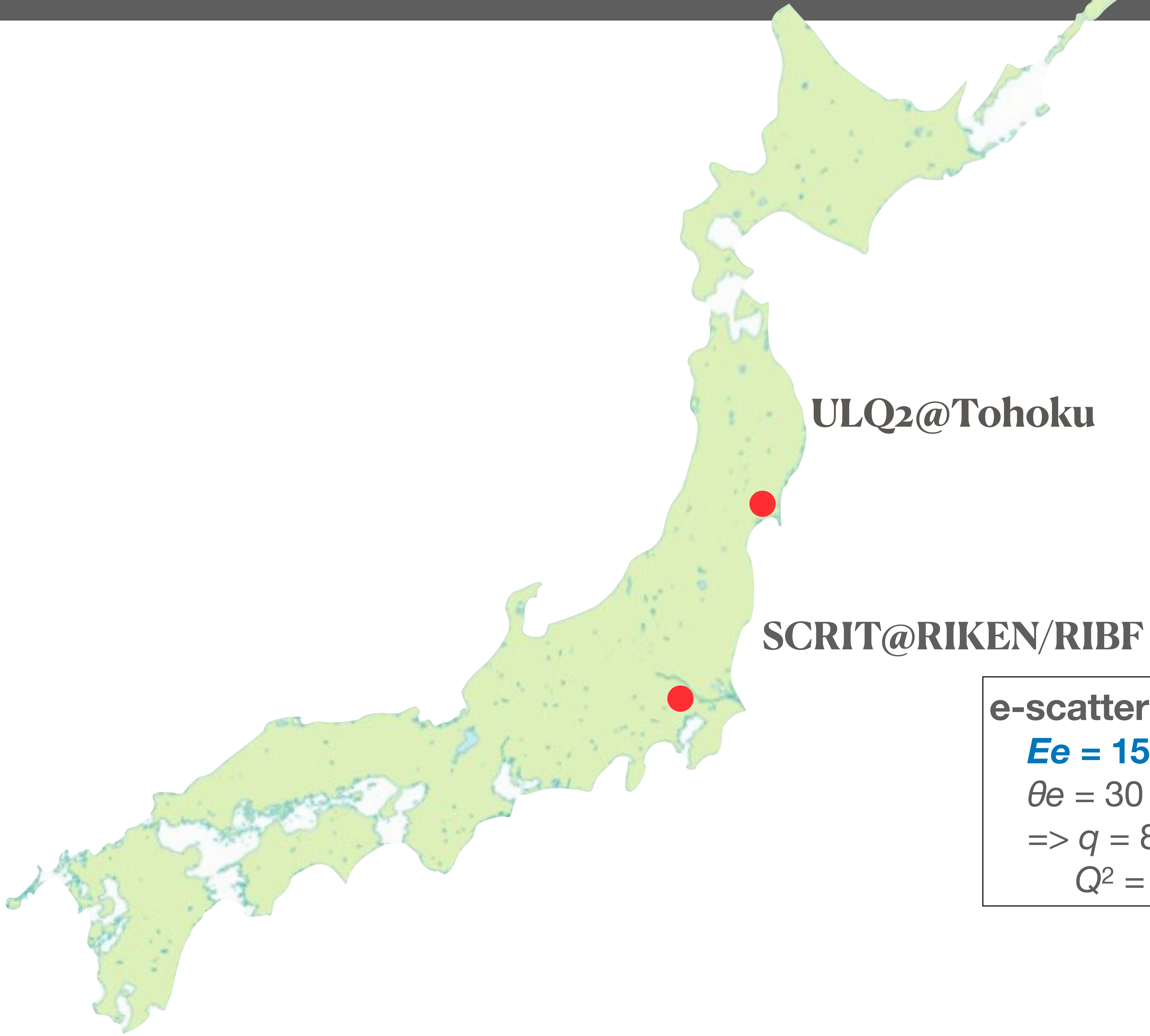

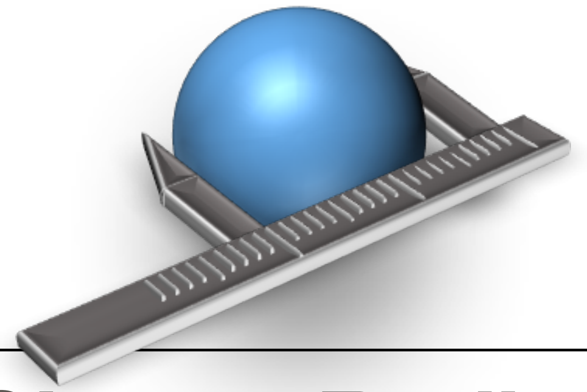

Proton Charge Radius
- ***Ee* = 10 - 60 MeV**
- θe = 30 - 150 deg.
- => $Q^2 = 3\times10^{-5}$ - 0.013 (GeV/c)^2

lowest-ever Q^2 !!

e-scattering for exotic nuclei (~10^8/sec)
- ***Ee* = 150 - 300 MeV**
- θe = 30 - 60 deg.
- => q = 80 - 300 MeV/c
- Q^2 = 0.006 - 0.09 (GeV/c)^2

world's first !!

Low-energy electron-scattering facilities in Japan

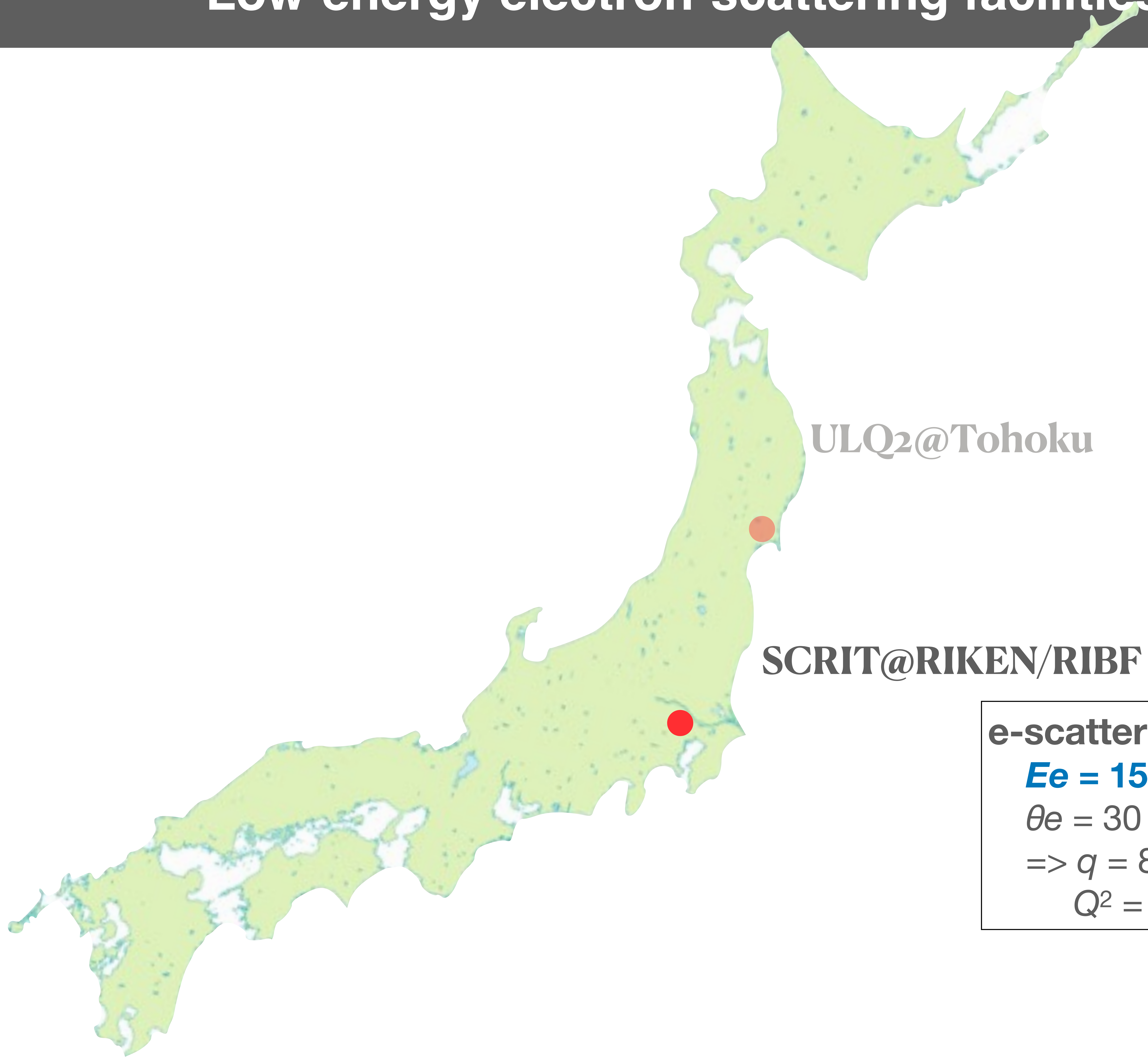

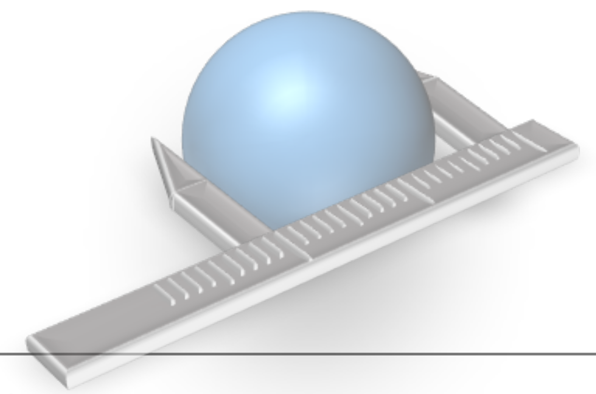

Proton Charge Radius

E_e = 10 - 60 MeV

θ_e = 30 - 150 deg.

=> $Q^2 = 3\text{x}10^{-5}$ - 0.013 (GeV/c)^2

lowest-ever Q^2 !!

e-scattering for exotic nuclei (~10^8/sec)

E_e = 150 - 300 MeV

θ_e = 30 - 60 deg.

=> q = 80 - 300 MeV/c

Q^2 = 0.006 - 0.09 (GeV/c)^2

world's first !!

Nuclei ever studied by electron scattering

- *strictly limited to stable nuclei*
- *never applied for exotic nuclei (short-lived)*

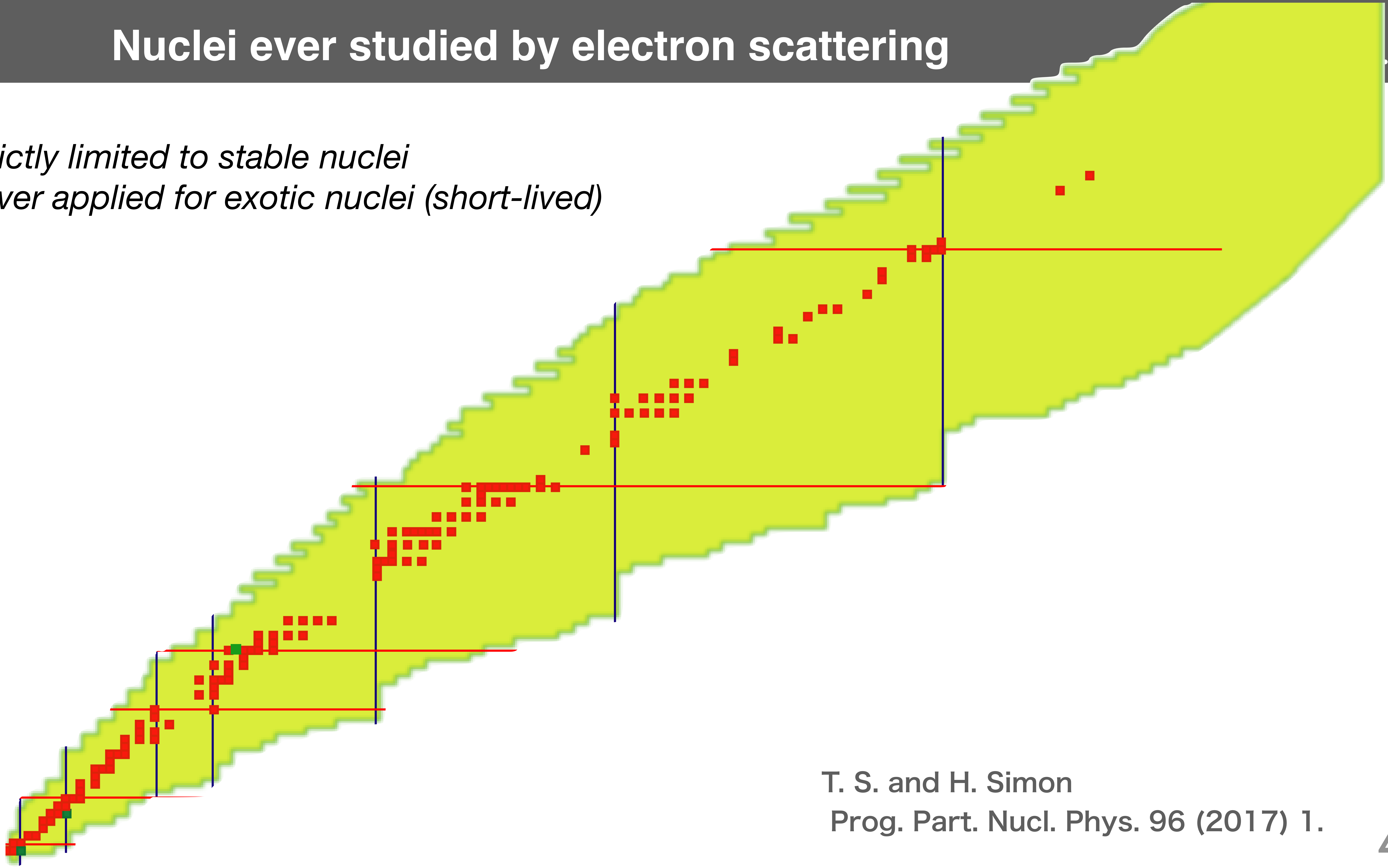

T. S. and H. Simon
Prog. Part. Nucl. Phys. 96 (2017) 1.

world's first demonstration of e-scattering for online-produced radioactive isotope

PHYSICAL REVIEW LETTERS **131,** 092502 (2023)

Editors' Suggestion | Featured in Physics

First Observation of Electron Scattering from Online-Produced Radioactive Target

K. Tsukada,[1,2] Y. Abe,[2] A. Enokizono,[2,3] T. Goke,[4] M. Hara,[2] Y. Honda,[2,4] T. Hori,[2] S. Ichikawa,[2,*]
Y. Ito,[1] K. Kurita,[3] C. Legris,[4] Y. Maehara,[1] T. Ohnishi,[2] R. Ogawara,[1,2] T. Suda,[2,4]
T. Tamae,[4] M. Wakasugi,[1,2] M. Watanabe,[2] and H. Wauke[2,4]

[1]*Institute for Chemical Research, Kyoto University, Uji, Kyoto 611-0011, Japan*
[2]*Nishina Center for Accelerator-Based Science, RIKEN, Wako, Saitama 351-0198, Japan*
[3]*Department of Physics, Rikkyo University, Toshima, Tokyo 171-8501, Japan*
[4]*Research Center for Electron Photon Science, Tohoku University, Sendai, Miyagi 982-0826, Japan*

(Received 7 March 2023; accepted 21 June 2023; published 30 August 2023)

We successfully performed electron scattering off unstable nuclei which were produced online from the photofission of uranium. The target ^{137}Cs ions were trapped with a new target-forming technique that makes a high-density stationary target from a small number of ions by confining them in an electron storage ring. After ... od to increase th... ity of 0.9×10^{26} ... tered electrons is consistent with a calculation. This success marks the realization of the anticipated femtoscope which clarifies the structures of exotic and short-lived unstable nuclei.

Phys. Rev. Lett. 131 (2023) 092502.

DOI: 10.1103/PhysRevLett.131.092502

Electron scattering provides a long-awaited view of unstable nuclei

Nuclear reactions produce a plethora of short-lived artificial isotopes. Figuring out what they look like has been a challenge.

The cartoon picture of an atomic nucleus looks kind of like the inside of a gumball machine that dispenses only two flavors: protons and neutrons, evenly mixed in a compact, spherical cluster.

That's not generally what real nuclei look like. Neutron-rich lead-208, for example, has a thick skin of neutrons encasing its proton-endowed core (see Physics Today, July 2021, page 12). Some nuclei are flattened, and some are elongated. Some are even pear shaped.

The more unstable a nucleus, the stranger the structures it can adopt. Short-lived nuclei might form bubble structures with depleted central density, or they might have a valence nucleon or two that form a halo around a compact central core. (See the article by Filomena Nunes, Physics Today, May 2021, page 34.) Frustratingly, though, those exotic structures are hard to experimentally confirm, because the gold standard for probing nuclear structure—electron scattering—has been off limits to short-lived nuclei.

That could change soon. Kyo Tsukada and colleagues, working at RIKEN's Radioactive Isotope Beam Factory (RIBF) in Wako, Japan, have performed the first electron-scattering experiment on unstable nuclei produced on the fly in a nuclear reaction.[1] Their isotope of choice, cesium-137, has a half-life of 30 years. It's not so exotic that the researchers expected—or found—anything unusual about its structure. But the technique they used is applicable to shorter-lived nuclei, so more experiments are on the way.

Backscatter

Probing nuclei through particle scattering dates back to the discovery of the nucleus itself, in 1911, when Ernest

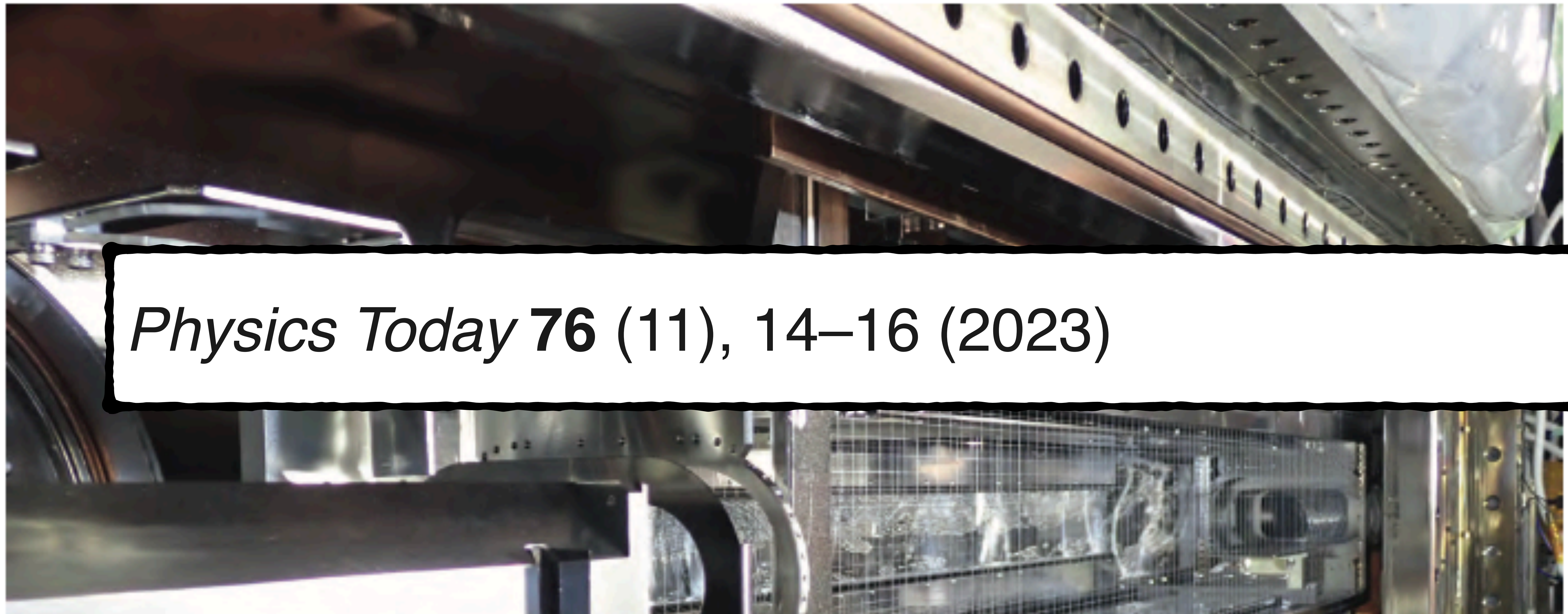

Physics Today **76** (11), 14–16 (2023)

Edit

Electron scattering provides a long-awaited view of unstable nuclei

Nuclear reactions produce a plethora of short-lived artificial isotopes. Figuring out what they look like has been a challenge.

The cartoon picture of an atomic nucleus looks kind of like the inside of a gumball machine that dispenses only two flavors: protons and neutrons, evenly mixed in a compact, spherical cluster.

That's not generally what real nuclei

stranger the structures it can adopt. Short-lived nuclei might form bubble structures with depleted central density, or they might have a valence nucleon or two that form a halo around a compact central core. (See the article by Filomena Nunes, Physics Today, May

and colleagues, working at RIKEN's Radioactive Isotope Beam Factory (RIBF) in Wako, Japan, have performed the first electron-scattering experiment on unstable nuclei produced on the fly in a nuclear reaction.[1] Their isotope of choice, cesium-137, has a half-life of 30 years. It's not so exotic that the researchers expected—or found—anything unusual about its structure. But the technique they used is applicable to shorter-

electron scattering - the gold standard for probing nuclear structure - has been off limits to short-lived nuclei

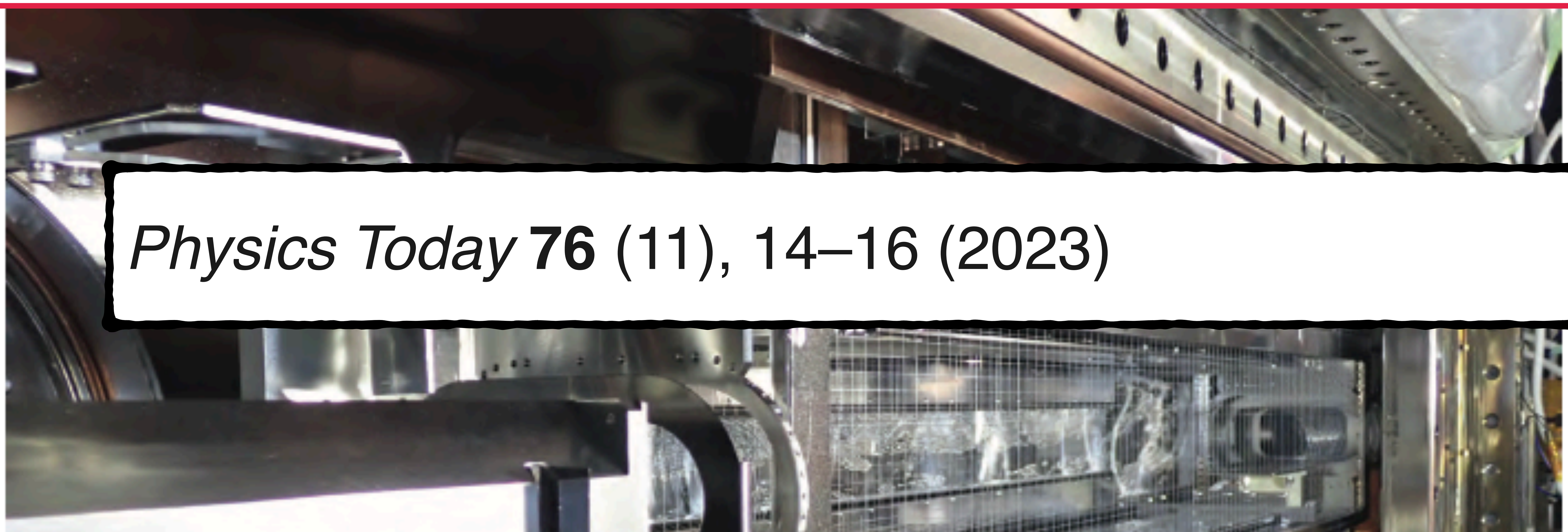

Physics Today **76** (11), 14–16 (2023)

SCRIT-based electron scattering facility

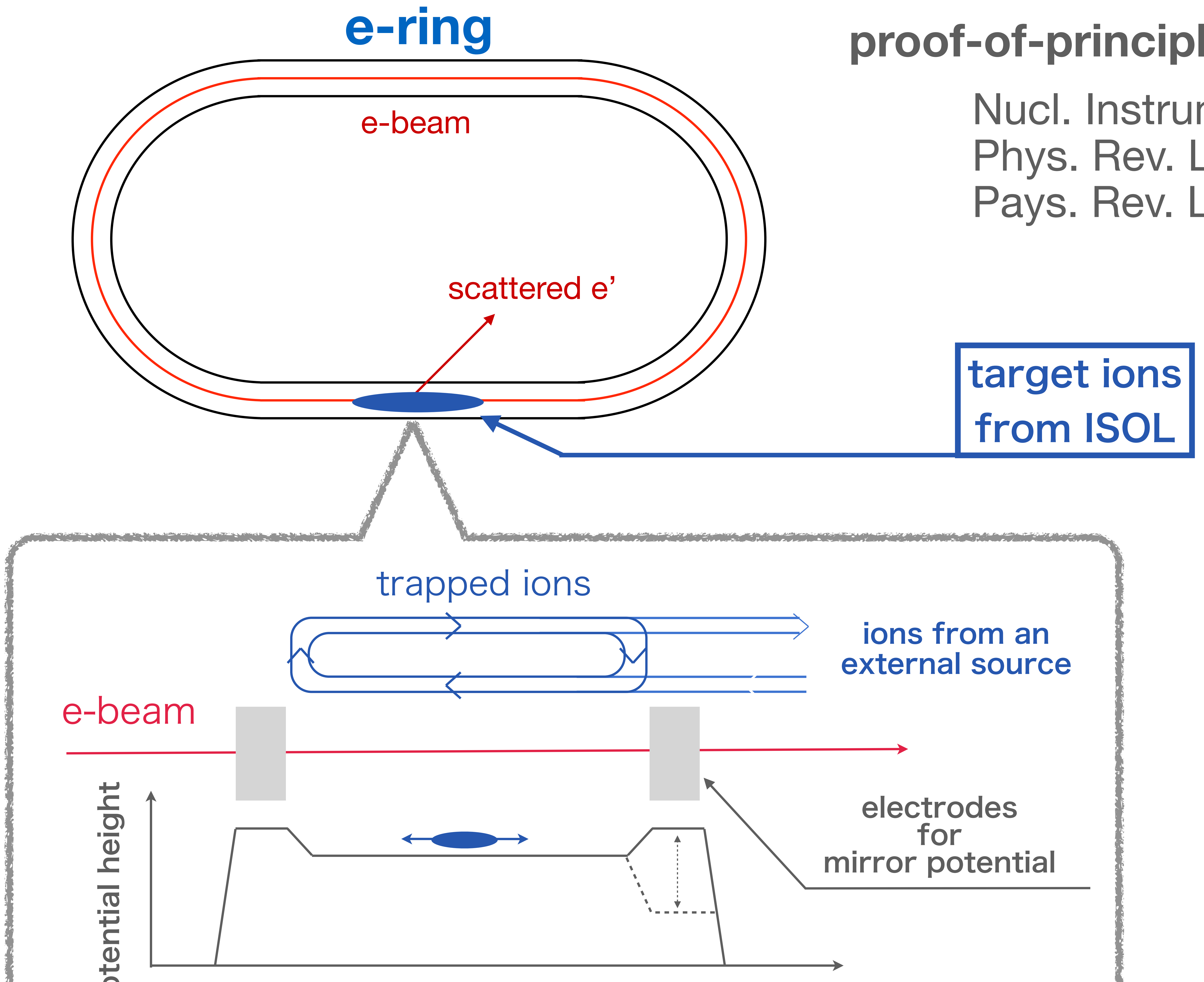

proof-of-principle studies

Nucl. Instrum. Methods A532 (2004) 216.
Phys. Rev. Lett. 100 (2008) 164801.
Pays. Rev. Lett. 102 (2009) 102501.

- **automatic collision by "ion trapping"**
- **fast ion manipulation for short-lived nuclei**

RIKEN SCRIT Electron Scattering Facility

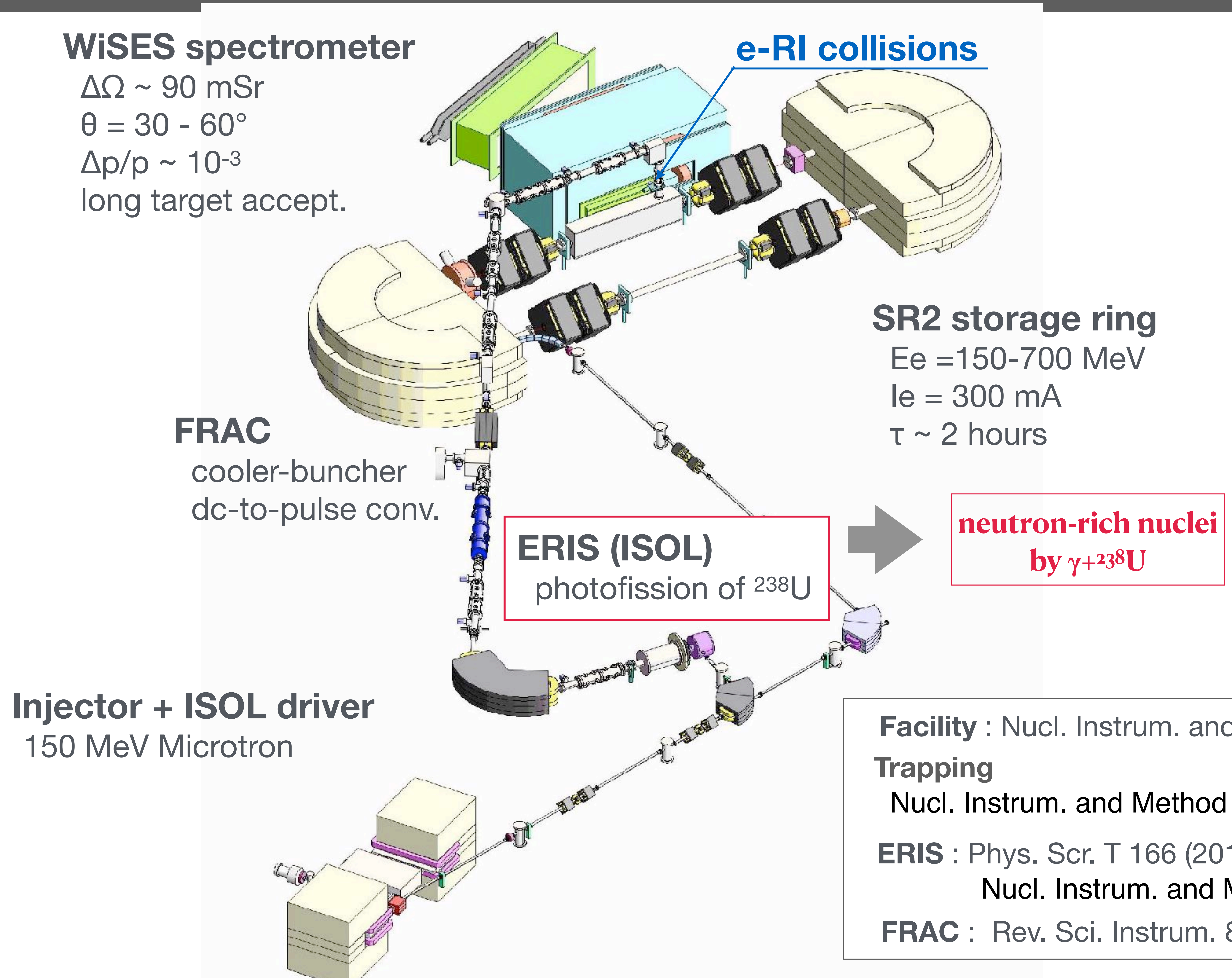

Facility : Nucl. Instrum. and Method B541 (2023) 380-384.

Trapping
Nucl. Instrum. and Method B541 (2023) 90-92

ERIS : Phys. Scr. T 166 (2015) 014071.
Nucl. Instrum. and Method B463 (2020) 290-292.

FRAC : Rev. Sci. Instrum. 89 (2018) 095107.

SCRIT electron scattering facility @ RIBF

World's first electron facility dedicated for exotic nuclei

RIKEN RI Beam Factory

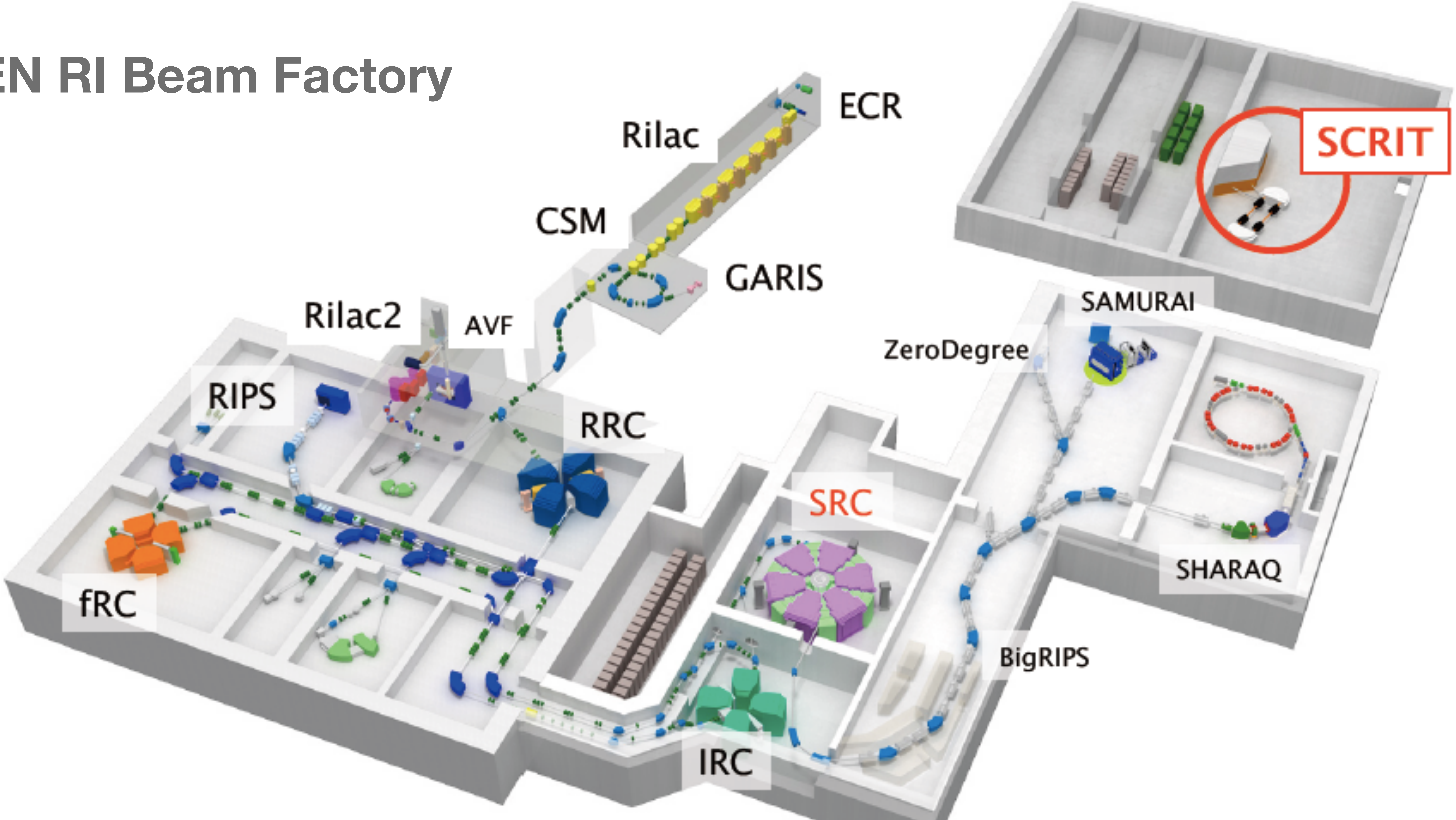

RIKEN SCRIT e-scattering facility

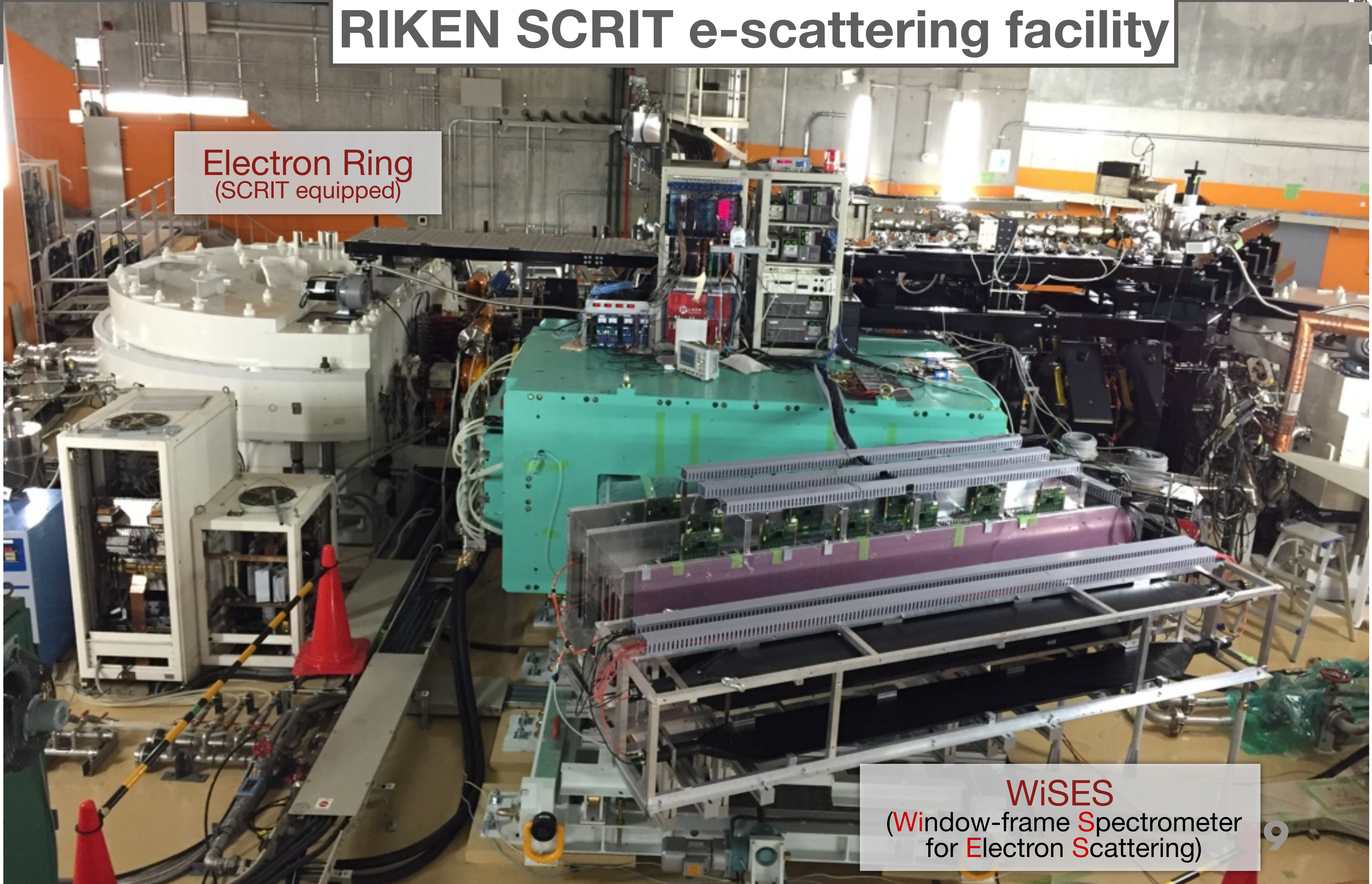

9

Region of our current studies

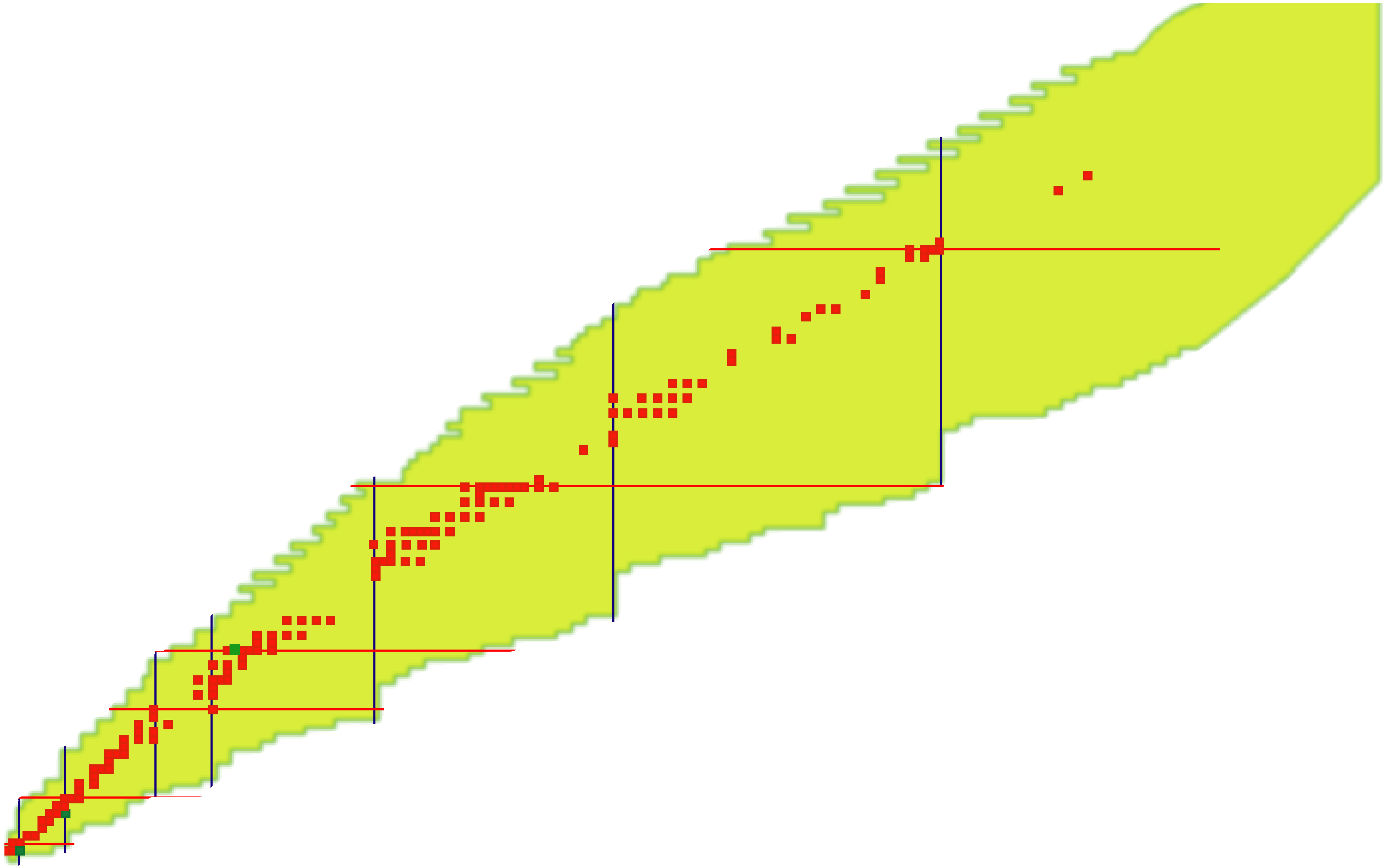

Region of our current studies

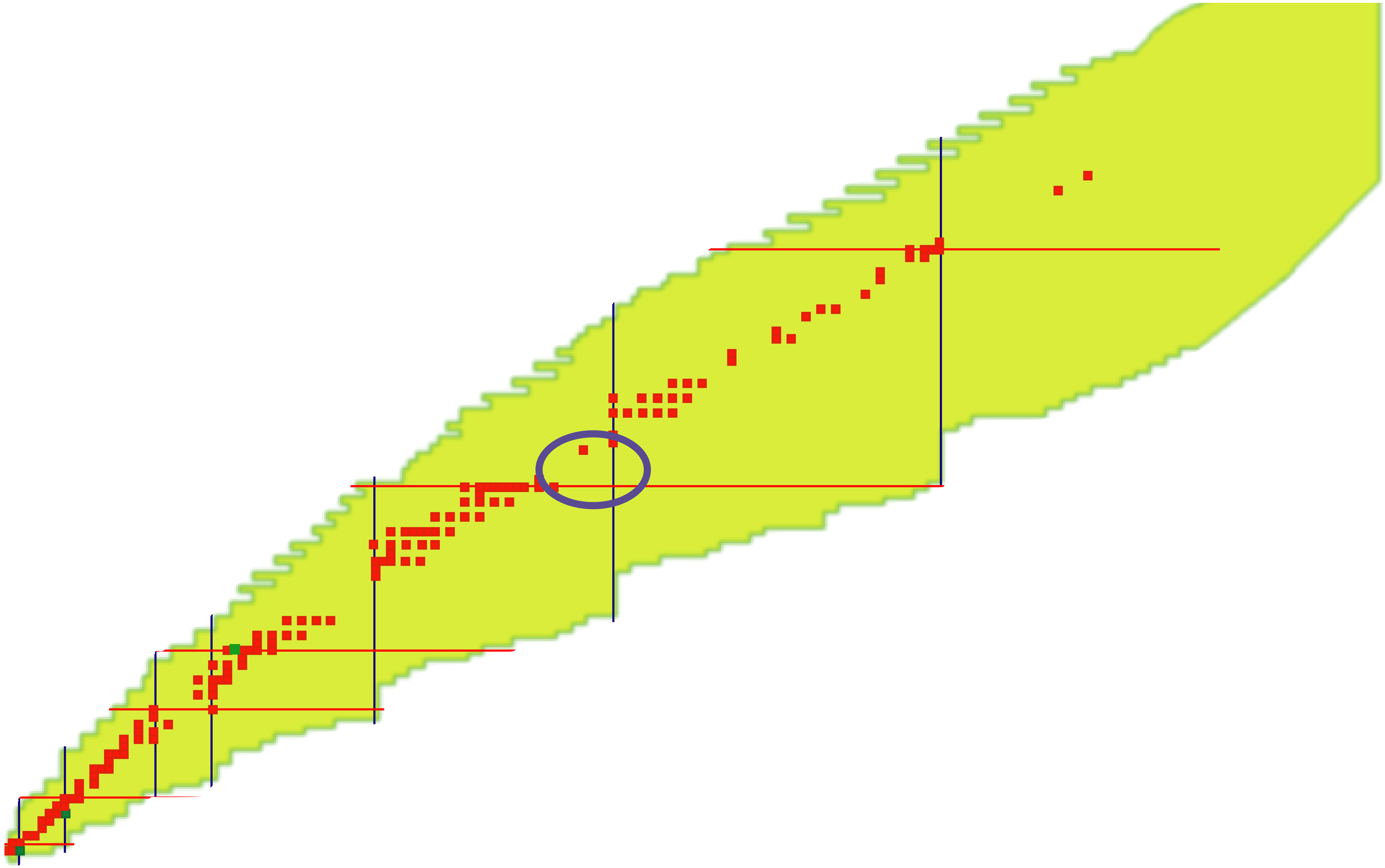

Region of our current studies

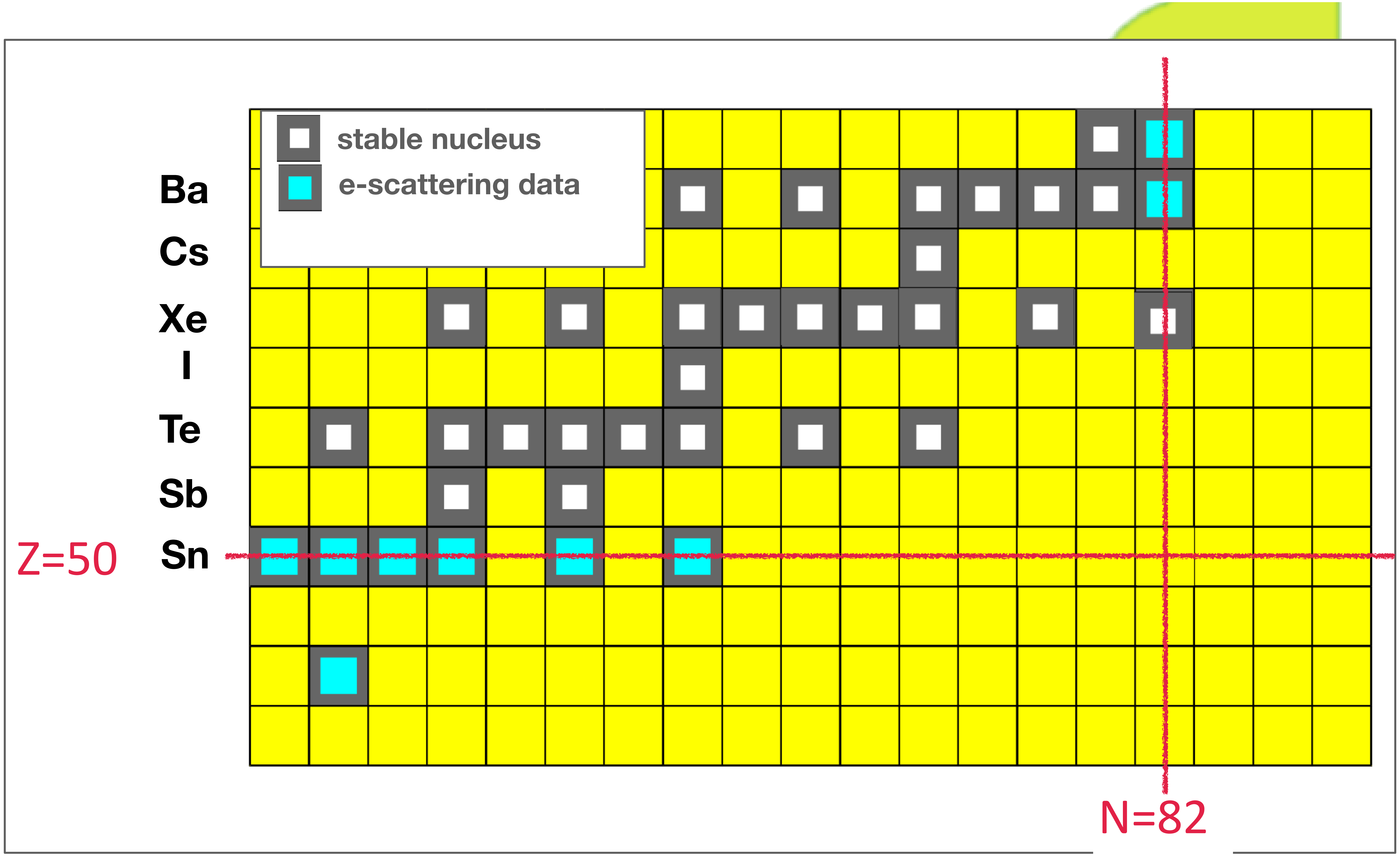

Region of our current studies

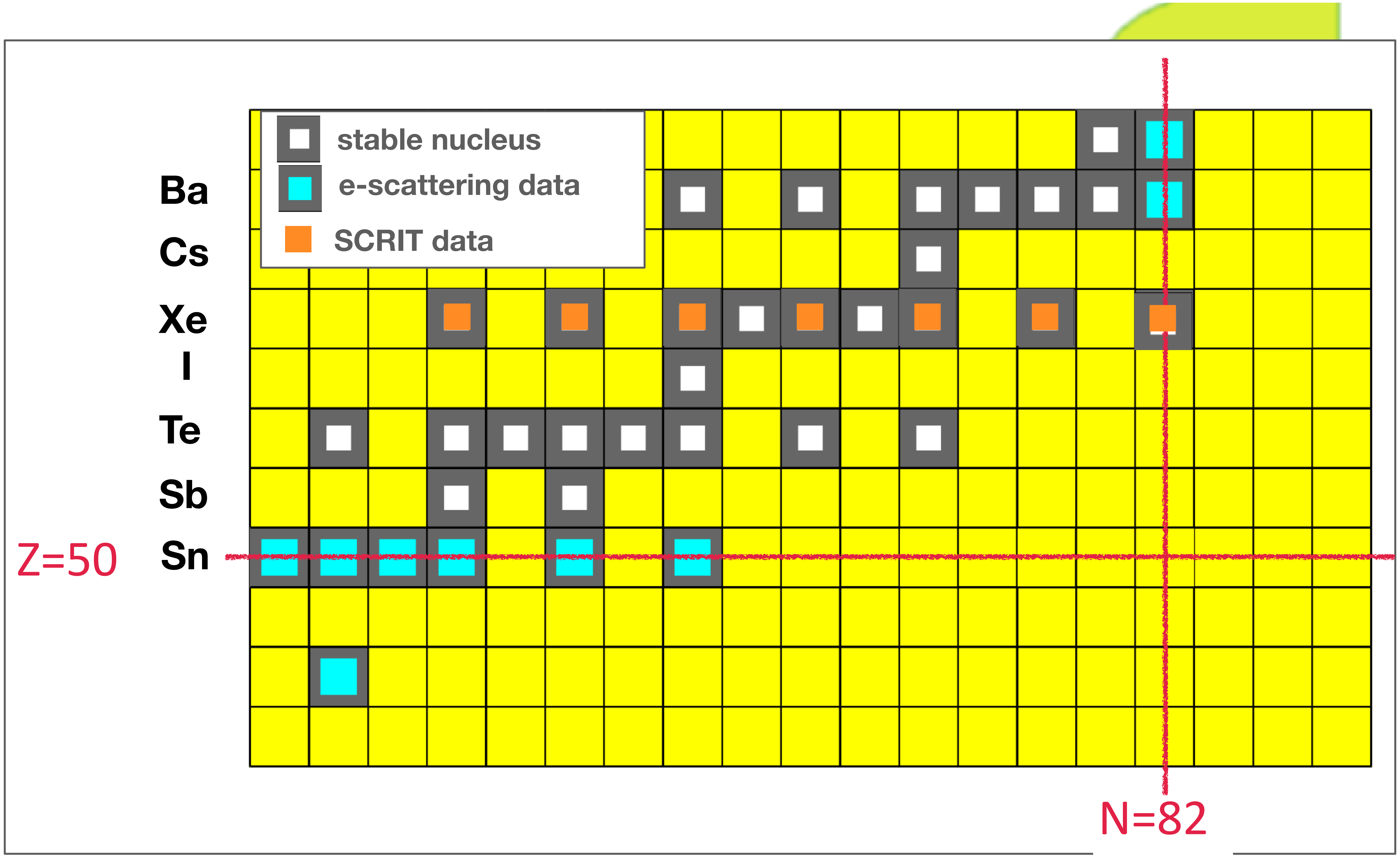

Facility Commissioning with Stable Xe(e,e')

trapping sequence

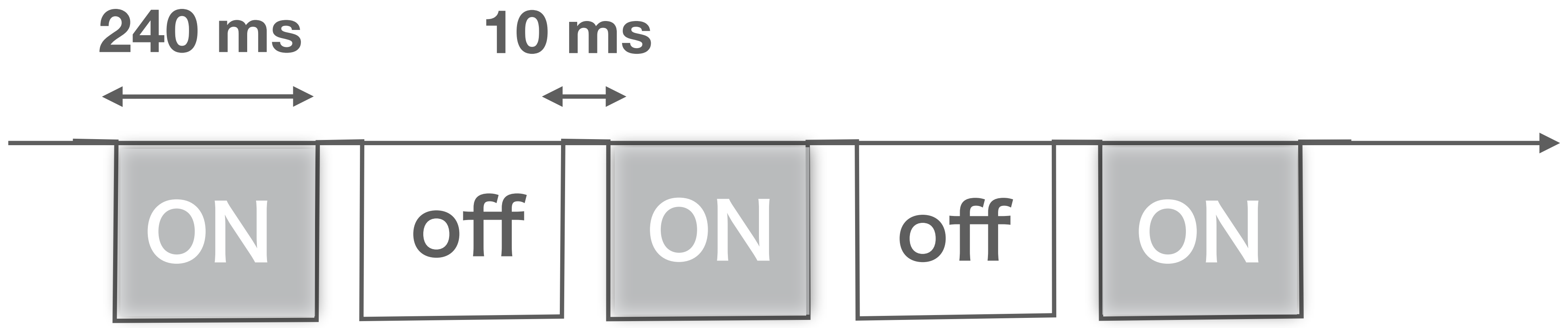

K. Tsukada et al.,
Phys. Rev. Lett. 118 (2017) 262501.

L ~ 10^{27} /cm²/s with $N_{trapped}$ ~ 10^7

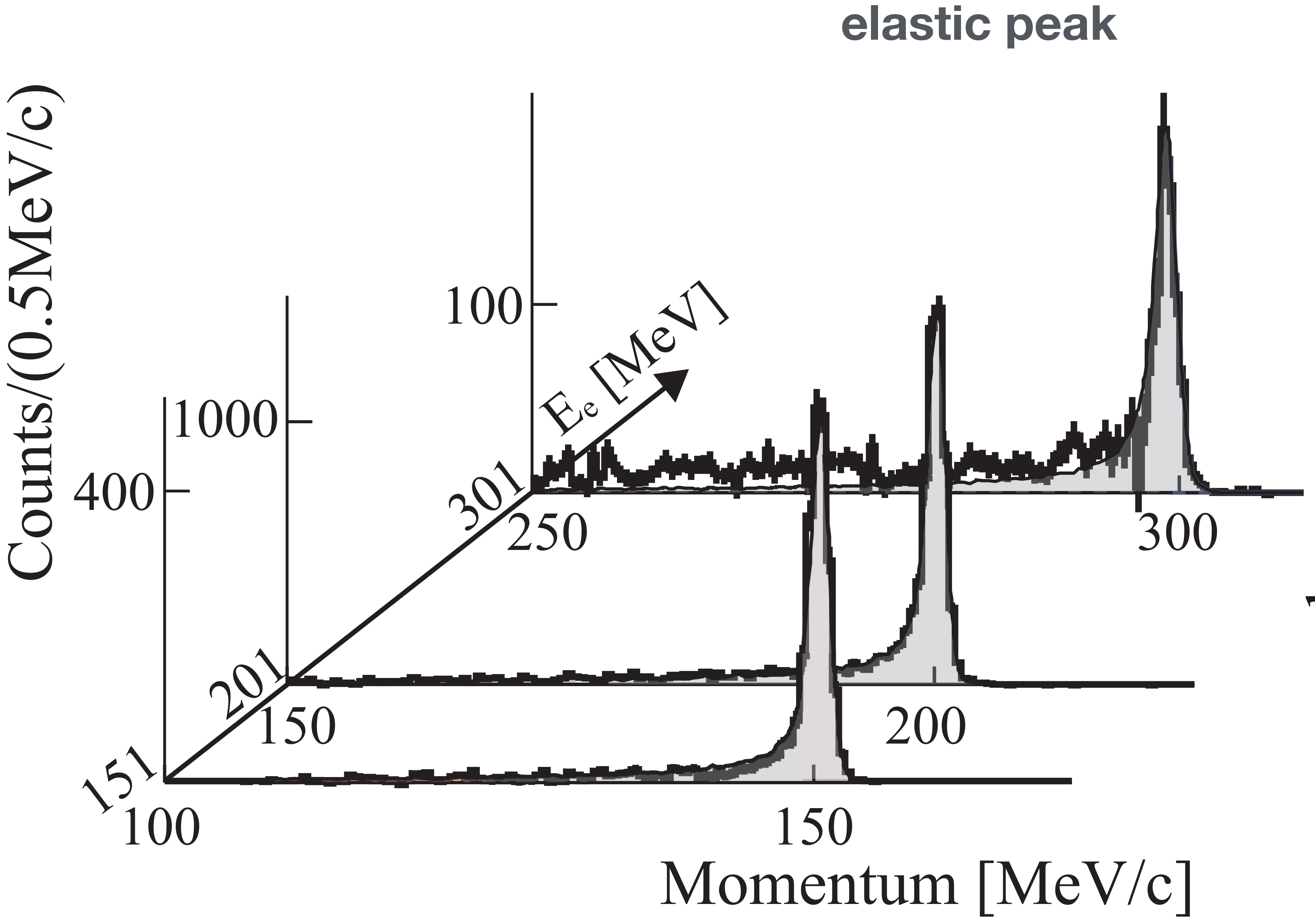

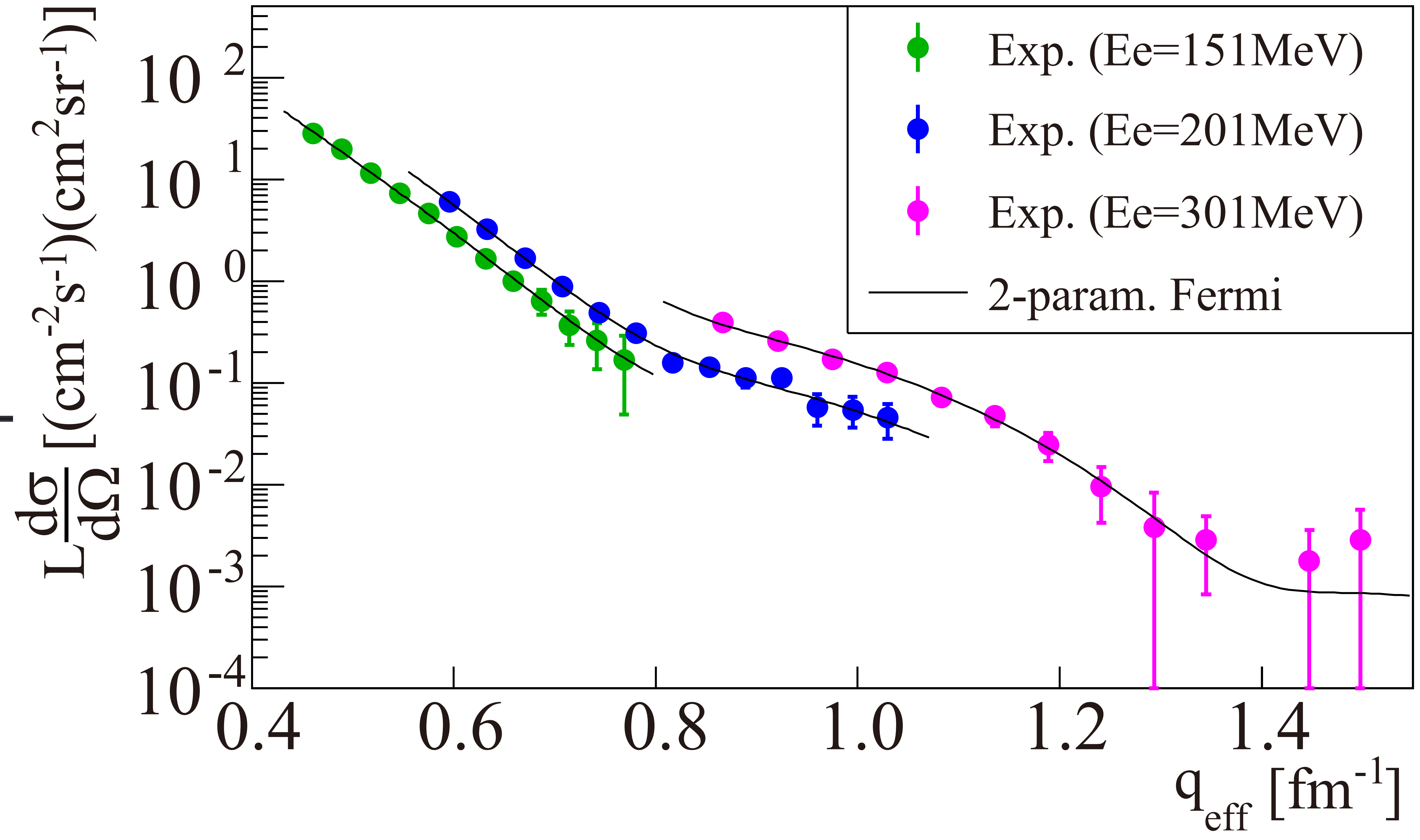

$\langle r^2\rangle^{1/2} = 4.789\,^{+0.12}_{-0.10}$ fm ⟷ $\langle r^2\rangle^{1/2} = 4.787$ fm(μ-atom X-rays)

$^{124-136}$Xe(e,e’) at SCRIT

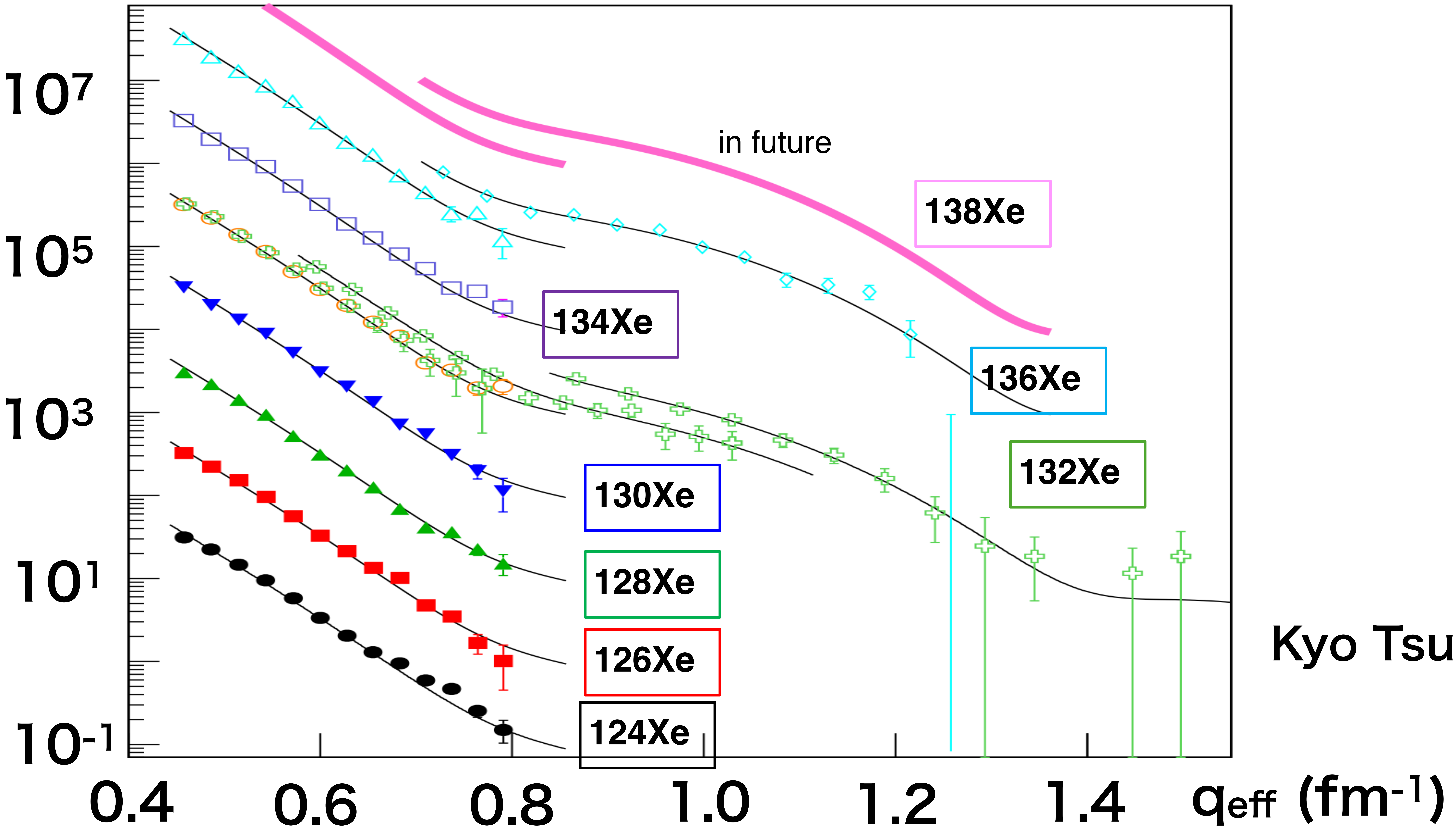

Kyo Tsukada

Region of our current studies

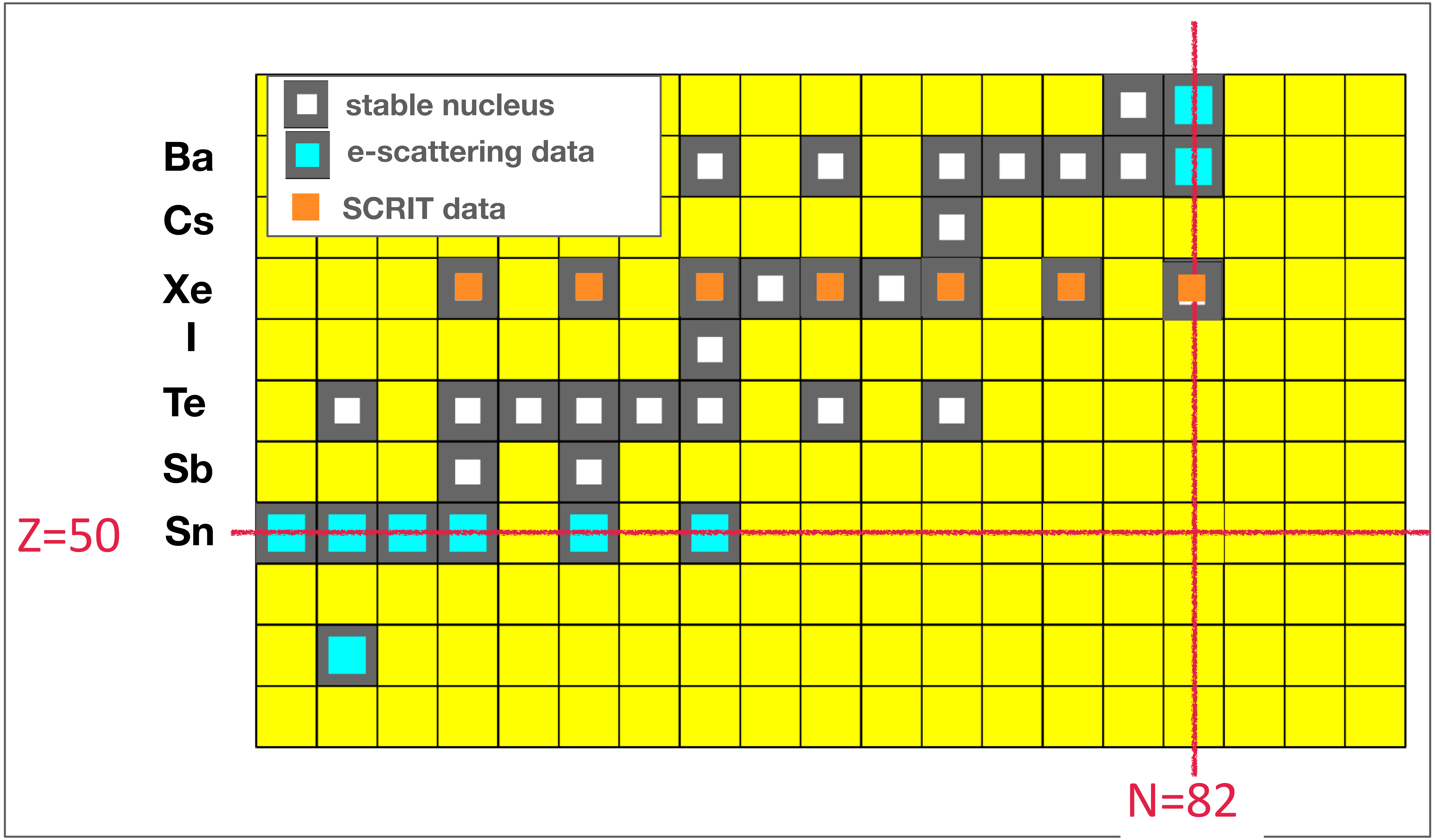

Region of our current studies

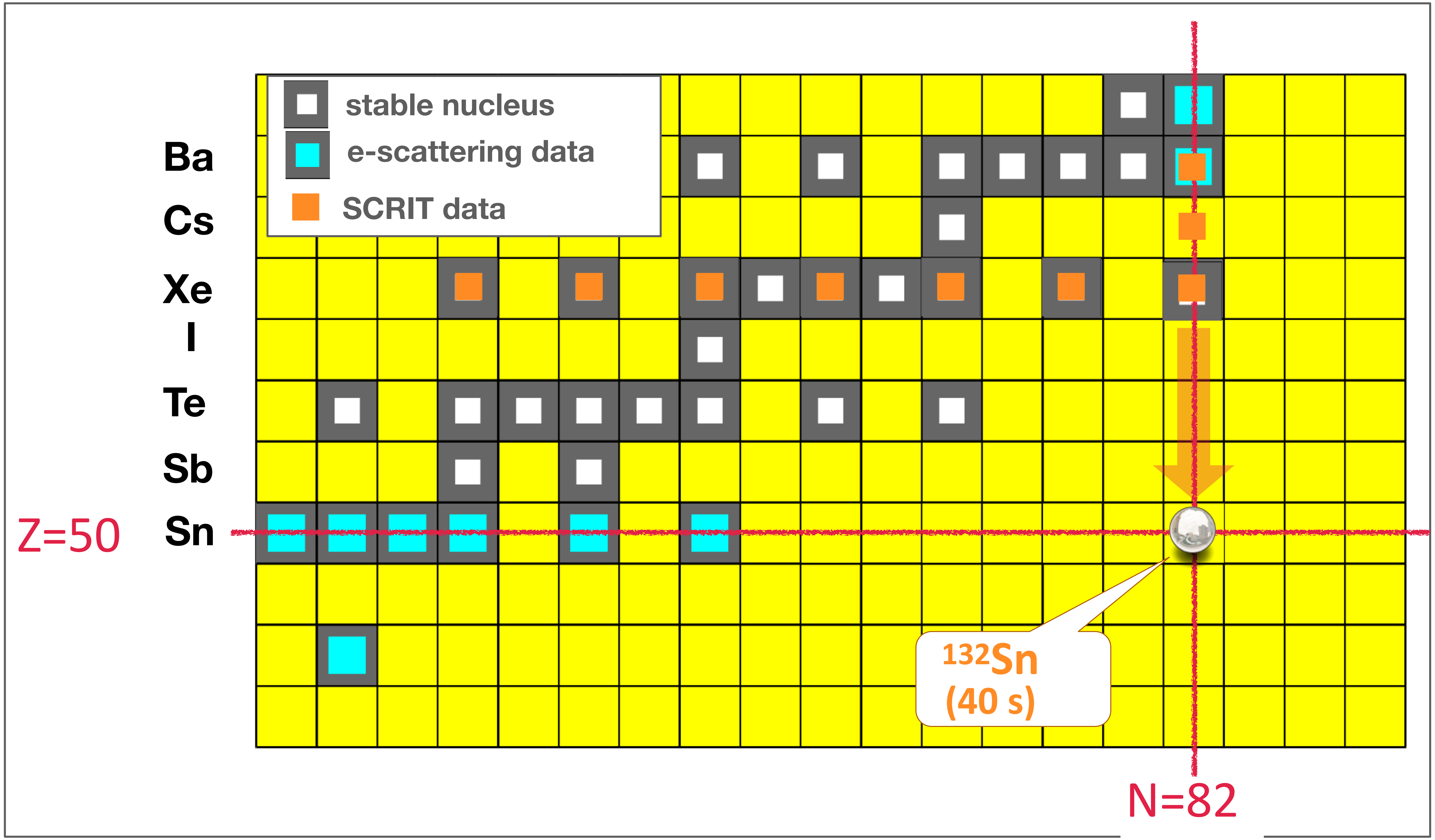

Region of our current studies

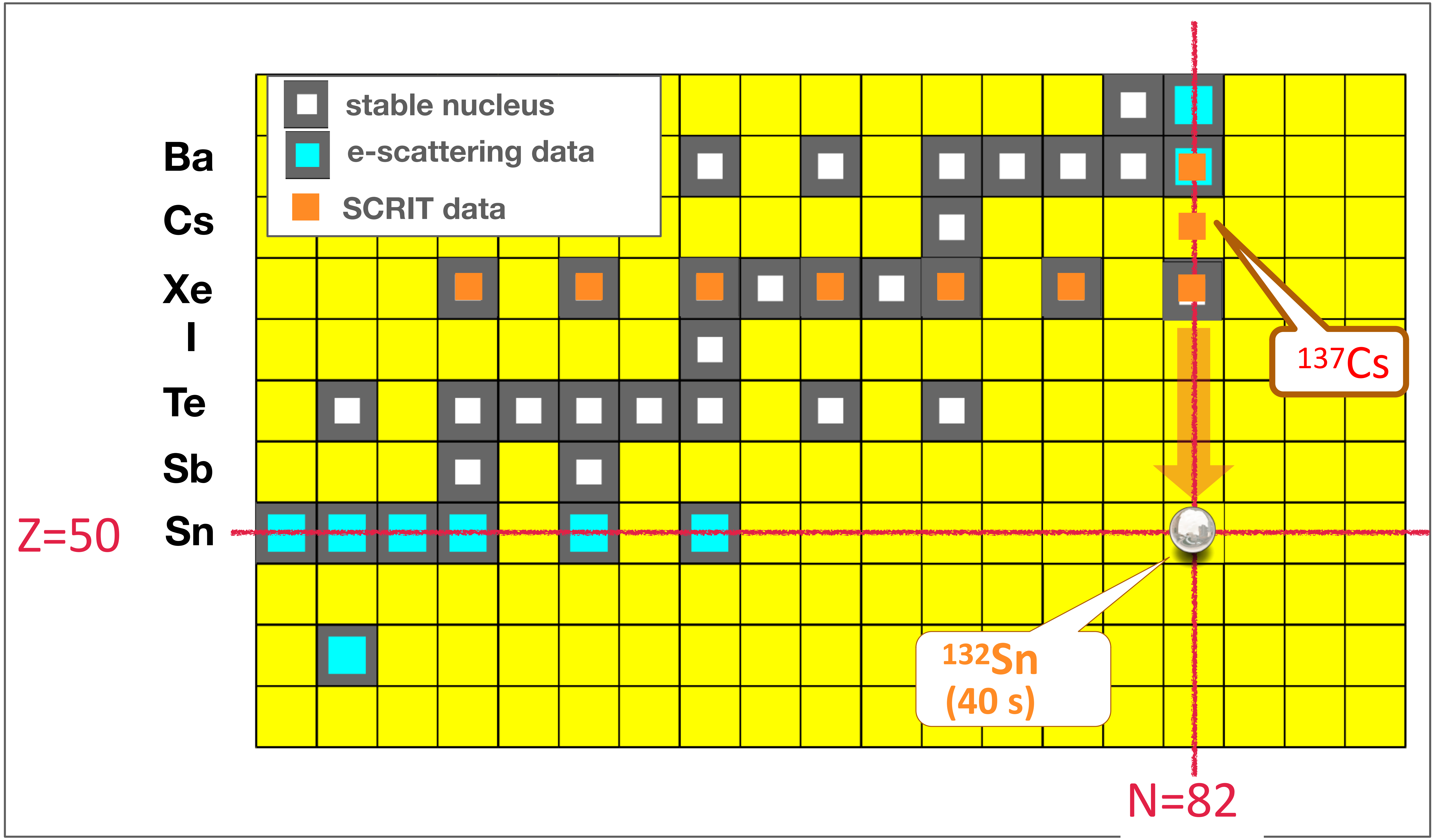

e-scattering for online-produced unstable Cs ions

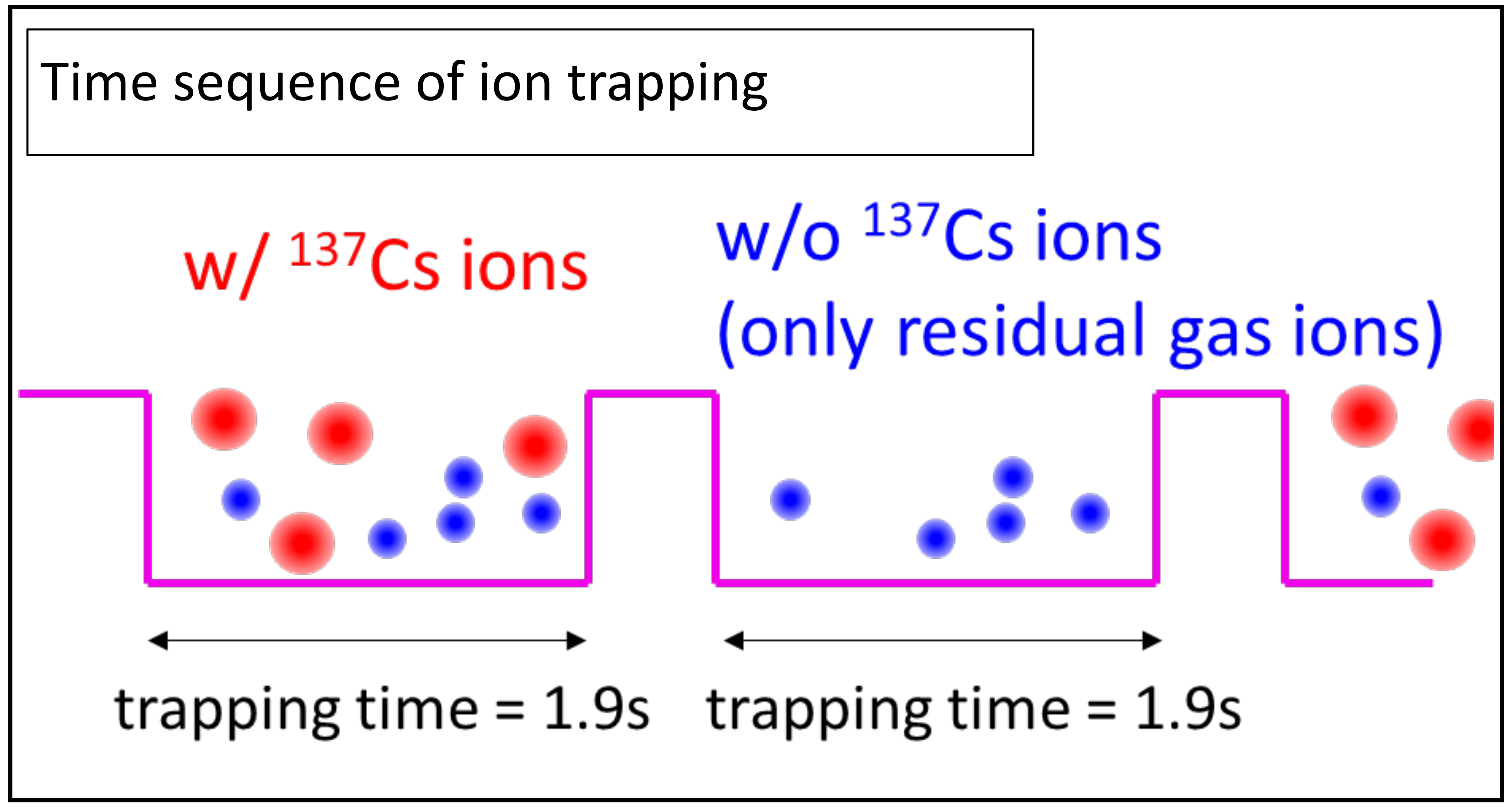

1.9 s trapping

=> mimicking "short-lived" nuclei

$N_{trapped}$ ~ 2 x10^7

=> L ~ 0.9 x 10^{26} /cm^2/s

successful demonstration for online-produced unstable nuclei

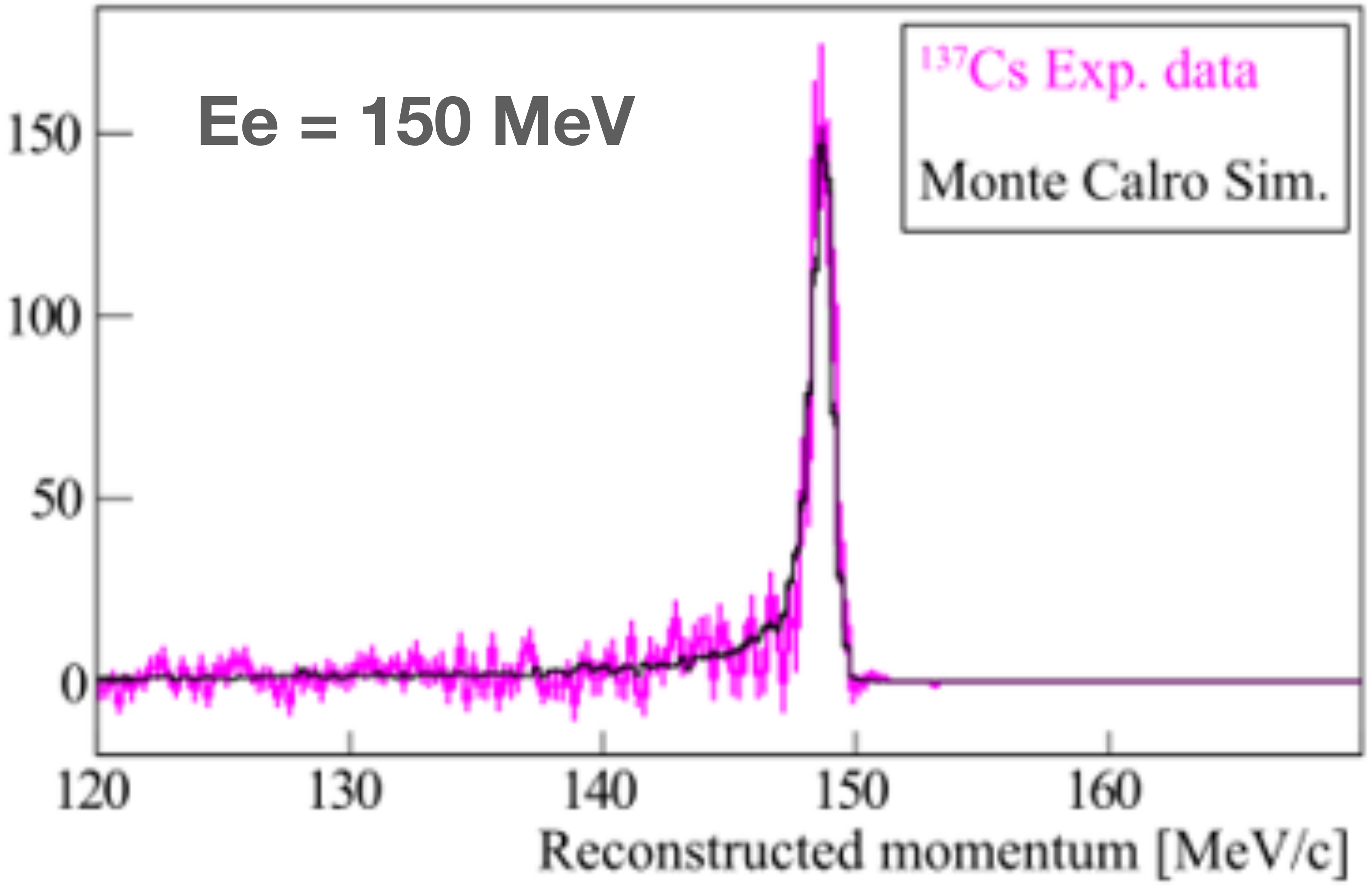

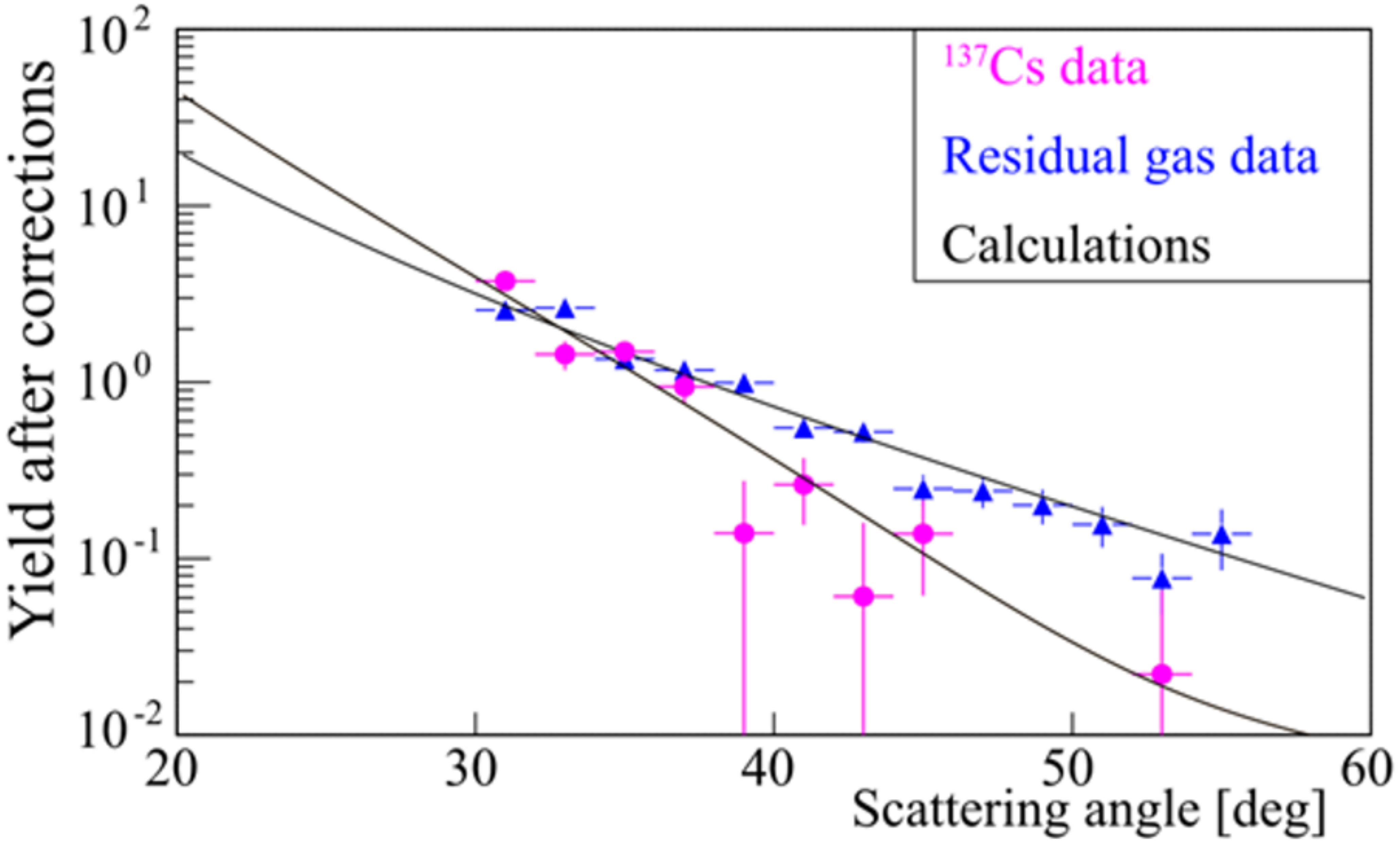

achieved luminosity with the SCRIT method

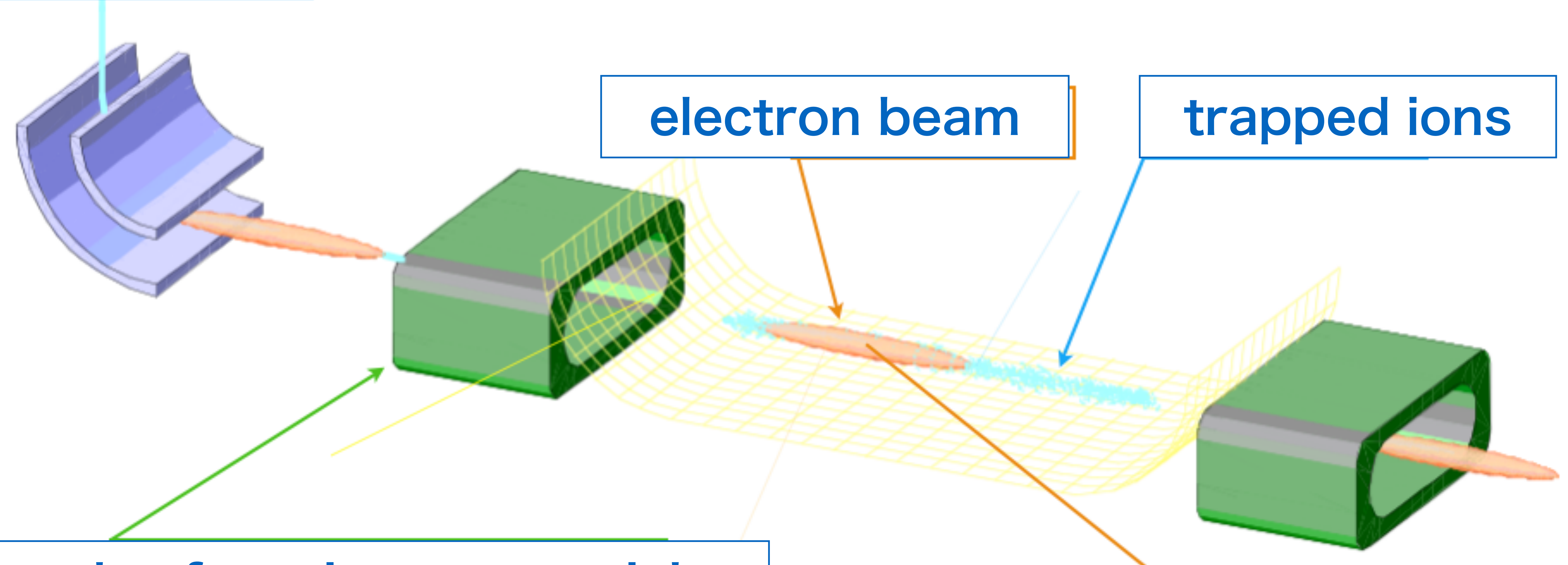

~10^7 ions are trapped on e-beam (~ 1 mm^2)

N_t ~10^7 /mm^2 => 10^9 /cm^2

	Ee	N_{beam}	ρ・t	L
Hofstadter's era (1950s)	150 MeV	~ 1nA (~10^9 /s)	~10^{19} /cm^2	~10^{28} /cm^2/s
JLAB	12 GeV	~100μA (~10^{14} /s)	~10^{22} /cm2	~10^{36} /cm^2/s
SCRIT	150 - 300 MeV	~200 mA (~10^{18} /s)	~ 10^9 /cm^2	~10^{27} /cm^2/s

achieved luminosity with the SCRIT method

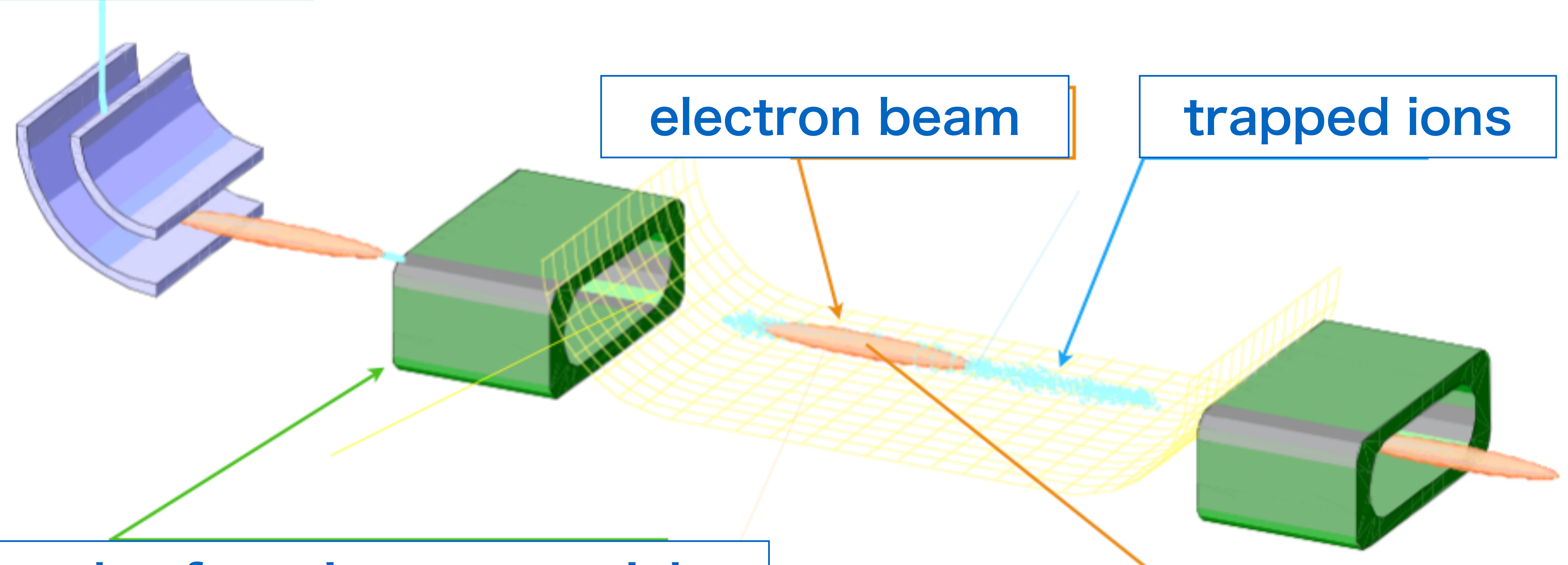

~10^7 ions are trapped on e-beam (~ 1 mm^2)

N_t ~10^7 /mm^2 => 10^9 /cm^2

REQUIRED TARGET THICKNESS 10^{-10}!!!

	Ee	N_{beam}	ρ・t	L
Hofstadter's era (1950s)	150 MeV	~ 1nA (~10^9 /s)	~10^{19} /cm^2	~10^{28} /cm^2/s
JLAB	12 GeV	~100μA (~10^{14} /s)	~10^{22} /cm2	~10^{36} /cm^2/s
SCRIT	150 - 300 MeV	~200 mA (~10^{18} /s)	~ 10^9 /cm^2	~10^{27} /cm^2/s

1) charge densities of exotic nuclei

systematic measurements for many unstable nuclei

^{132}Sn : symbolic target for “day-one” exp

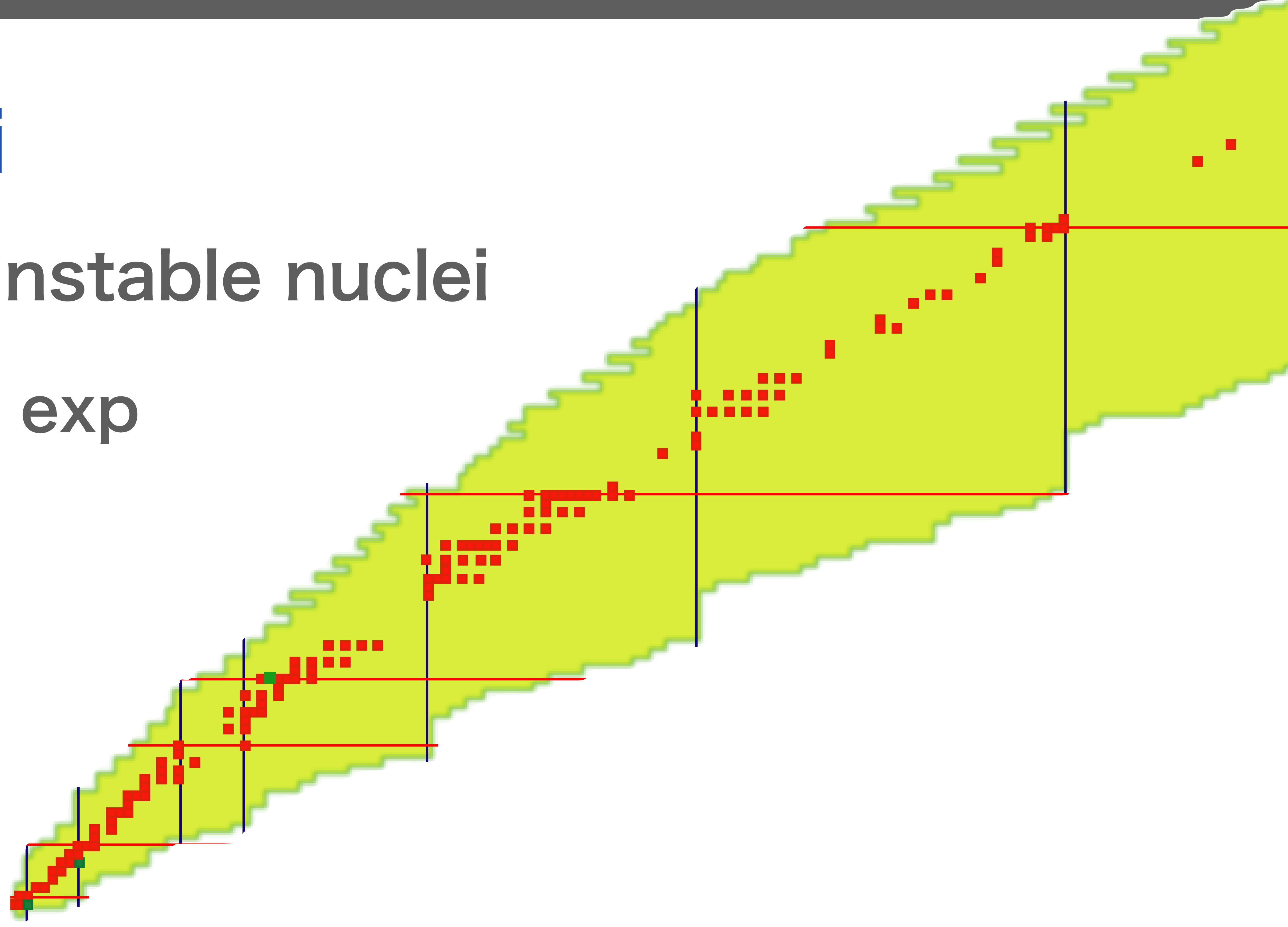

ISOL upgrade: towards ^{132}Sn (40s)

Production Rate
$N_{fission}$ ~ 10^8 /watt
$N_{^{132}Sn}$ ~ 10^6 /watt * 1% ($\varepsilon_{trans.}$)
beam power : ~ 20W (today)
~ 2 kW (underway)

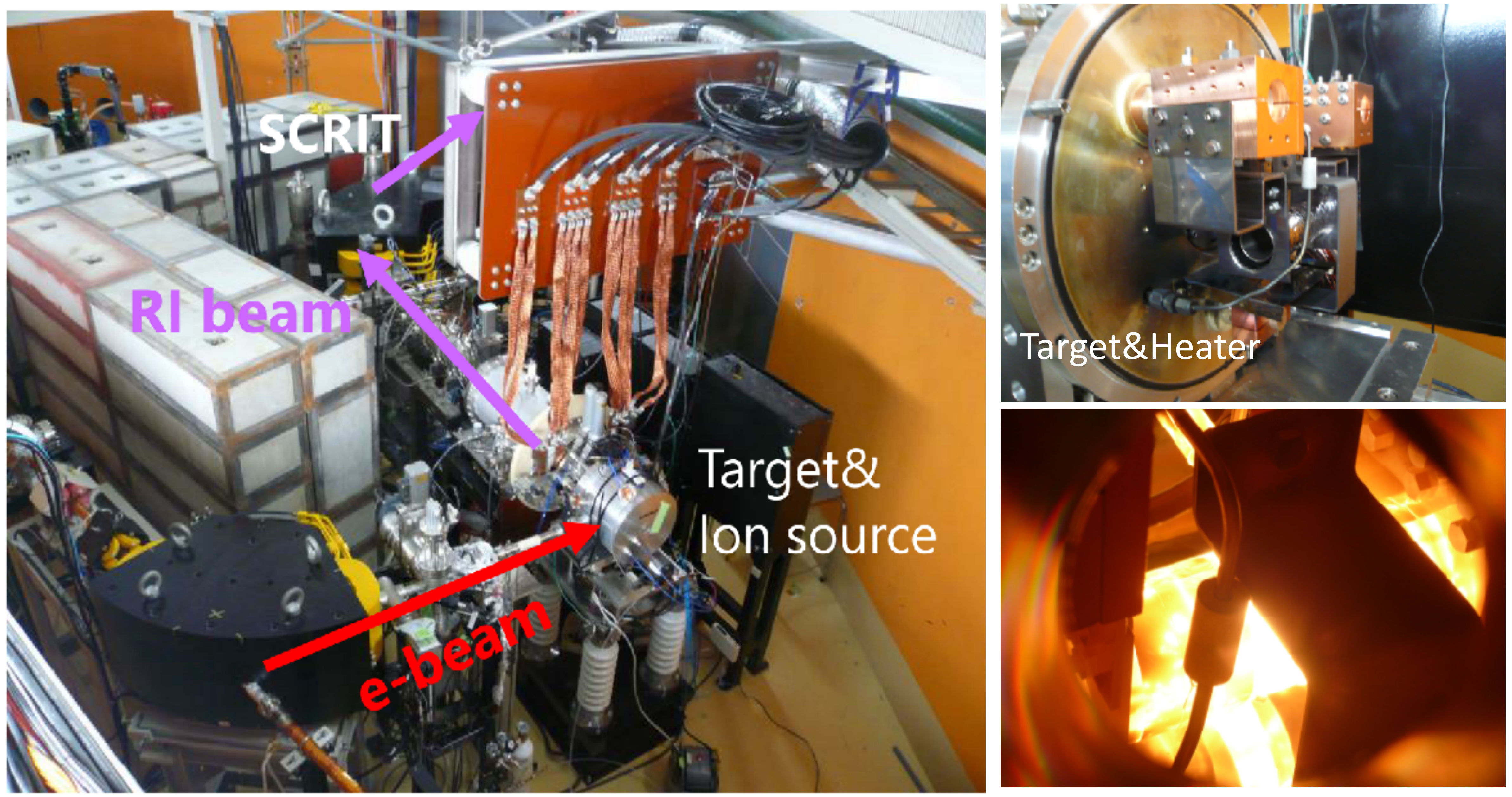

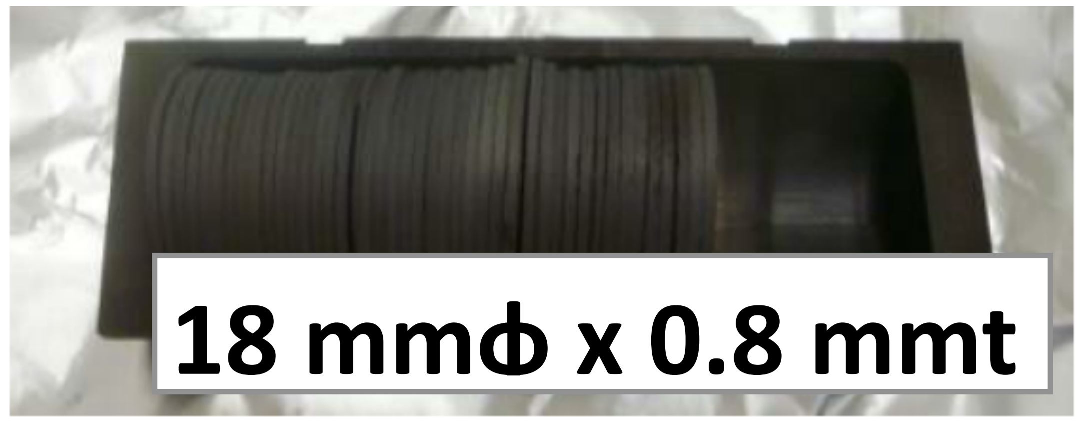

House-made
Uranium carbide (UCx)

T. Ohnishi *et al.* NIM B317 (2013) 357.

towards 2 kW e-beam
higher repetition
higher peak intensity

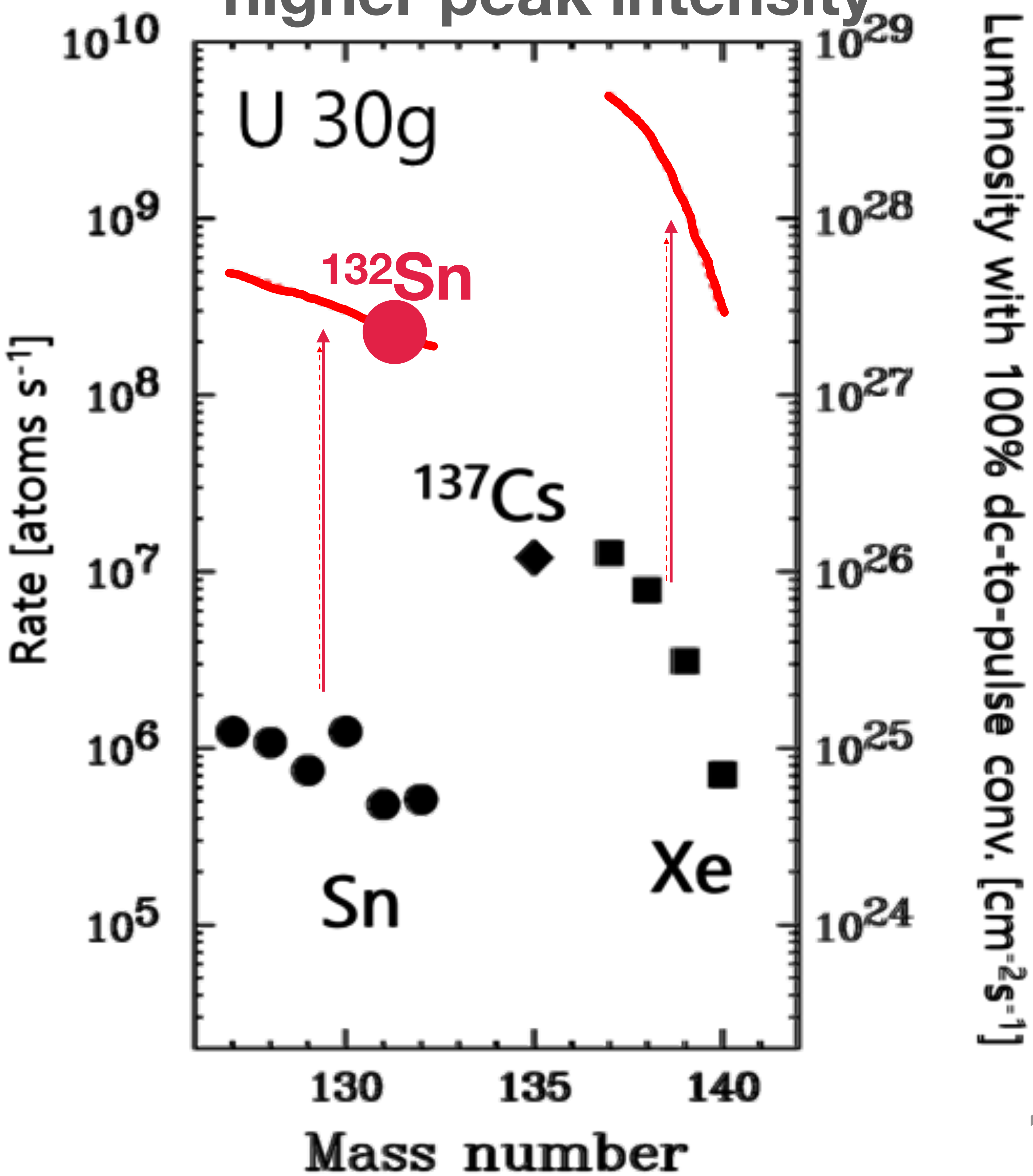

^{238}U photo-fission yields

R_f ~ 2x10^8 fissions/W

mass region : A~100 and 130

Tetsuya Oonishi

1) charge densities of exotic nuclei

systematic measurements for many unstable nuclei

^{132}Sn : symbolic target for “day-one” exp

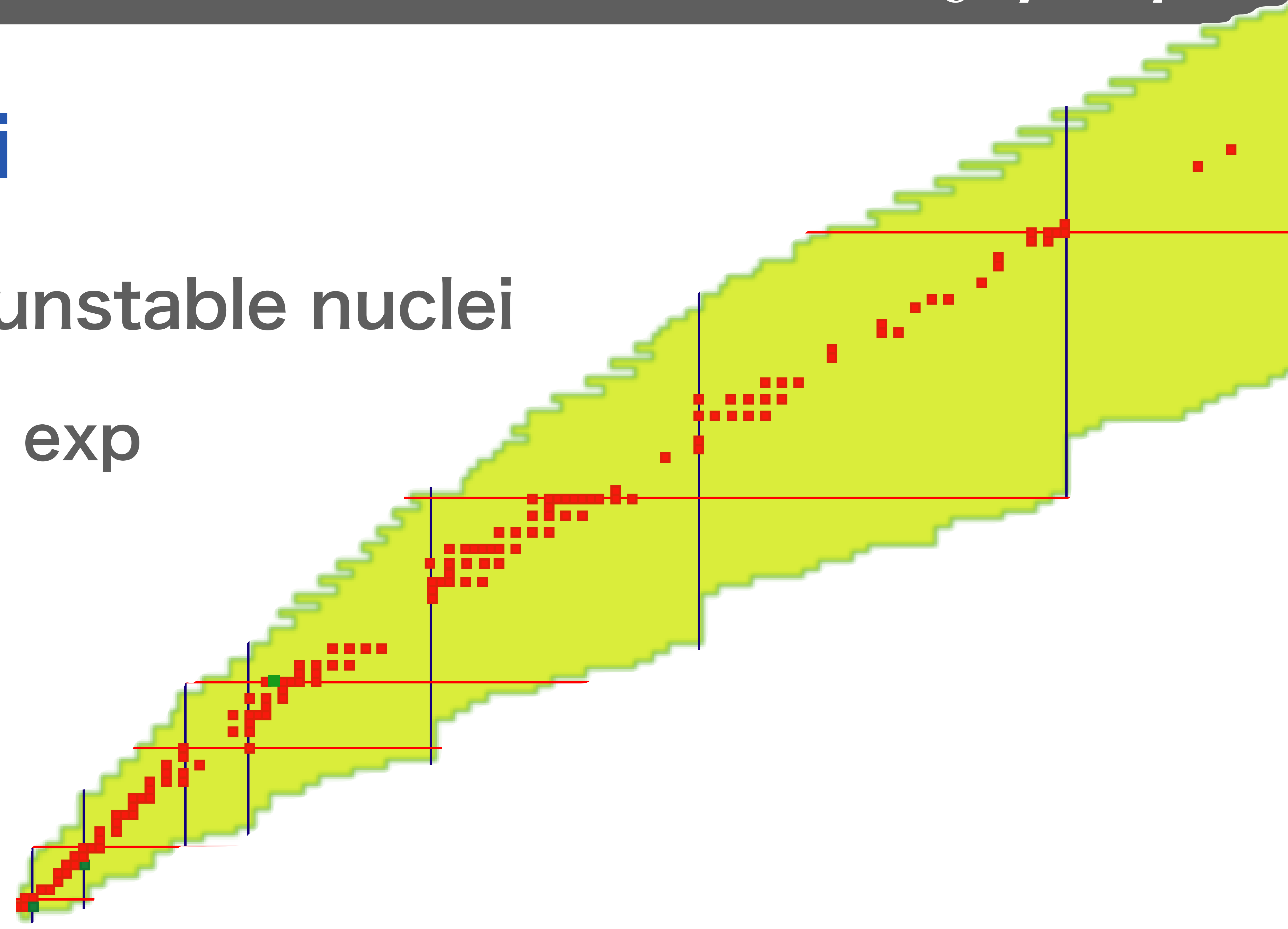

1) charge densities of exotic nuclei

systematic measurements for many unstable nuclei

^{132}Sn : symbolic target for “day-one” exp

^{46}Ar : Stefano Brolli

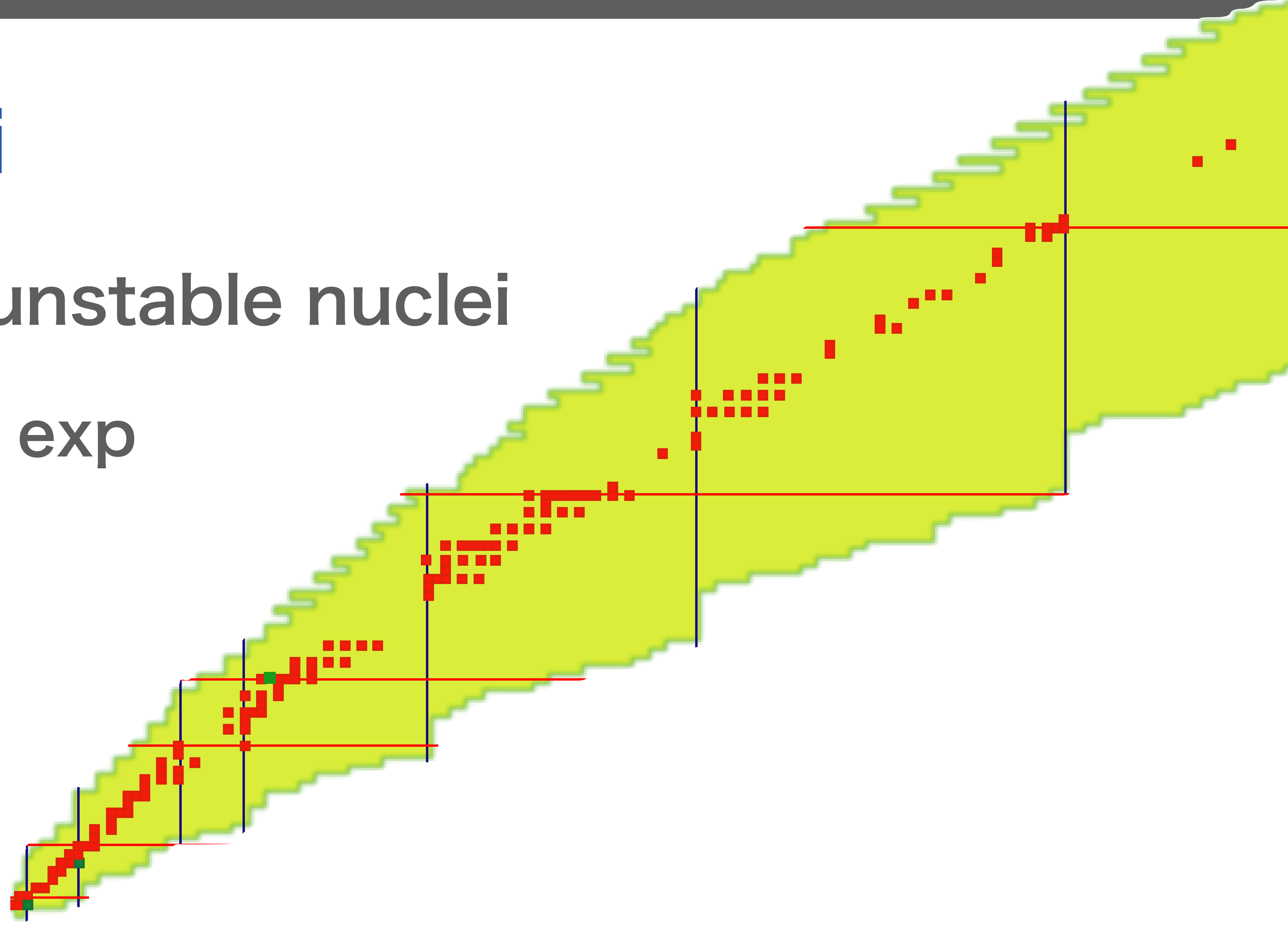

“^{46}Ar : proton-bubble” nucleus (8.4s)

Courtesy: Stefano Brolli

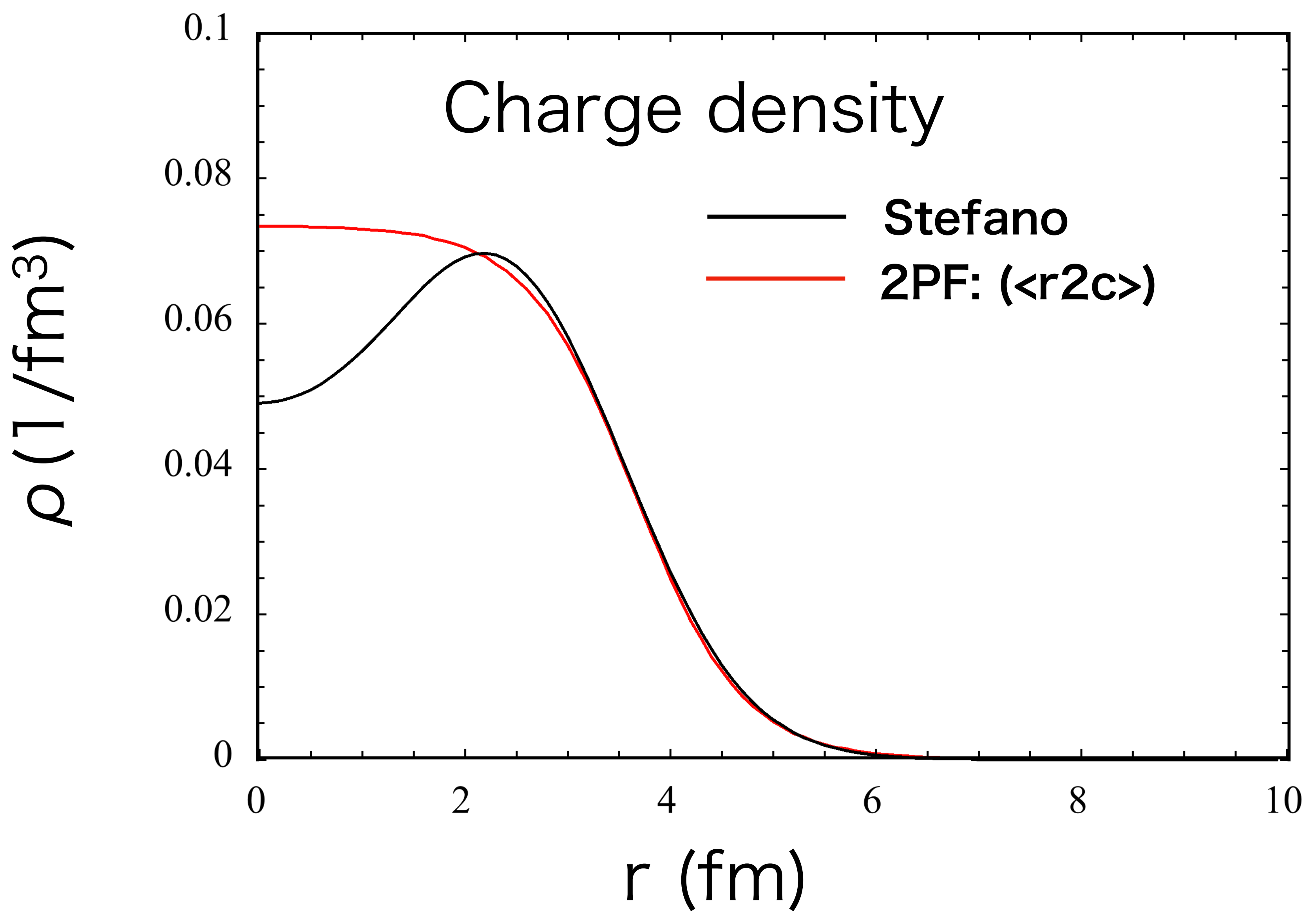

"^{46}Ar : proton-bubble" nucleus (8.4s)

Courtesy: Stefano Brolli

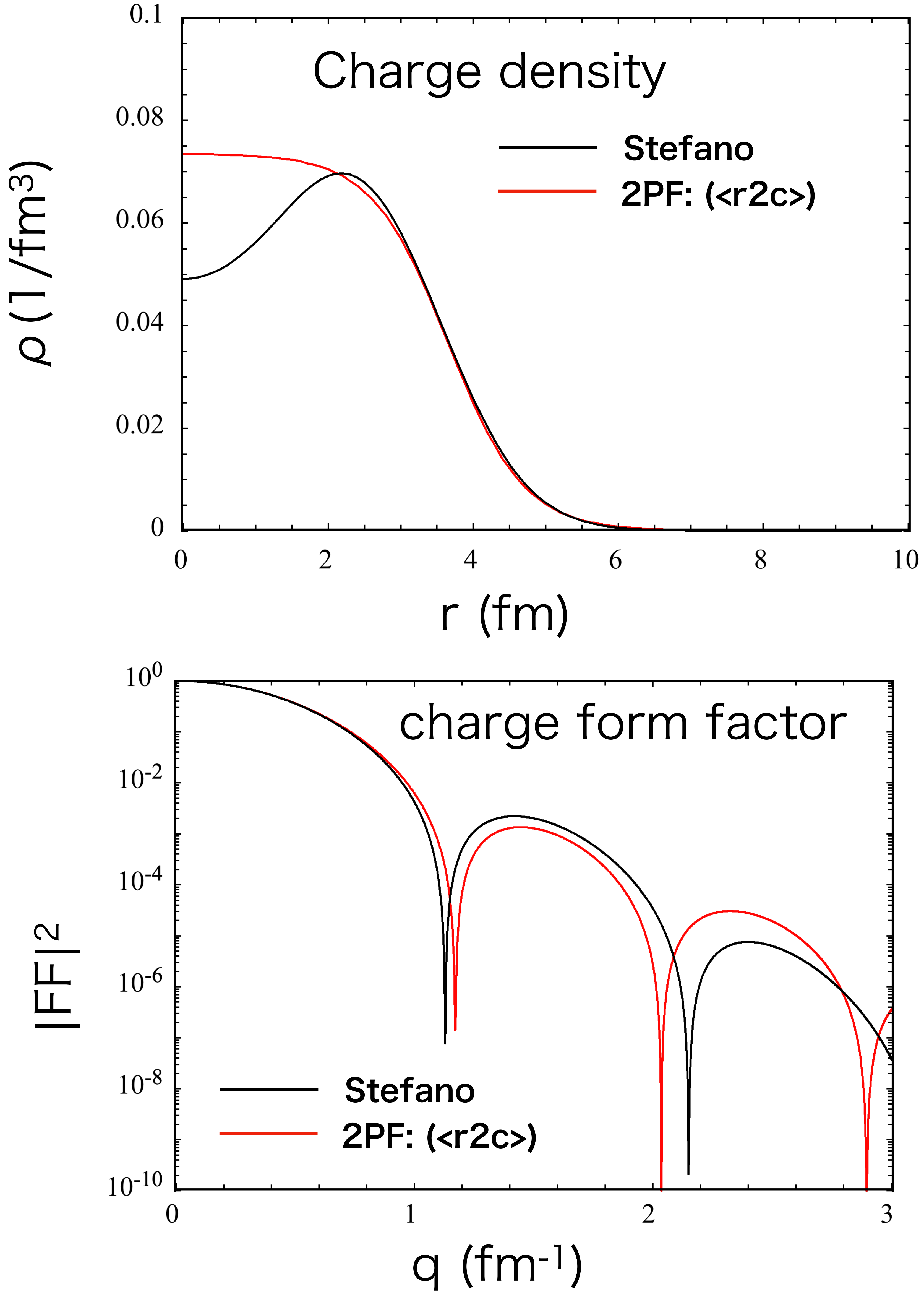

“^{46}Ar : proton-bubble” nucleus (8.4s)

Courtesy: Stefano Brolli

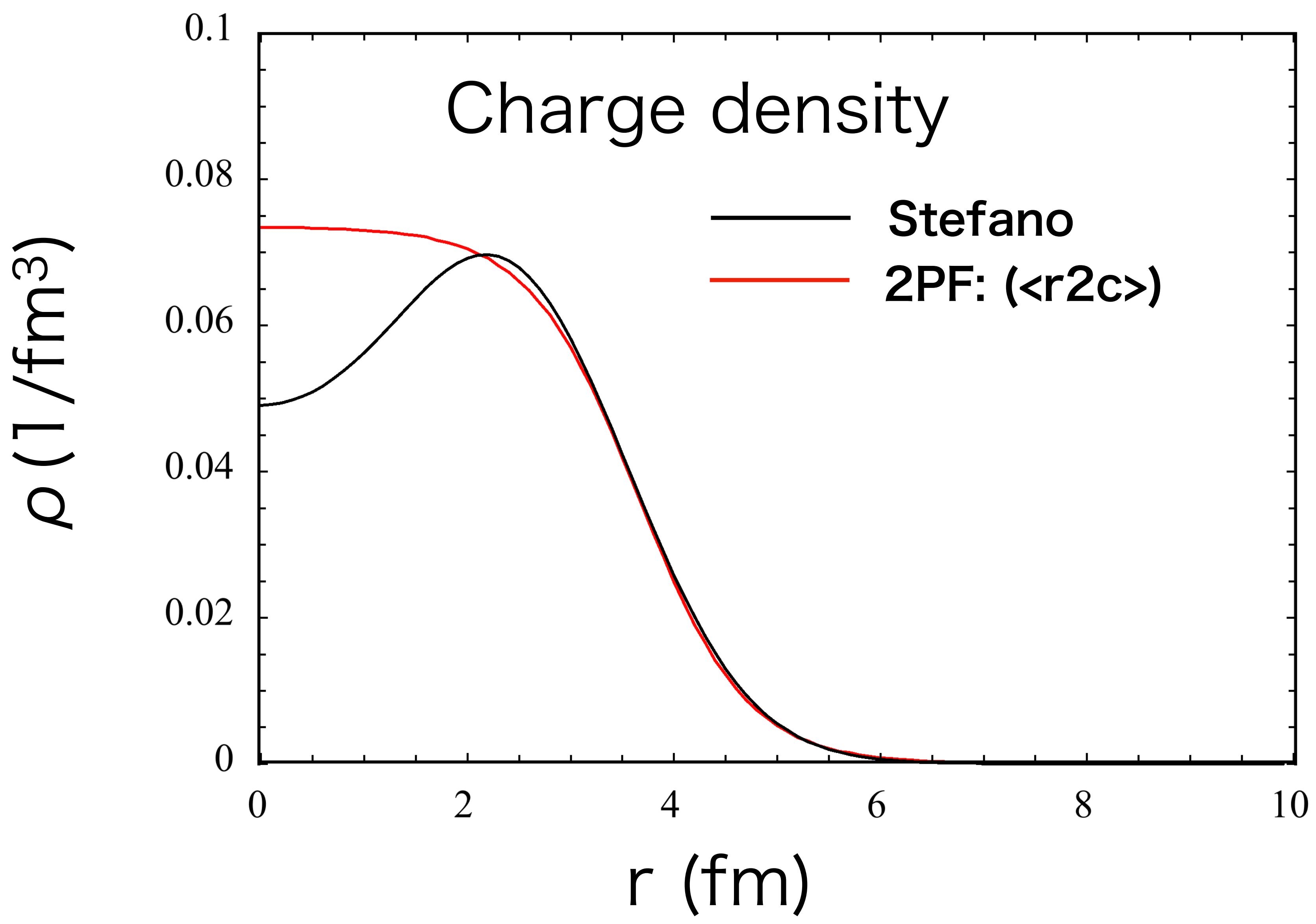

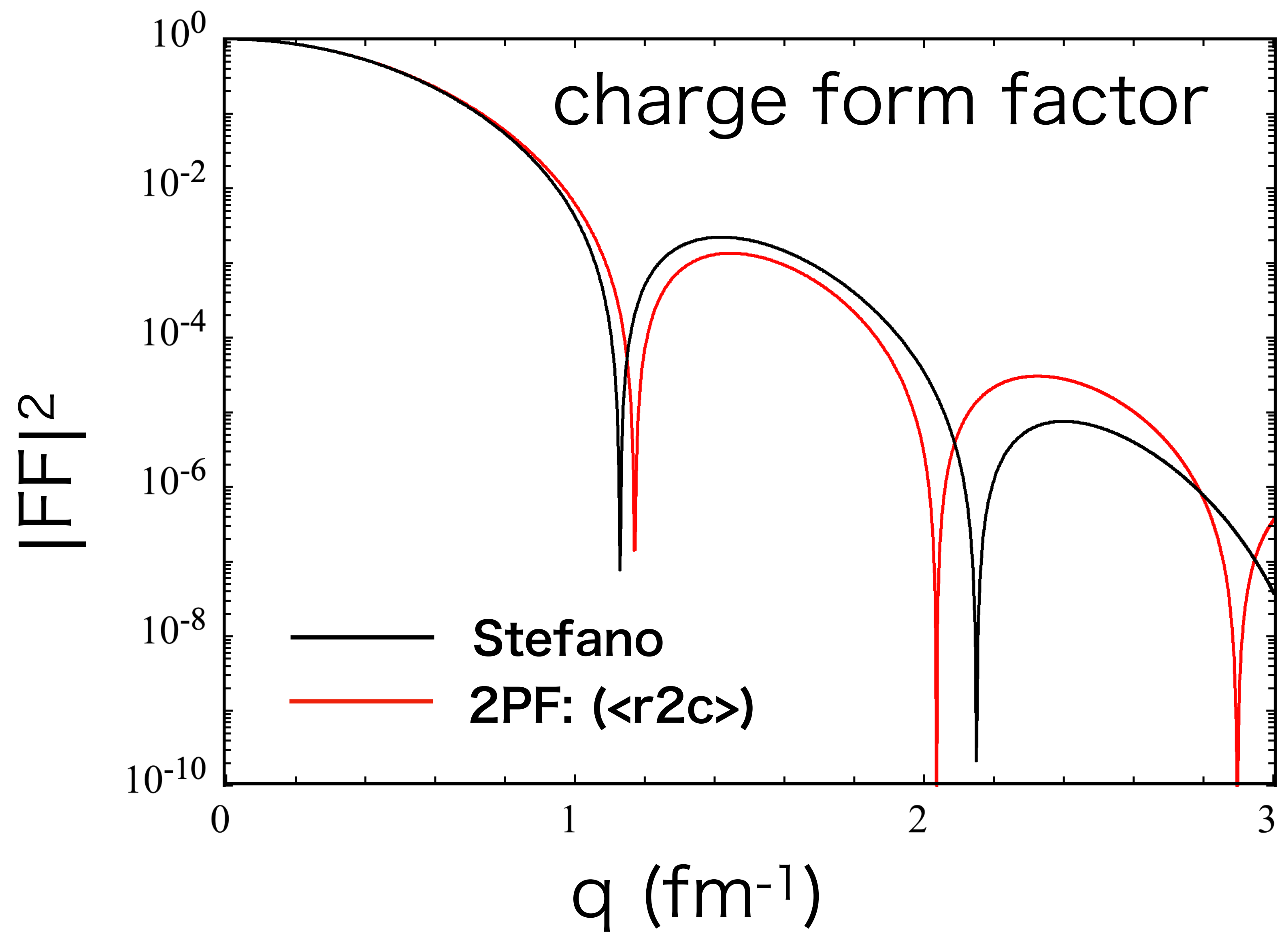

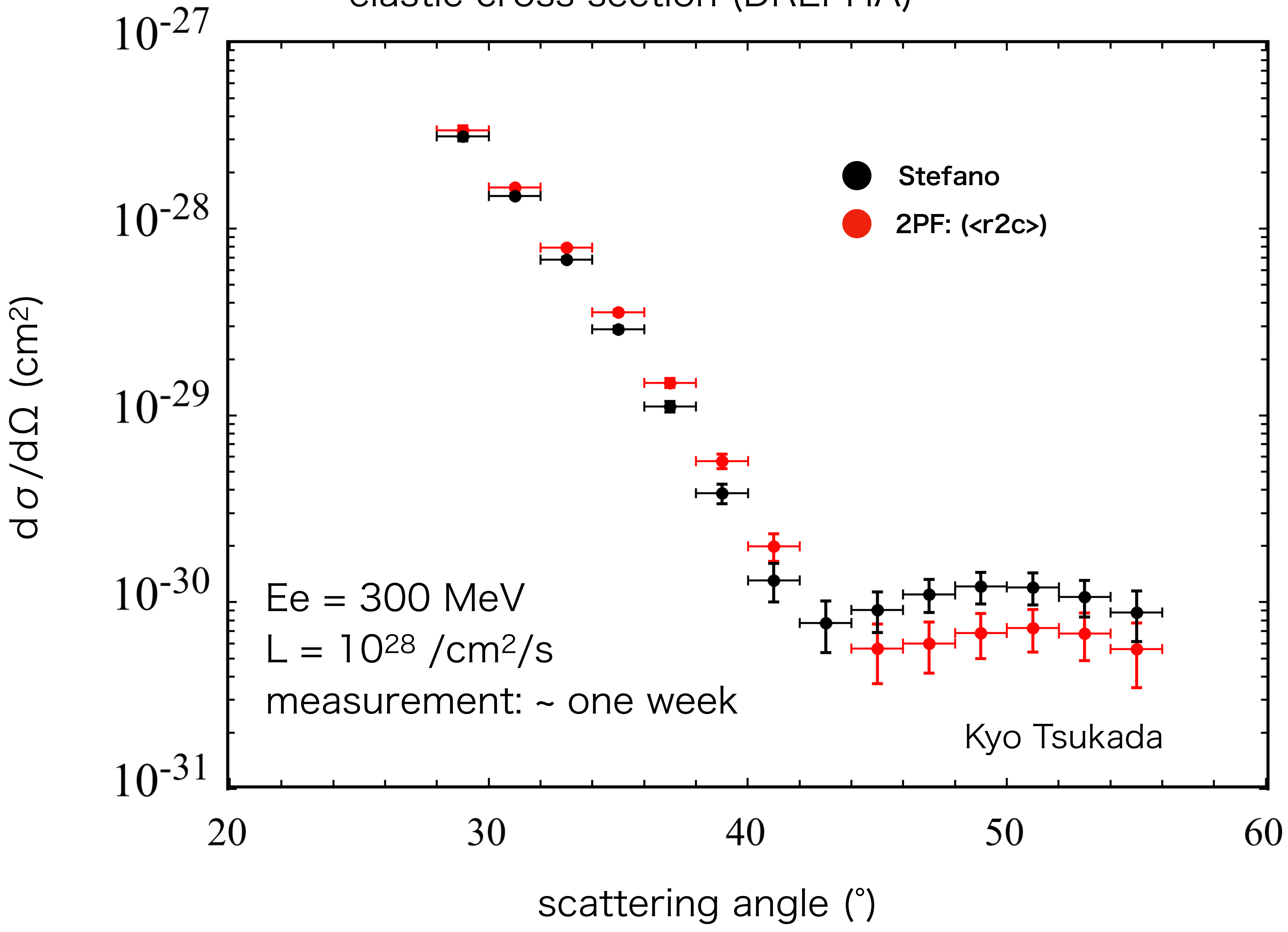

1) charge densities of exotic nuclei

systematic measurements for many unstable nuclei

^{132}Sn : symbolic target for “day-one” exp

^{46}Ar : Stefano Brolli

……

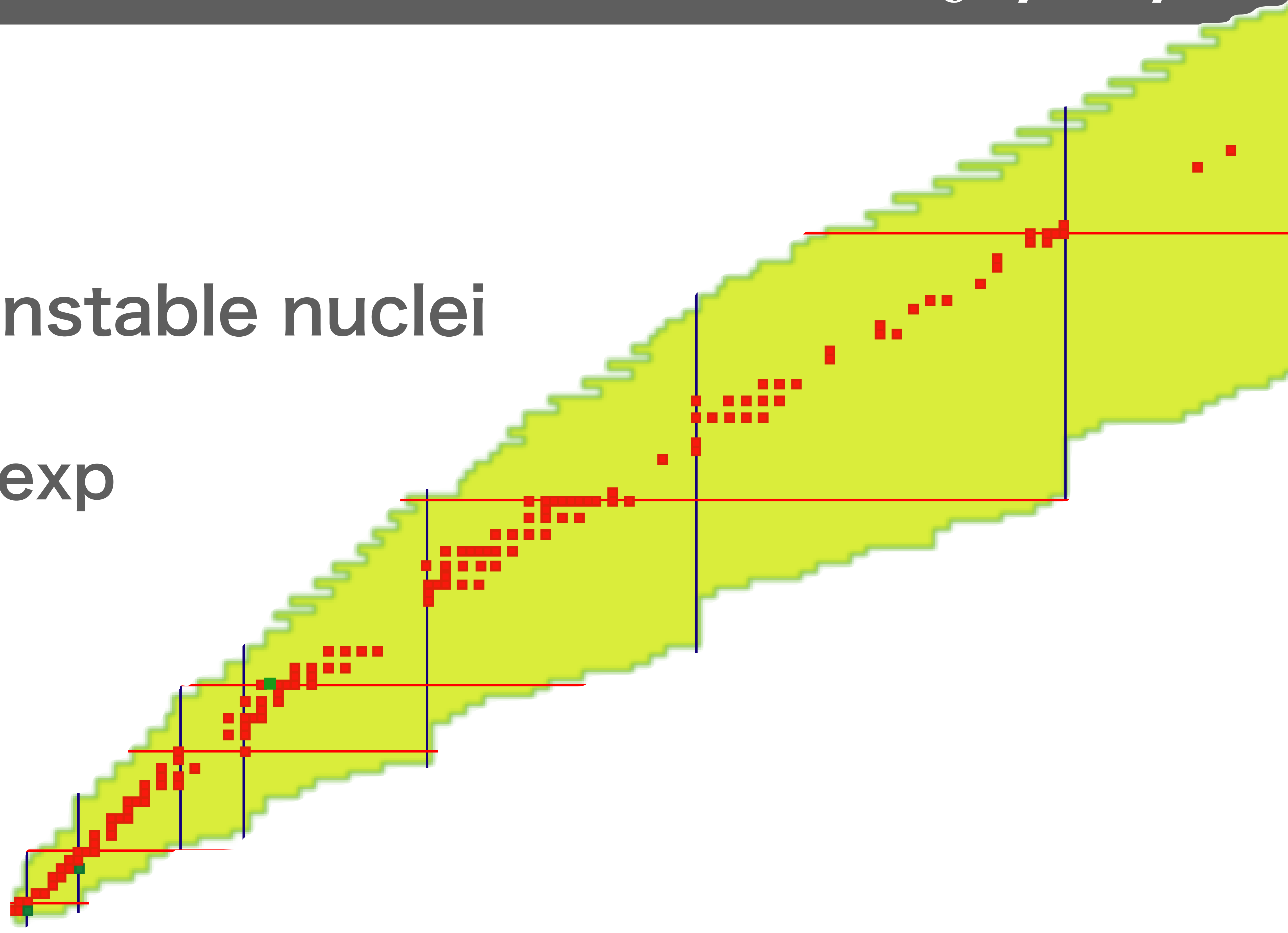

research possibilities of SCRIT for nuclear physics

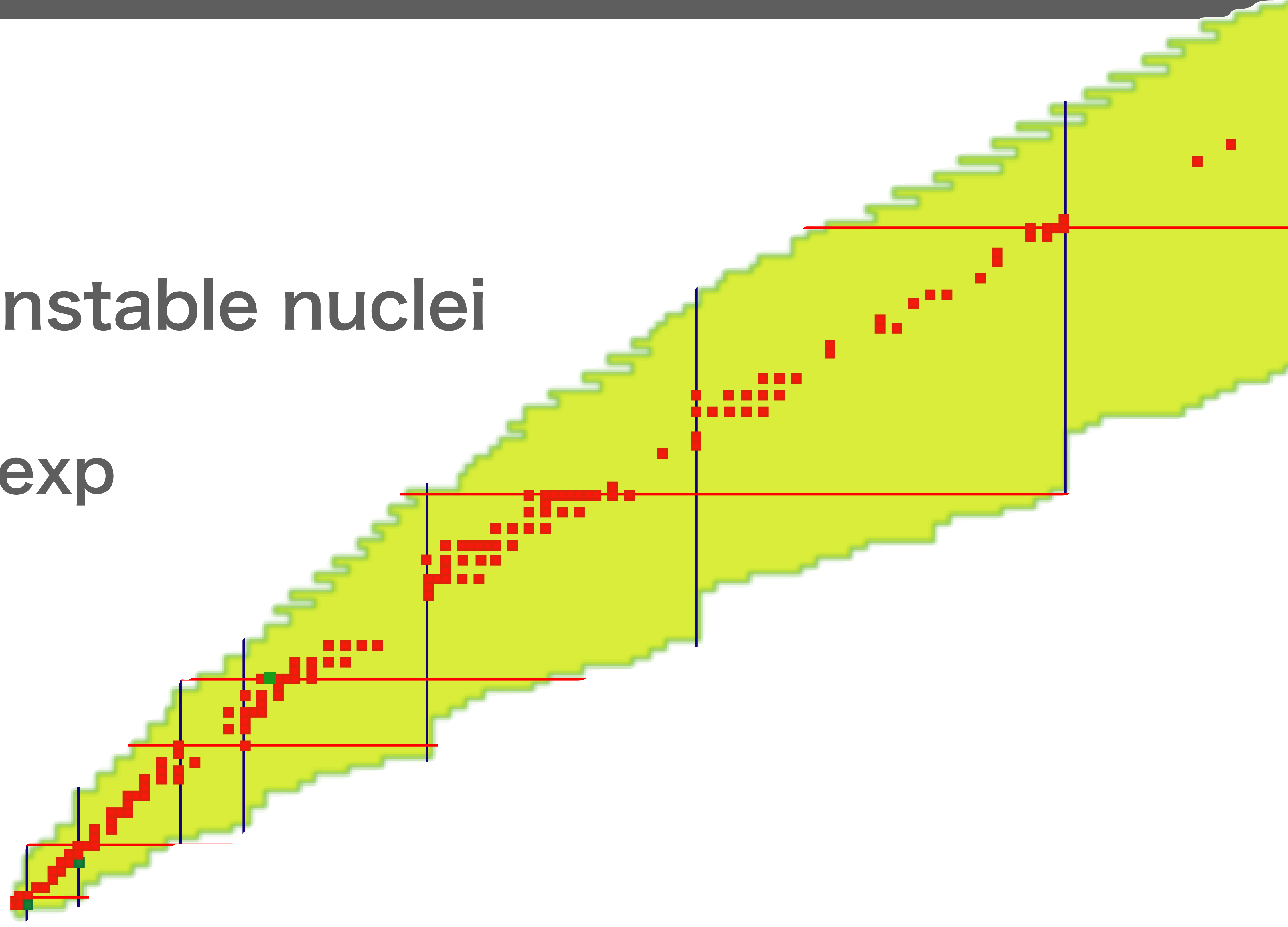

1) charge densities of exotic nuclei

systematic measurements for many unstable nuclei

^{132}Sn : symbolic target for “day-one” exp

^{46}Ar : Stefano Brolli

……

2) $<r_c^4>$ and neutron distribution

$$< r_c^4 > = \int r^4 \rho_c(r)\, \mathrm{d}^3 r$$

1) H. Kurasawa and T. Suzuki, Prog. Theor. Exp. Phys. 2019, 113D01
2) H. Kurasawa, T. S. and T. Suzuki, Prog. Theor. Exp. Phys. 2021, 013D02
3) H. Kurasawa and T. Suzuki, Prog. Theor. Exp. Phys. 2022, 023D03
4) T. Suzuki, Prog. Theor. Exp. Phys. 2023, 013D02
5) T. Suzuki et al., Front. Phys. 13 (2025) 1490337

nuclear charge density

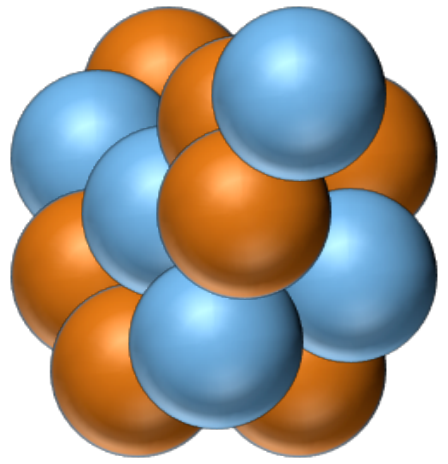

Proton

Neutron

nuclear charge density

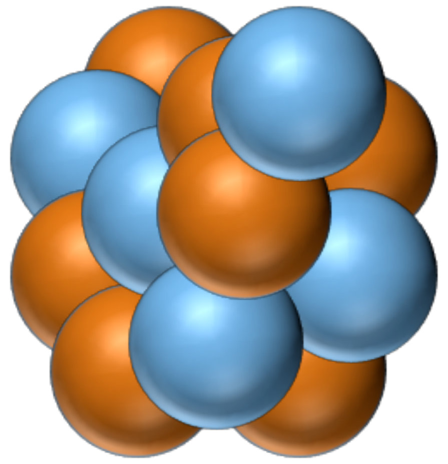

Proton

Neutron

$$\rho_c(r) = \rho_c^p(r) + \rho_c^n(r)$$

nuclear charge density

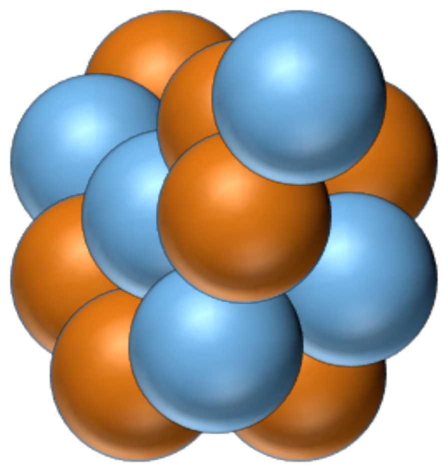

Proton

Neutron

$$\rho_c(r) = \rho_c^p(r) + \rho_c^n(r)$$

$$\rho_c^p(r) = \int \rho_p(r)\ \rho_{p(point)}(r - r')\ \mathrm{d}^3 r'$$

$$\rho_c^n(r) = \int \rho_n(r)\ \rho_{n(point)}(r - r')\ \mathrm{d}^3 r'$$

nuclear charge density

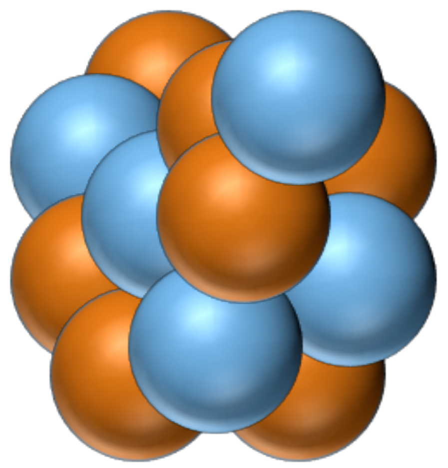

$$\rho_c(r) = \rho_c^p(r) + \rho_c^n(r)$$

$$\rho_c^p(r) = \int \rho_p(r)\ \rho_{p(point)}(r - r')\ \mathrm{d}^3 r'$$

$$\rho_c^n(r) = \int \rho_n(r)\ \rho_{n(point)}(r - r')\ \mathrm{d}^3 r'$$

^{208}Pb

(point) nucleon density

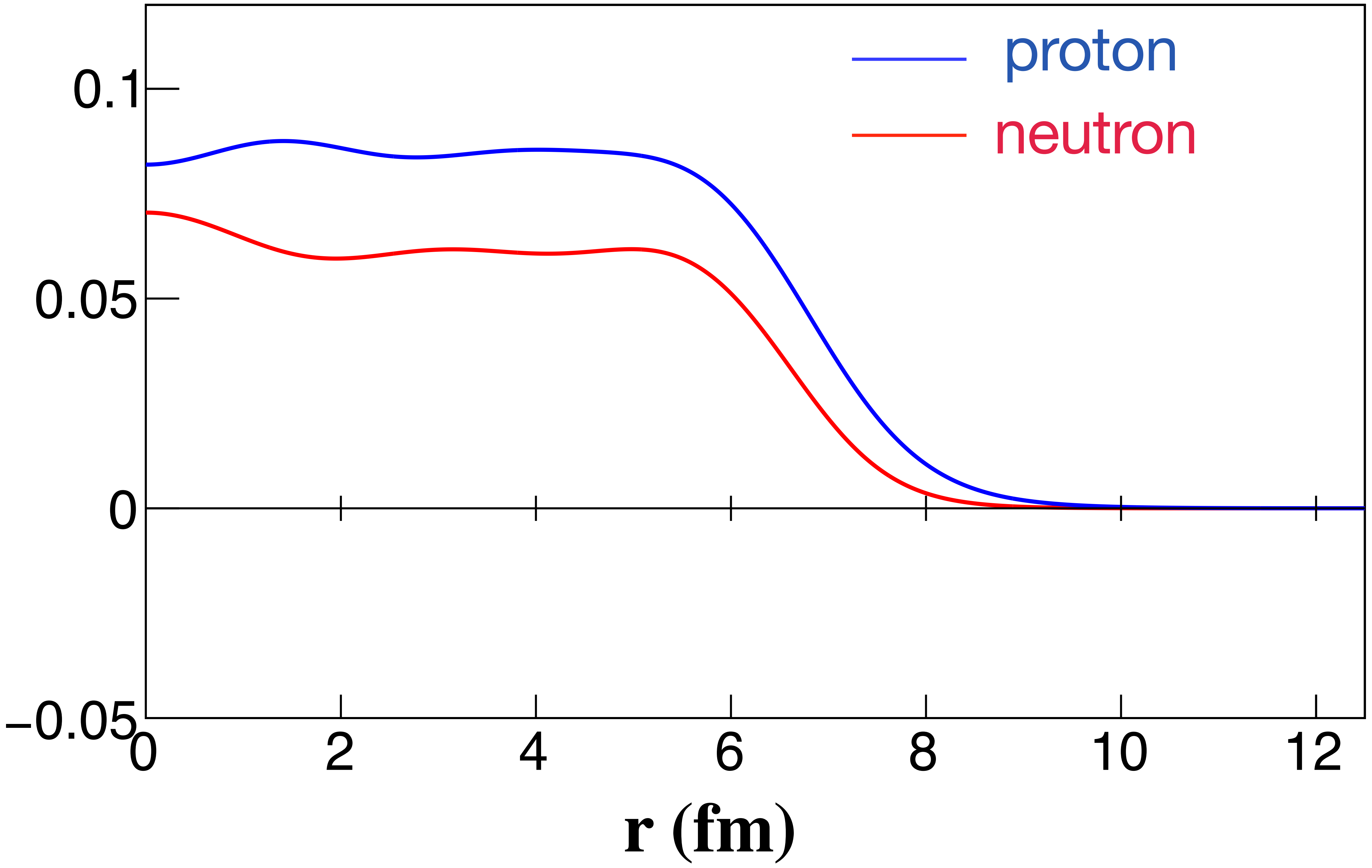

nuclear charge density

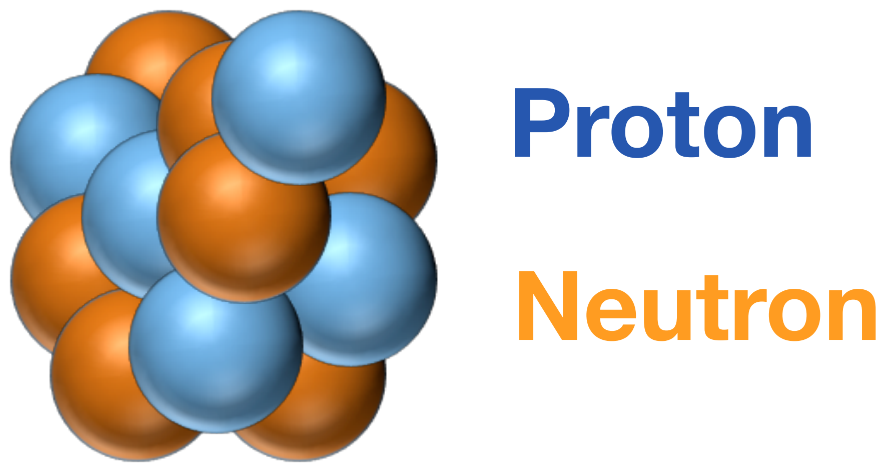

$$\rho_c(r) = \rho_c^p(r) + \rho_c^n(r)$$

$$\rho_c^p(r) = \int \rho_p(r)\, \rho_{p(point)}(r - r')\, \mathrm{d}^3 r'$$

$$\rho_c^n(r) = \int \rho_n(r)\, \rho_{n(point)}(r - r')\, \mathrm{d}^3 r'$$

^{208}Pb

RMF NL3
(H. Kurasawa)

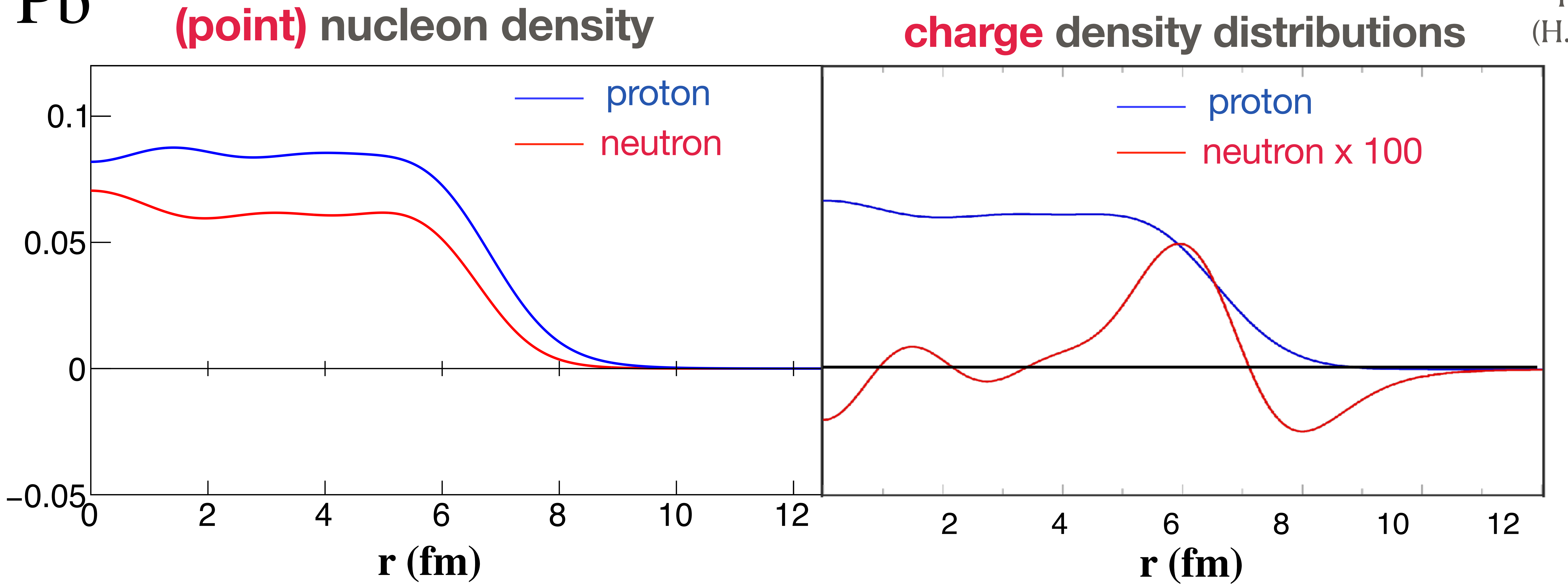

2nd moment of the charge density

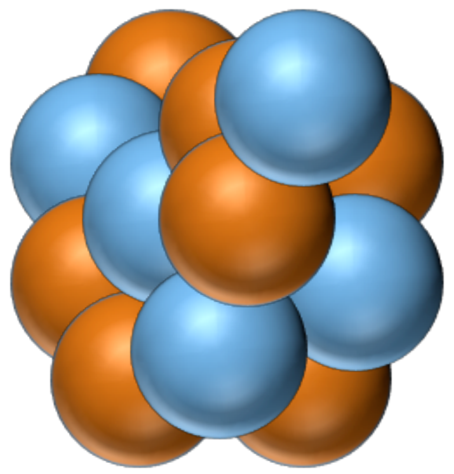

Proton

Neutron

2nd moment of the charge density

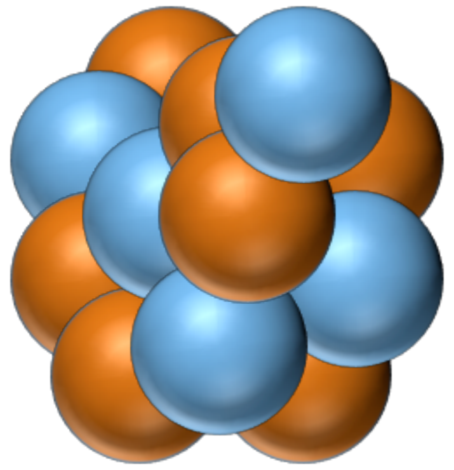

Proton

Neutron

$$< r_c^2 > = \int r^2 \, \rho_c(r) \, \mathrm{d}^3 r$$

2nd moment of the charge density

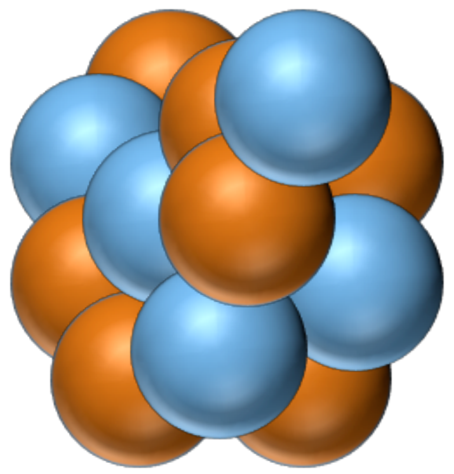

$$< r_c^2 > = \int r^2 \rho_c(r) \, \mathrm{d}^3 r$$

$$= < r^2_{p(point)} > + < r_p^2 > + < r^2_{n(point)} > + \frac{N}{Z} < r_n^2 > + \mathrm{rel.corr.}$$

2nd moment of the charge density

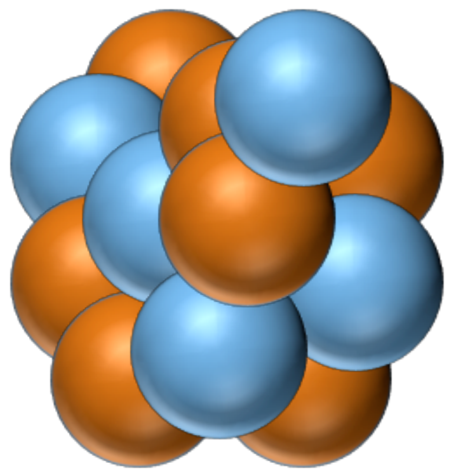

$$< r_c^2 > = \int r^2 \rho_c(r)\, \mathrm{d}^3 r$$

$e_n = 0$

$$= < r^2_{p(point)} > + < r_p^2 > + < r^2_{n(point)} > + \frac{N}{Z} < r_n^2 > + \mathrm{rel.corr.}$$

2nd moment of the charge density

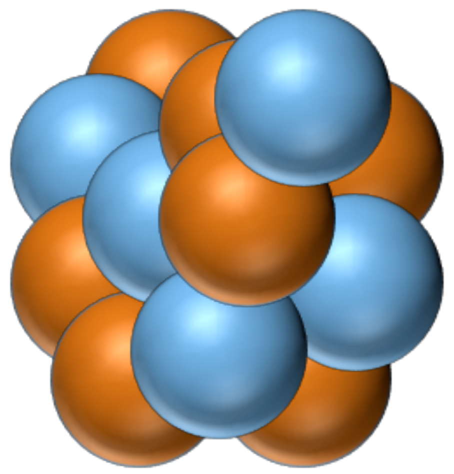

Proton

Neutron

$$< r_c^2 > = \int r^2 \rho_c(r)\, \mathrm{d}^3 r$$

Proton 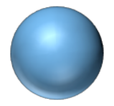

$e_n = 0$

Neutron 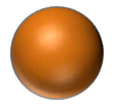

$$= < r^2_{p(point)} > + < r_p^2 > + < r^2_{n(point)} > + \frac{N}{Z} < r_n^2 > + \mathrm{rel.corr.}$$

2nd moment of the charge density

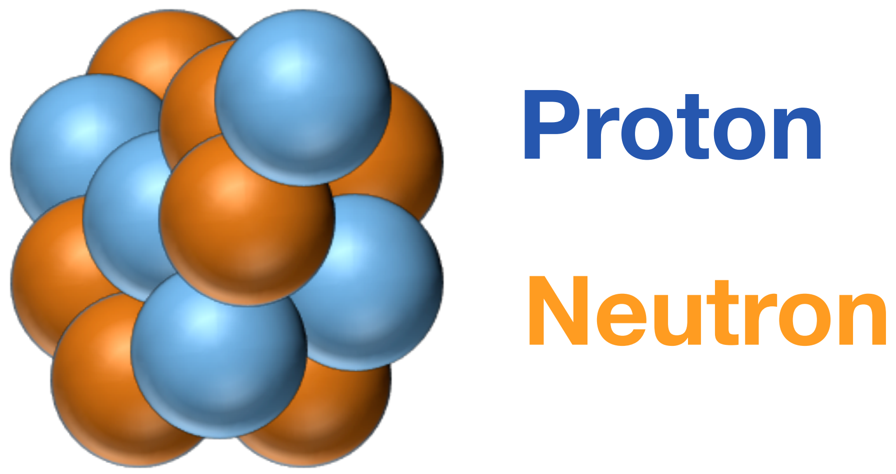

$$< r_c^2 > = \int r^2 \rho_c(r)\, d^3r$$

Proton

$e_n = 0$

Neutron

$$= < r^2_{p(point)} > + < r_p^2 > + \cancel{< r^2_{n(point)} >} + \frac{N}{Z} < r_n^2 > + \mathrm{rel.corr.}$$

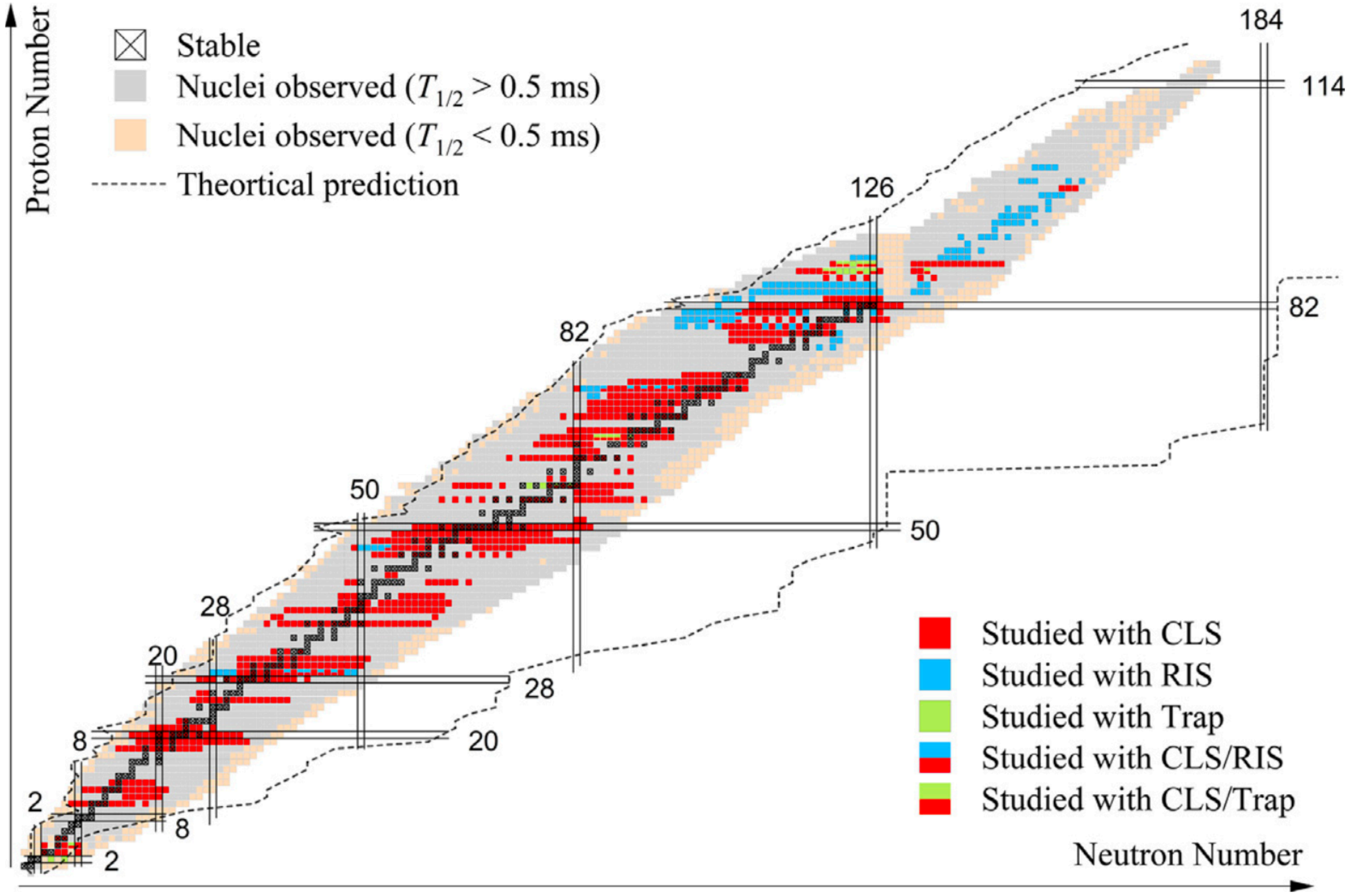

X. F. Yang et al.,PPNP **129, 104005 (2023)**

4th moment of the charge density

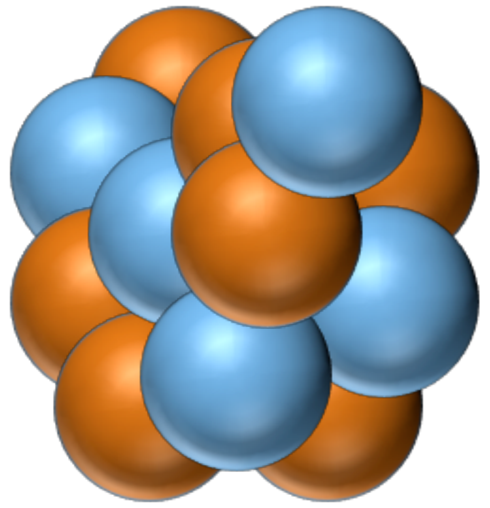

Proton

Neutron

4th moment of the charge density

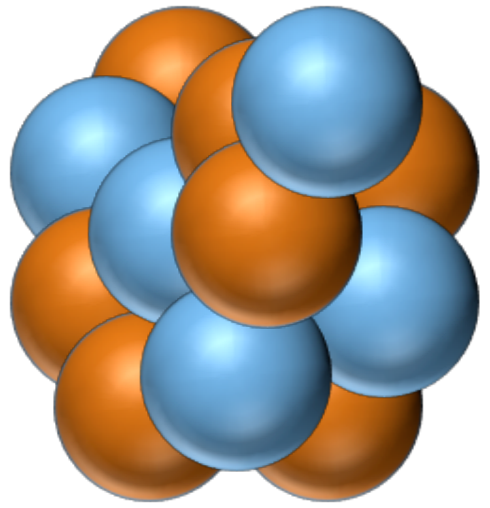

Proton

Neutron

$$< r_c^4 > = \int r^4 \rho_c(r) \, \mathrm{d}^3 r$$

4th moment of the charge density

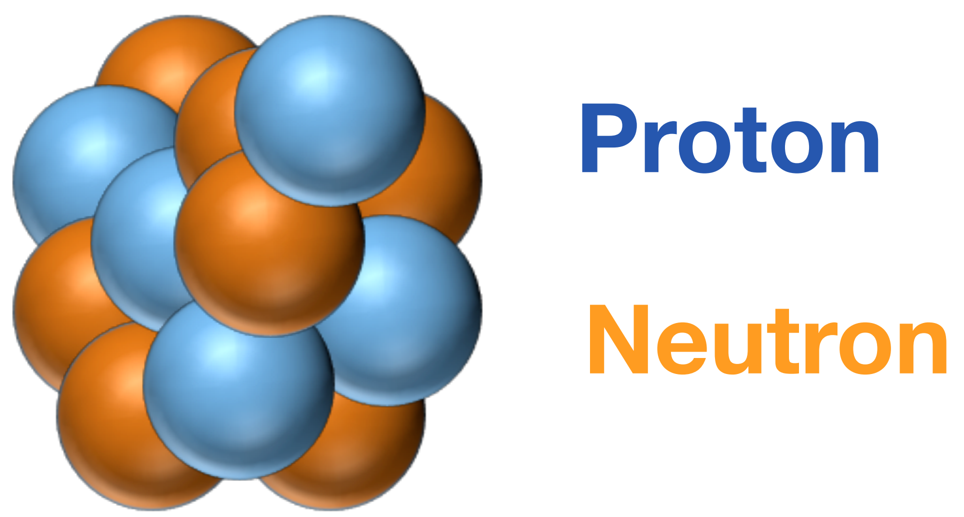

$$< r_c^4 > = \int r^4 \rho_c(r)\ \mathrm{d}^3 r$$
$$= < r^4_{p(point)} > + \frac{10}{3} < r^2_{p(point)} > < r_p^2 >$$
$$+ < r^4_{n(point)} > + \frac{10}{3} < r^2_{n(point)} > < r_n^2 > \frac{N}{Z} + \mathrm{rel.corr.}$$

H. Kurasawa, T. S. and T. Suzuki, Prog. Theor. Exp. Phys. 2021, 013D02

4th moment of the charge density

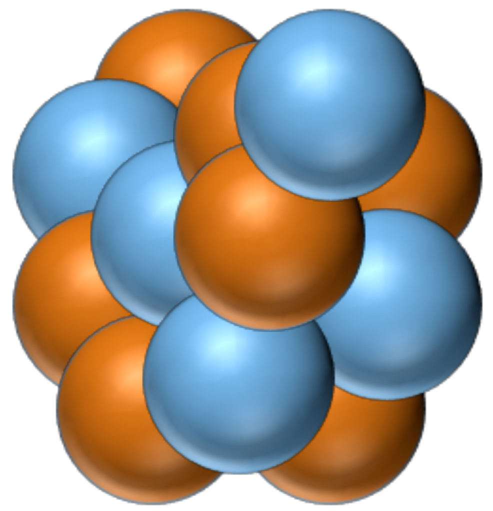

$$< r_c^4 > = \int r^4 \rho_c(r)\, \mathrm{d}^3 r$$

$$= < r^4_{p(point)} > + \frac{10}{3} < r^2_{p(point)} > < r_p^2 >$$

$$+ < r^4_{n(point)} > + \frac{10}{3} < r^2_{n(point)} > < r_n^2 > \frac{N}{Z} + \mathrm{rel.corr.}$$

H. Kurasawa, T. S. and T. Suzuki,
Prog. Theor. Exp. Phys. 2021, 013D02

4th moment of the charge density

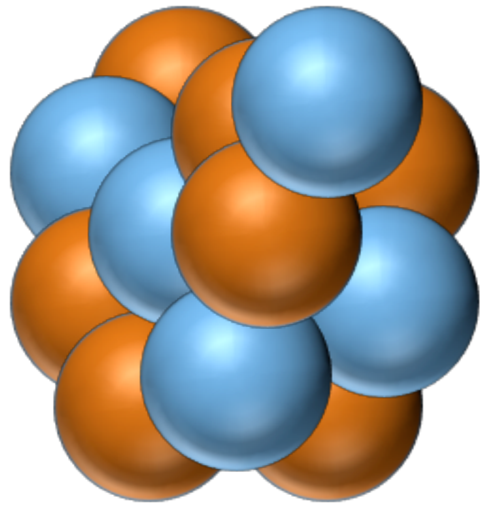

H. Kurasawa, T. S. and T. Suzuki, Prog. Theor. Exp. Phys. 2021, 013D02

$$< r_c^4 > = \int r^4 \rho_c(r)\, \mathrm{d}^3 r$$

$$= < r^4_{p(point)} > + \frac{10}{3} < r^2_{p(point)} > < r_p^2 >$$

$e_n = 0$

$$+ \cancel{< r^4_{n(point)} >} + \frac{10}{3} < r^2_{n(point)} > < r_n^2 > \frac{N}{Z} + \mathrm{rel.\,corr.}$$

4th moment of the charge density

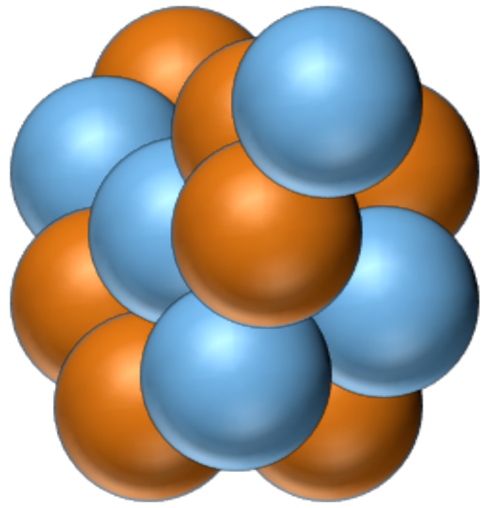

Proton

Neutron

$$< r_c^4 > = \int r^4 \rho_c(r)\, \mathrm{d}^3 r$$

$$= < r^4_{p(point)} > + \frac{10}{3} < r^2_{p(point)} > < r_p^2 >$$

$e_n = 0$

$$+ < r^4_{n(point)} > + \frac{10}{3} < r^2_{n(point)} > < r_n^2 > \frac{N}{Z} + \mathrm{rel.corr.}$$

RMS n-radius

H. Kurasawa, T. S. and T. Suzuki, Prog. Theor. Exp. Phys. 2021, 013D02

4th moment of the charge density

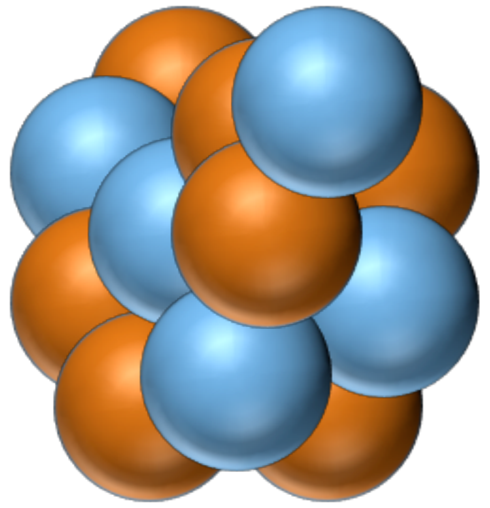

Proton

Neutron

$$< r_c^4 > = \int r^4 \rho_c(r)\, \mathrm{d}^3 r$$

$$= < r^4_{p(point)} > + \frac{10}{3} < r^2_{p(point)} > < r_p^2 >$$

$e_n = 0$

$$+ < r^4_{n(point)} > + \frac{10}{3} < r^2_{n(point)} > < r_n^2 > \frac{N}{Z} + \mathrm{rel.\ corr.}$$

RMS n-radius

H. Kurasawa, T. S. and T. Suzuki,
Prog. Theor. Exp. Phys. 2021, 013D02

$$< r_c^4 > = Q_{cp}^4 - Q_{cn}^4$$

4th moment of the charge density

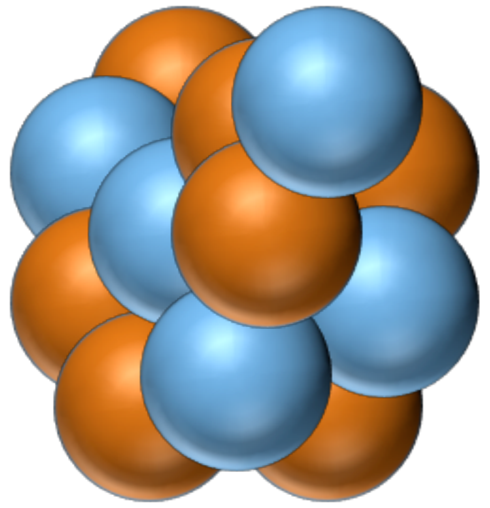

Proton

Neutron

$$< r_c^4 > = \int r^4 \rho_c(r)\, d^3r$$

$$= < r^4_{p(point)} > + \frac{10}{3} < r^2_{p(point)} > < r_p^2 >$$

$e_n = 0$

$$+ < r^4_{n(point)} > + \frac{10}{3} < r^2_{n(point)} > < r_n^2 > \frac{N}{Z} + \mathrm{rel.corr.}$$

RMS n-radius

H. Kurasawa, T. S. and T. Suzuki,
Prog. Theor. Exp. Phys. 2021, 013D02

$$< r_c^4 > = Q^4_{cp} - Q^4_{cn}$$

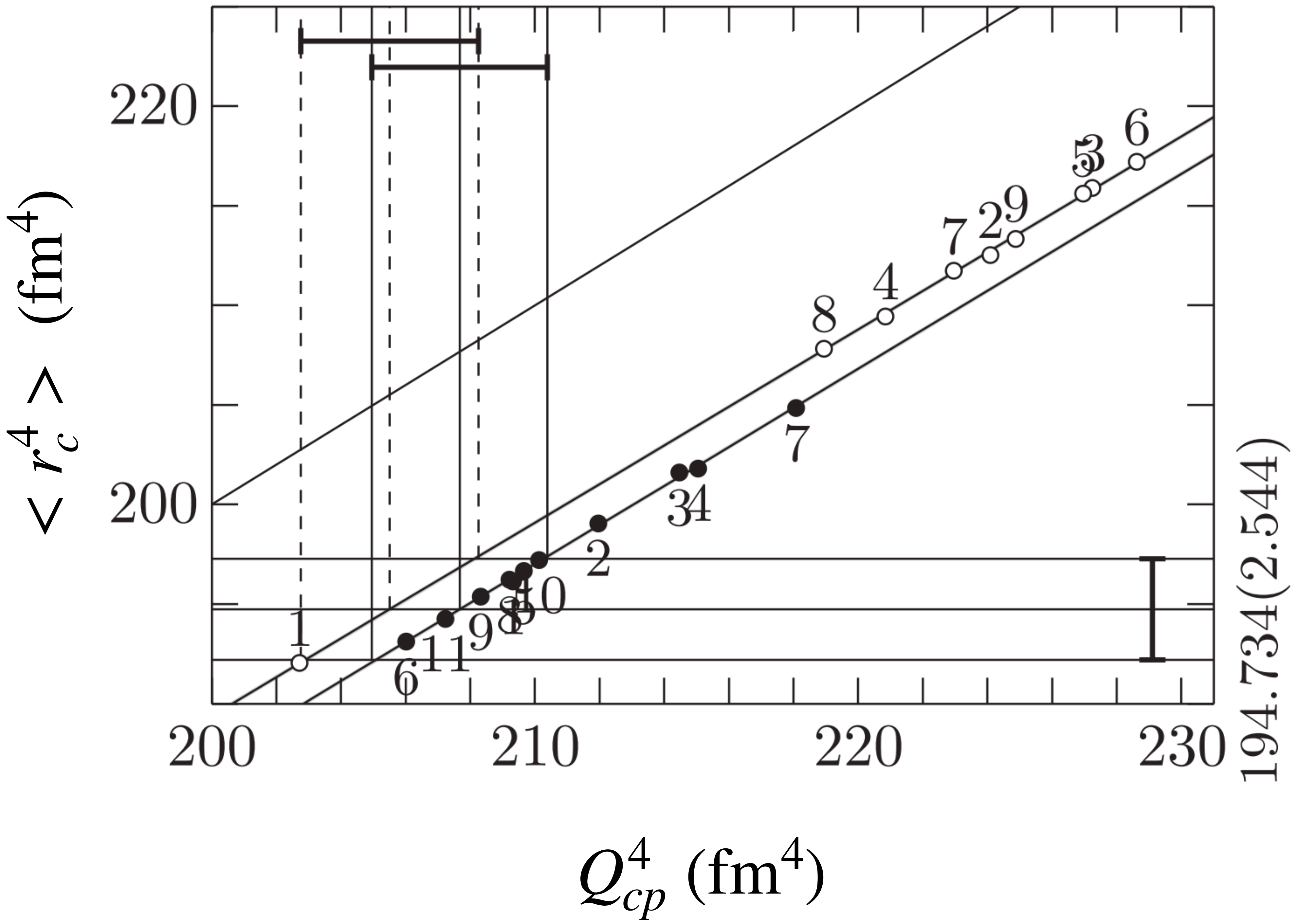

non-rel. MF (SK1, SKIII, SLy4,,,,)

rel. MF (NL2, NL3, NL-SH, FSUGold,,,,)

4th moment of the charge density

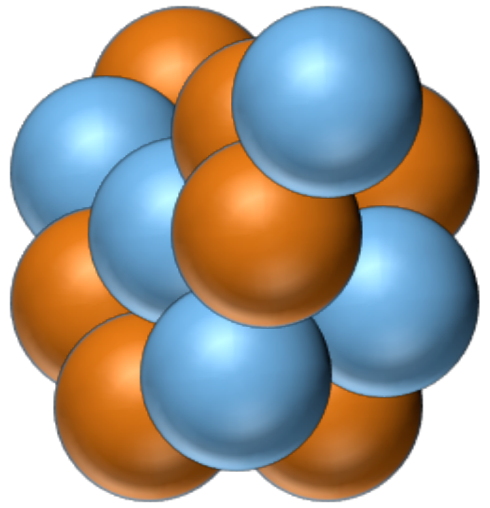

Proton

Neutron

$$< r_c^4 > = \int r^4 \rho_c(r)\, d^3 r$$

$$= < r^4_{p(point)} > + \frac{10}{3} < r^2_{p(point)} > < r_p^2 >$$

$e_n = 0$

$$+ < r^4_{n(point)} > + \frac{10}{3} < r^2_{n(point)} > < r_n^2 > \frac{N}{Z} + \text{rel. corr.}$$

RMS n-radius

H. Kurasawa, T. S. and T. Suzuki, Prog. Theor. Exp. Phys. 2021, 013D02

$$< r_c^4 > = Q^4_{cp} - Q^4_{cn}$$

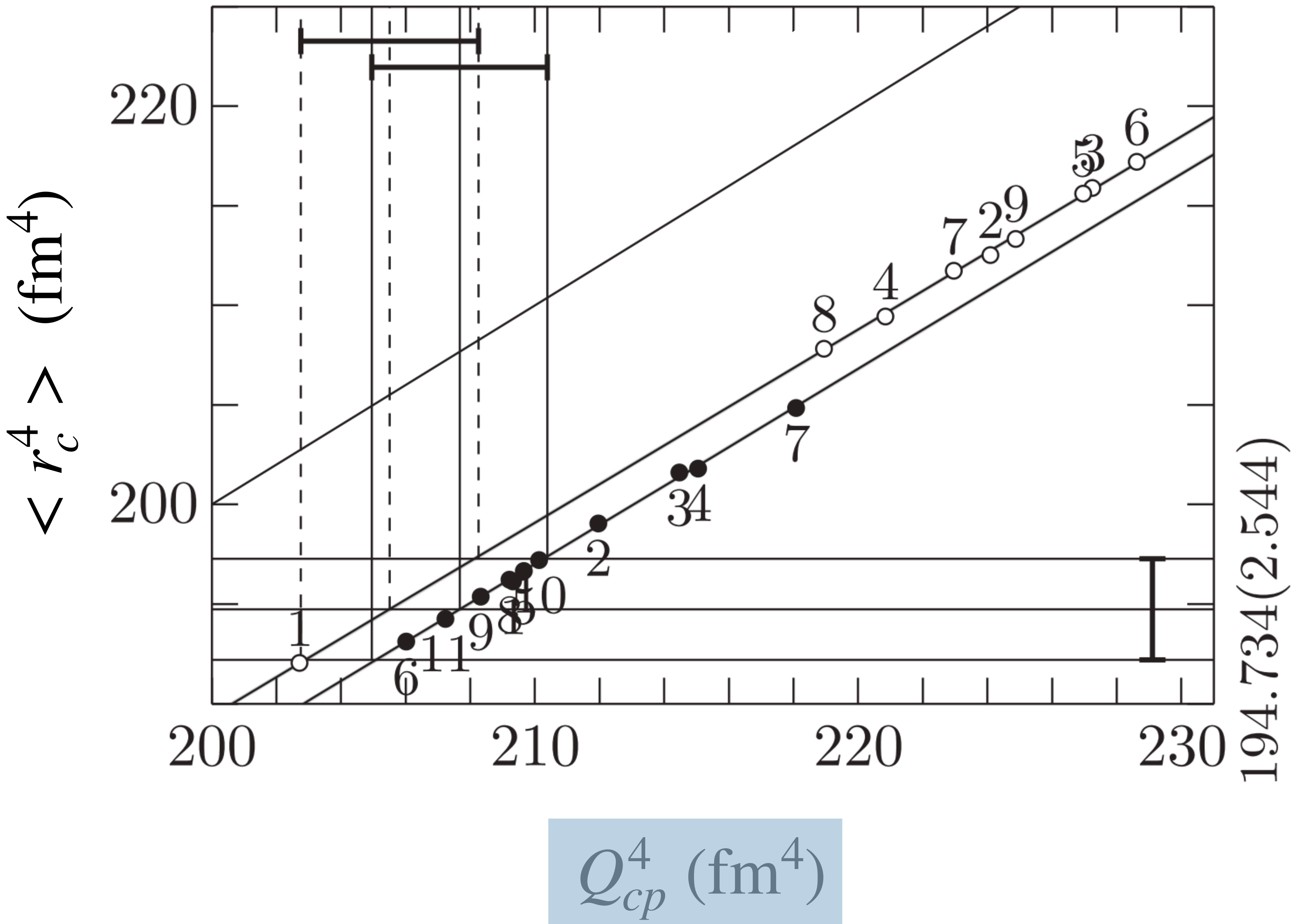

○ non-rel. MF (SK1, SKIII, SLy4,,,,)

● rel. MF (NL2, NL3, NL-SH, FSUGold,,,,)

4th moment of the charge density

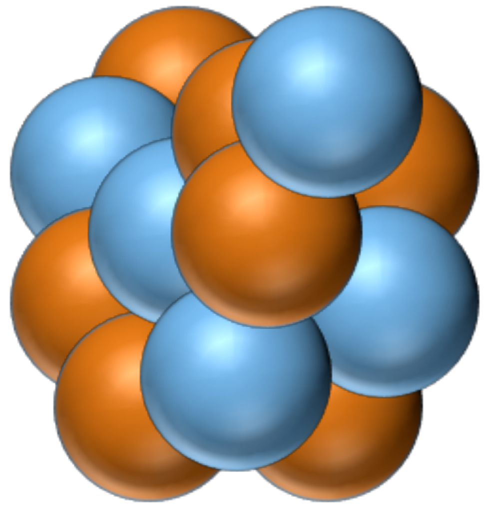

Proton

Neutron

$$< r_c^4 > = \int r^4 \rho_c(r)\, d^3r$$

$$= < r^4_{p(point)} > + \frac{10}{3} < r^2_{p(point)} > < r_p^2 >$$

$e_n = 0$

$$+ < r^4_{n(point)} > + \frac{10}{3} < r^2_{n(point)} > < r_n^2 > \frac{N}{Z} + \mathrm{rel.\,corr.}$$

RMS n-radius

H. Kurasawa, T. S. and T. Suzuki, Prog. Theor. Exp. Phys. 2021, 013D02

$$< r_c^4 > = Q^4_{cp} - Q^4_{cn}$$

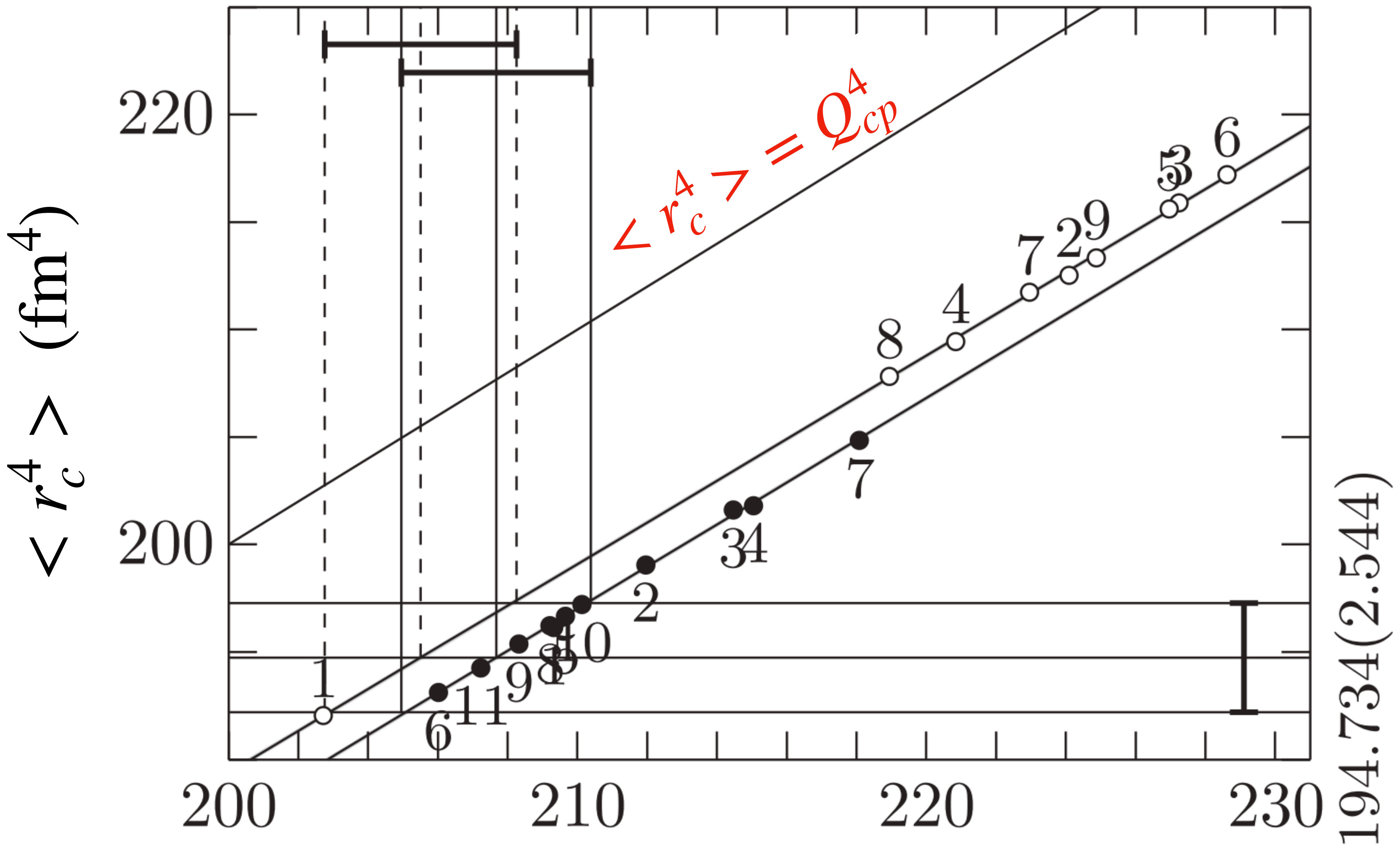

○ non-rel. MF (SK1, SKIII, SLy4,,,,)

● rel. MF (NL2, NL3, NL-SH, FSUGold,,,,)

4th moment of the charge density

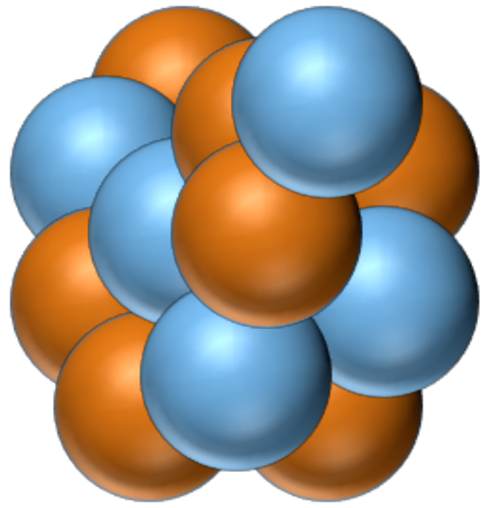

$$< r_c^4 > = \int r^4 \rho_c(r)\, d^3 r$$

$$= < r^4_{p(point)} > + \frac{10}{3} < r^2_{p(point)} > < r_p^2 >$$

$e_n = 0$

$$+ < r^4_{n(point)} > + \frac{10}{3} < r^2_{n(point)} > < r_n^2 > \frac{N}{Z} + \mathrm{rel.\ corr.}$$

RMS n-radius

H. Kurasawa, T. S. and T. Suzuki,
Prog. Theor. Exp. Phys. 2021, 013D02

$$< r_c^4 > = Q_{cp}^4 - Q_{cn}^4$$

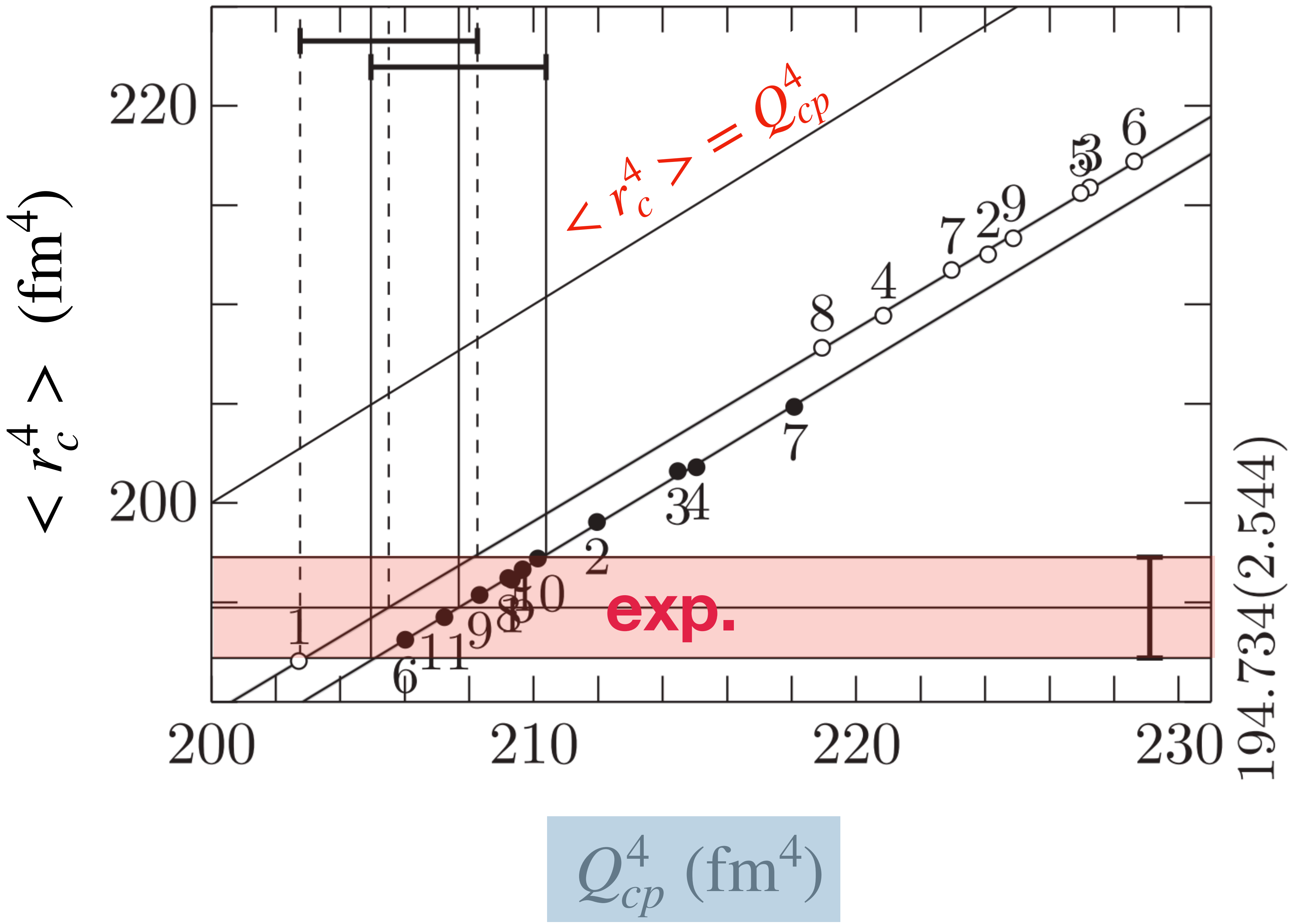

○ non-rel. MF (SK1, SKIII, SLy4,,,,)

● rel. MF (NL2, NL3, NL-SH, FSUGold,,,,)

4th moment of the charge density

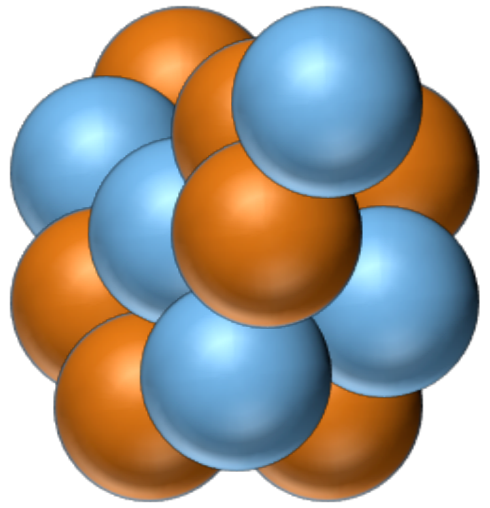

Proton

Neutron

$$< r_c^4 > = \int r^4 \rho_c(r)\, d^3 r$$

$$= < r^4_{p(point)} > + \frac{10}{3} < r^2_{p(point)} > < r_p^2 >$$

$e_n = 0$

$$+ < r^4_{n(point)} > + \frac{10}{3} < r^2_{n(point)} > < r_n^2 > \frac{N}{Z} + \text{rel. corr.}$$

RMS n-radius

H. Kurasawa, T. S. and T. Suzuki,
Prog. Theor. Exp. Phys. 2021, 013D02

$$< r_c^4 > = Q^4_{cp} - Q^4_{cn}$$

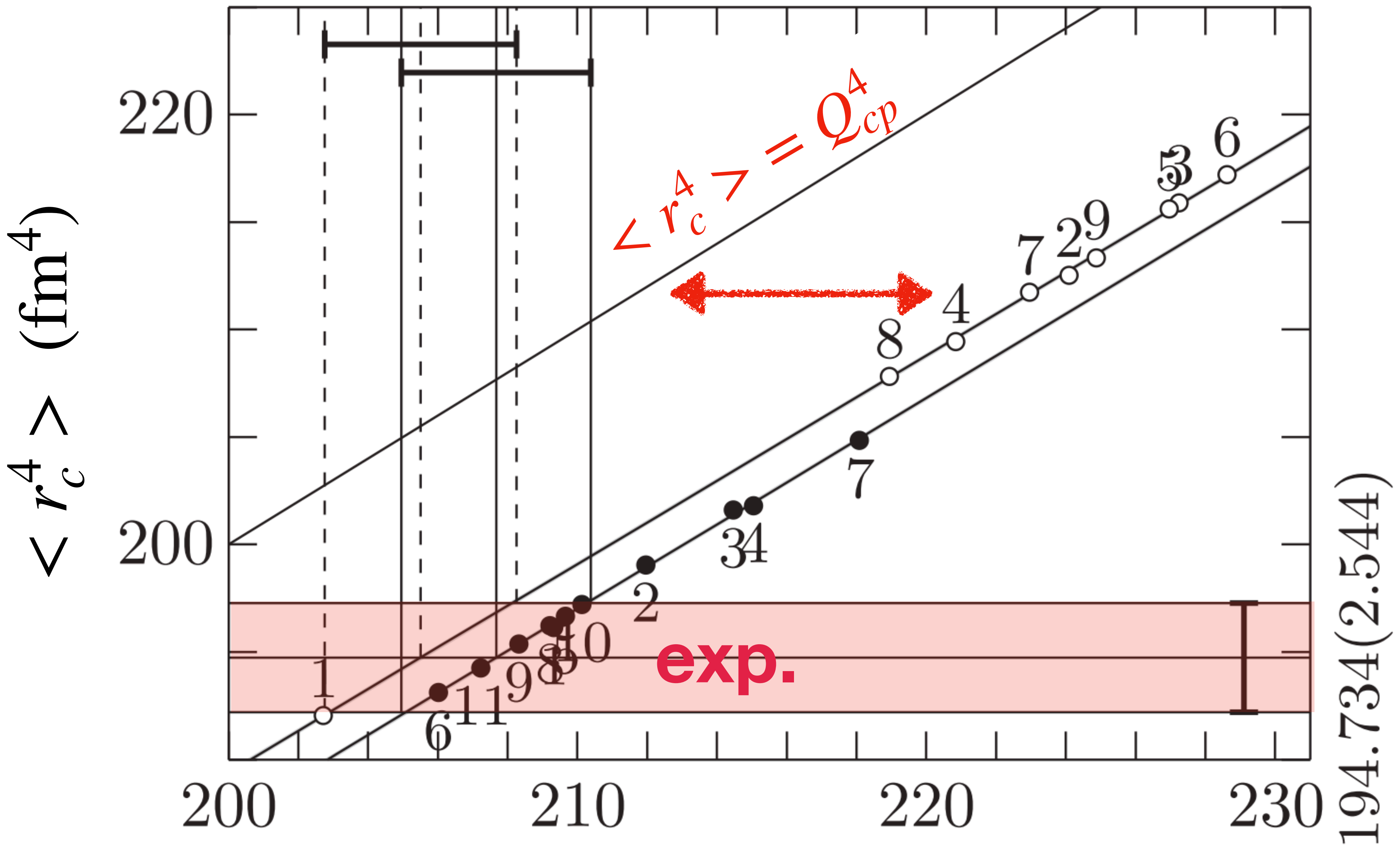

neutron contribution (~ 6%)

○ non-rel. MF (SK1, SKIII, SLy4,,,,)

● rel. MF (NL2, NL3, NL-SH, FSUGold,,,,)

Many relativistic MF models for ^{208}Pb

There are more than 100 phenomenological models

+ relativistic models

1 L2, 2 NLB, 3 NL1, 4 NL2, 5 NL3,
6 NL-SH, 7 NL-Z, 8 NL-C, 9 NL3II,
10FSUGold・・・・・・・・・・・・・・・・・.

**All based on
mean field approximation
accumulated for 50 years !**

**Each model has each aim with
different parameters .**

***It is not the best way
to choose
a few models among them.***

STONE, MILLER, KONCEWICZ, STEVENSON, AND STRAYER PHYSICAL REVIEW C 68, 034324 (2003)

TABLE I. Properties of symmetric nuclear matter at nuclear saturation density n_0 (fm^{-3}) as predicted by different types of Skyrme interaction: Fermi momentum k_F (fm^{-1}), mean distance between adjacent nucleons $r_0=(9\pi)^{1/3}/2k_F$ (fm), total binding energy per particle $\mathcal{E}$ (MeV), incompressibility modulus K_∞ (MeV), asymmetry coefficient a_s (MeV), speed of sound v_s/c, and the isoscalar effective mass $m_{eff}=m_s^*/m$.

Skyrme	n_0	k_F	r_0	$\mathcal{E}$	a_s	K_∞	v_s	m_{eff}	Skyrme	n_0	k_F	r_0	$\mathcal{E}$	a_s	K_∞	v_s	m_{eff}
SI	0.156	1.320	1.154	−15.99	29.25	372.1	0.212	0.91	SLy0	0.160	1.334	1.142	−15.97	32.03	230.7	0.167	0.70
SII	0.148	1.300	1.172	−15.96	34.15	341.6	0.203	0.58	SLy1	0.161	1.334	1.141	−15.98	32.04	230.8	0.167	0.70
SkT	0.148	1.298	1.174	−15.40	24.90	334.0	0.200	0.60	SLy2	0.161	1.335	1.141	−15.99	32.05	230.9	0.167	0.70
SIII	0.145	1.291	1.180	−15.85	28.17	355.9	0.207	0.76	SLy3	0.161	1.335	1.141	−15.97	32.03	230.9	0.167	0.70
SIV	0.151	1.308	1.165	−15.96	31.24	325.4	0.198	0.47	SLy4	0.160	1.332	1.143	−15.97	32.04	230.9	0.167	0.69
SV	0.155	1.320	1.154	−16.05	32.86	306.8	0.192	0.38	SLy5	0.161	1.335	1.141	−15.98	32.05	230.9	0.167	0.70
SVI	0.144	1.286	1.185	−15.75	26.89	364.0	0.209	0.95	SLy6	0.159	1.331	1.145	−15.92	32.00	230.8	0.167	0.69
SVII	0.143	1.285	1.185	−15.79	26.96	366.9	0.210	1.00	SLy7	0.159	1.329	1.146	−15.90	32.03	230.6	0.167	0.69
SIII*	0.151	1.307	1.165	−16.57	32.67	372.9	0.212	0.79	SLy8	0.161	1.334	1.141	[illegible]	32.04	230.9	0.167	0.70
SkM	0.160	1.334	1.142	−15.77	30.77	217.5	0.162	0.79	SLy9	0.151	1.308	1.164	−15.79	32.02	230.3	0.166	0.67
SGI	0.155	1.318	1.156	−15.89	28.35	262.6	0.178	0.61	SLy10	0.156	1.321	1.153	−15.90	32.02	230.4	0.167	0.68
SGII	0.159	1.329	1.146	−15.59	26.85	215.4	0.161	0.79	SkM1	0.160	1.334	[illegible]	−15.77	25.19	217.5	0.162	0.79
SkM*	0.160	1.334	1.142	−15.77	30.06	217.5	0.162	0.79	Skyrme1′	0.156	1.320	1.154	−15.99	29.37	372.1	0.211	0.91
RATP	0.160	1.333	1.143	−16.05	29.28	240.6	0.170	0.67	SkI6	0.159	1.331	[illegible]	−15.92	30.13	249.7	0.173	0.64
SkT1	0.161	1.336	1.140	−15.98	32.05	237.2	0.169	1.00	SkXce	0.155	[illegible]	1.154	−15.86	30.16	269.1	0.180	1.01
SkT2	0.161	1.336	1.140	−15.94	32.03	236.8	0.169	1.00	SkXm	0.159	[illegible]	1.145	−16.04	31.22	239.1	0.170	0.97
SkT3	0.161	1.336	1.140	−15.94	31.53	236.8	0.169	1.00	SkX	0.156	1.321	1.153	−16.05	31.11	272.0	0.181	0.99
SkT4	0.159	1.331	1.145	−15.95	35.49	236.5	0.169	1.00	MSk1	[illegible]	1.326	1.148	−15.83	30.02	234.6	0.168	1.00
SkT5	0.164	1.345	1.133	−16.00	37.05	202.7	0.156	1.00	MSk2	0.158	1.326	1.148	−15.83	30.02	232.5	0.167	1.05
SkT6	0.161	1.336	1.140	−15.96	29.99	237.0	0.169	1.00	MSk3	0.158	1.327	1.148	−15.82	28.00	234.4	0.168	1.00
SkT7	0.161	1.335	1.141	−15.94	29.54	236.7	0.169	0.83	MSk4	0.158	1.326	1.148	−15.79	28.01	232.0	0.167	1.05
SkT8	0.161	1.335	1.141	−15.94	29.95	236.8	0.169	0.83	MSk5	0.158	1.326	1.148	−15.79	28.01	232.0	0.167	1.05
SkT9	0.161	1.334	1.142	−15.88	29.78	235.9	0.169	0.83	MSk5*	0.156	1.322	1.152	−15.78	28.01	244.6	0.172	0.80
SkP	0.163	1.341	1.136	−15.95	30.02	201.9	0.156	1.00	MSk6	0.158	1.326	1.148	−15.79	28.01	232.0	0.167	1.05
E	0.159	1.331	1.144	−16.12	27.65	335.3	0.201	0.87	MSk7	0.158	1.326	1.148	−15.79	27.96	232.1	0.167	1.05
Es	0.163	1.341	1.136	−16.02	26.44	249.9	0.173	0.84	SKRA	0.160	1.332	1.144	−15.78	31.35	217.9	0.162	0.75
Z	0.159	1.331	1.145	−15.97	26.81	332.1	[illegible]	0.84	SkO	0.161	1.335	1.141	−15.83	32.01	224.3	0.164	0.90
Zs	0.163	1.342	1.135	−15.88	26.70	234.5	[illegible]	0.78	SkO′	0.160	1.334	1.142	−15.75	31.98	223.3	0.164	0.90
Zs*	0.163	1.340	1.136	−15.96	28.82	236.0	0.169	0.77	SLy230a	0.160	1.333	1.142	−15.99	32.04	230.9	0.167	0.70
Rs	0.158	1.327	1.148	−15.59	30.61	238.3	0.169	0.78	v110	0.158	1.326	1.148	−15.79	28.01	232.0	0.167	1.05
Gs	0.158	1.327	1.148	−15.59	31.40	[illegible]	0.169	0.78	v105	0.158	1.326	1.148	−15.79	28.01	232.0	0.167	1.05
SkMP	0.157	1.325	1.149	−15.56	29.91	231.7	0.167	0.65	v100	0.158	1.326	1.148	−15.79	28.01	232.0	0.167	1.05
SkSC1	0.161	1.335	1.141	−15.85	[illegible]	235.6	0.168	1.00	v090	0.158	1.326	1.148	−15.79	28.01	232.0	0.167	1.05
SkSC2	0.161	1.335	1.141	−15.90	24.75	236.2	0.169	1.00	v080	0.158	1.326	1.148	−15.79	28.01	232.0	0.167	1.05
SkSC3	0.161	1.335	1.141	[illegible]	27.02	235.5	0.168	1.00	v075	0.158	1.326	1.148	−15.80	28.01	232.1	0.167	1.05
SkSC4	0.161	1.335	1.141	[illegible]	28.82	235.8	0.168	1.00	v070	0.158	1.326	1.148	−15.80	28.00	232.1	0.167	1.05
SkSC5	0.161	1.335	1.141	−15.85	31.00	235.6	0.168	1.00	BSk1	0.157	1.326	1.149	−15.80	27.82	232.1	0.167	1.05
SkSC6	0.161	1.336	1.141	−15.92	24.59	236.5	0.169	1.00	Skz-1	0.160	1.334	1.142	−16.00	32.02	231.1	0.167	0.70
SkSC10	0.161	1.336	1.141	−15.96	22.84	237.0	0.169	1.00	Skz0	0.160	1.334	1.142	−16.00	32.02	231.1	0.167	0.70
SkI1	0.161	1.335	1.141	−15.95	37.59	243.8	0.171	0.69	Skz1	0.160	1.334	1.142	−16.00	32.03	231.1	0.167	0.70
SkI2	0.158	1.327	1.148	−15.77	33.42	241.9	0.171	0.68	Skz2	0.160	1.334	1.142	−16.00	32.04	231.1	0.167	0.70
SkI3	0.158	1.327	1.148	−15.98	34.89	259.2	0.177	0.58	Skz3	0.160	1.334	1.142	−16.01	32.05	231.1	0.167	0.70
SkI4	0.160	1.334	1.142	−15.94	29.54	249.1	0.173	0.65	Skz4	0.160	1.334	1.142	−16.01	32.05	231.1	0.167	0.70
SkI5	0.156	1.322	1.153	−15.85	36.69	256.7	0.176	0.58									

<r^2>c を input にしているから区別が付かない。

4th moment of the charge density

^{208}Pb

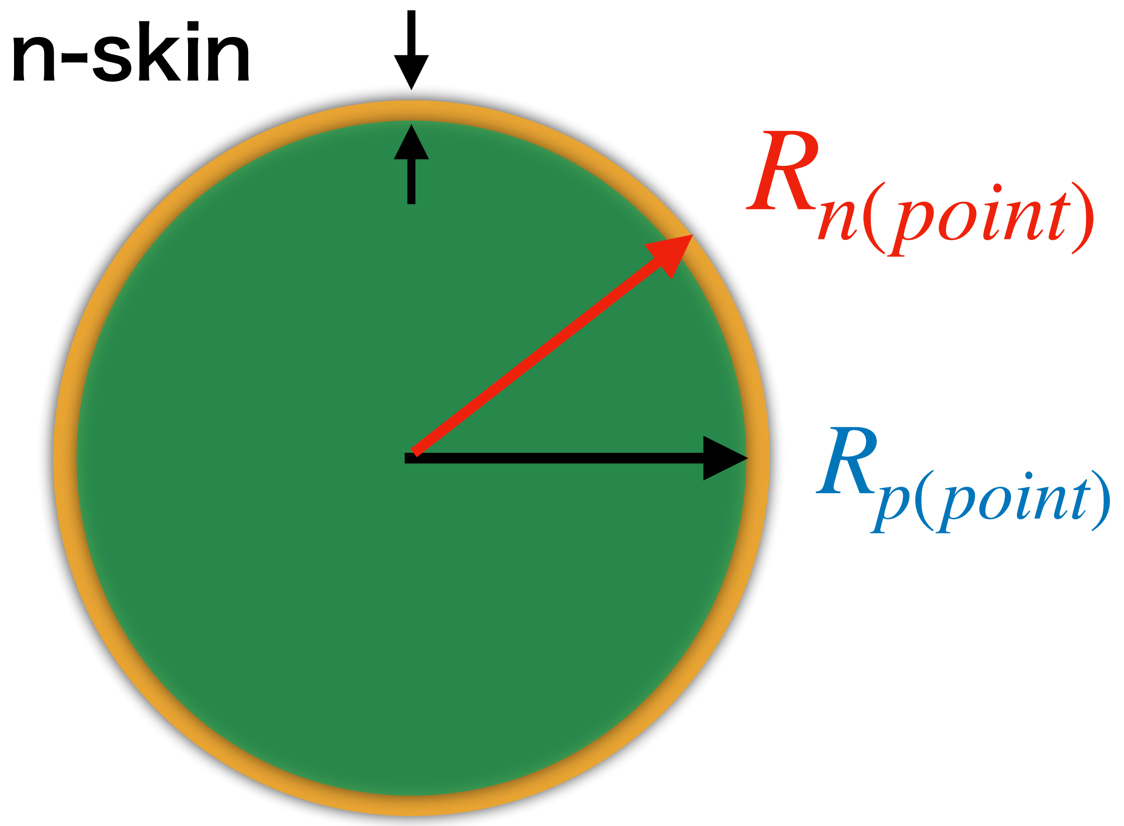

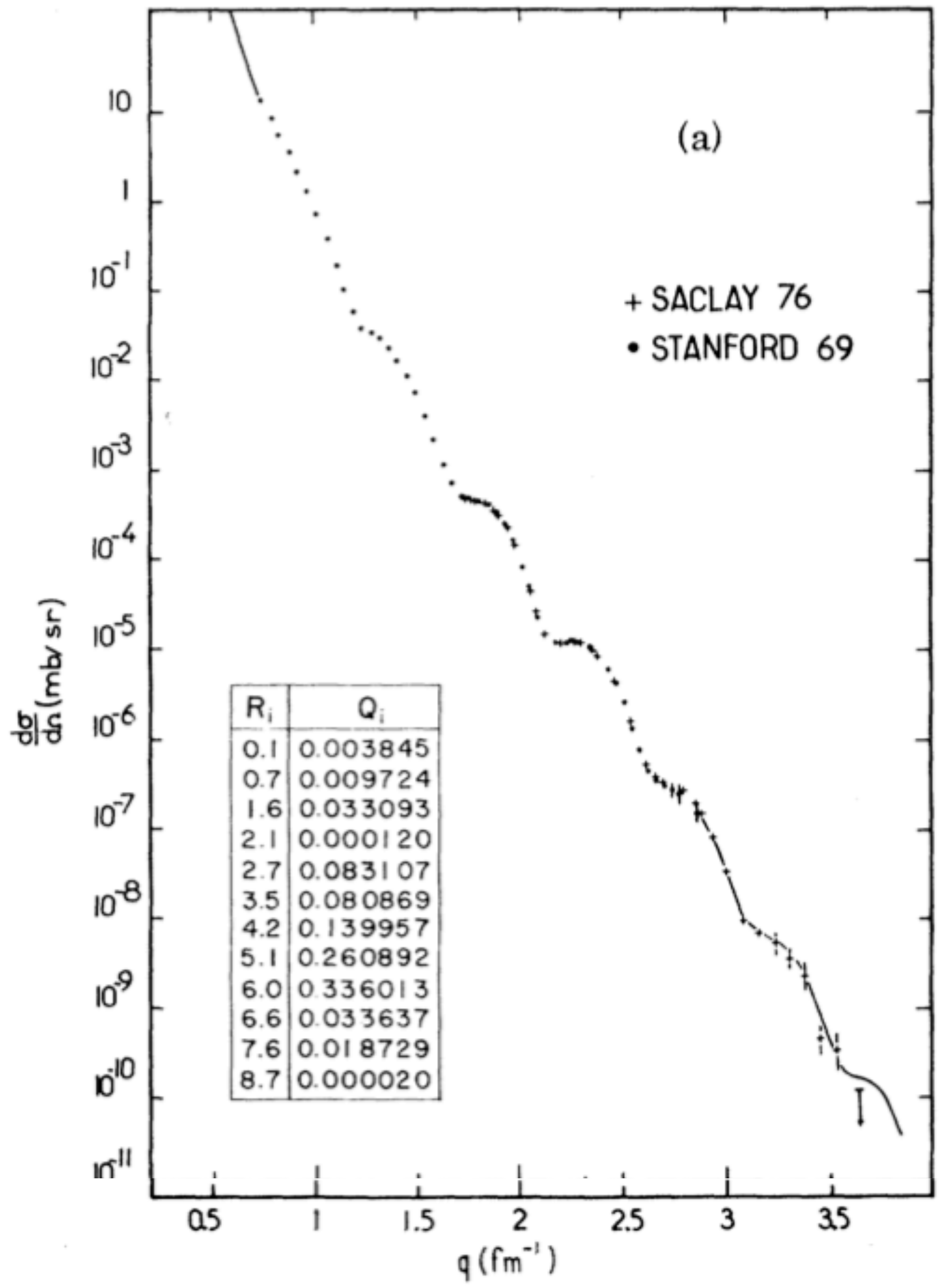

		R_p	R_n	δR
^{208}Pb	Rel.	5.454(0.013)	5.728(0.057)	0.275(0.070)
	Non.	5.447(0.014)	5.609(0.054)	0.162(0.068)
	Exp.	$R_c = 5.503(0.014)$		

^{48}Ca

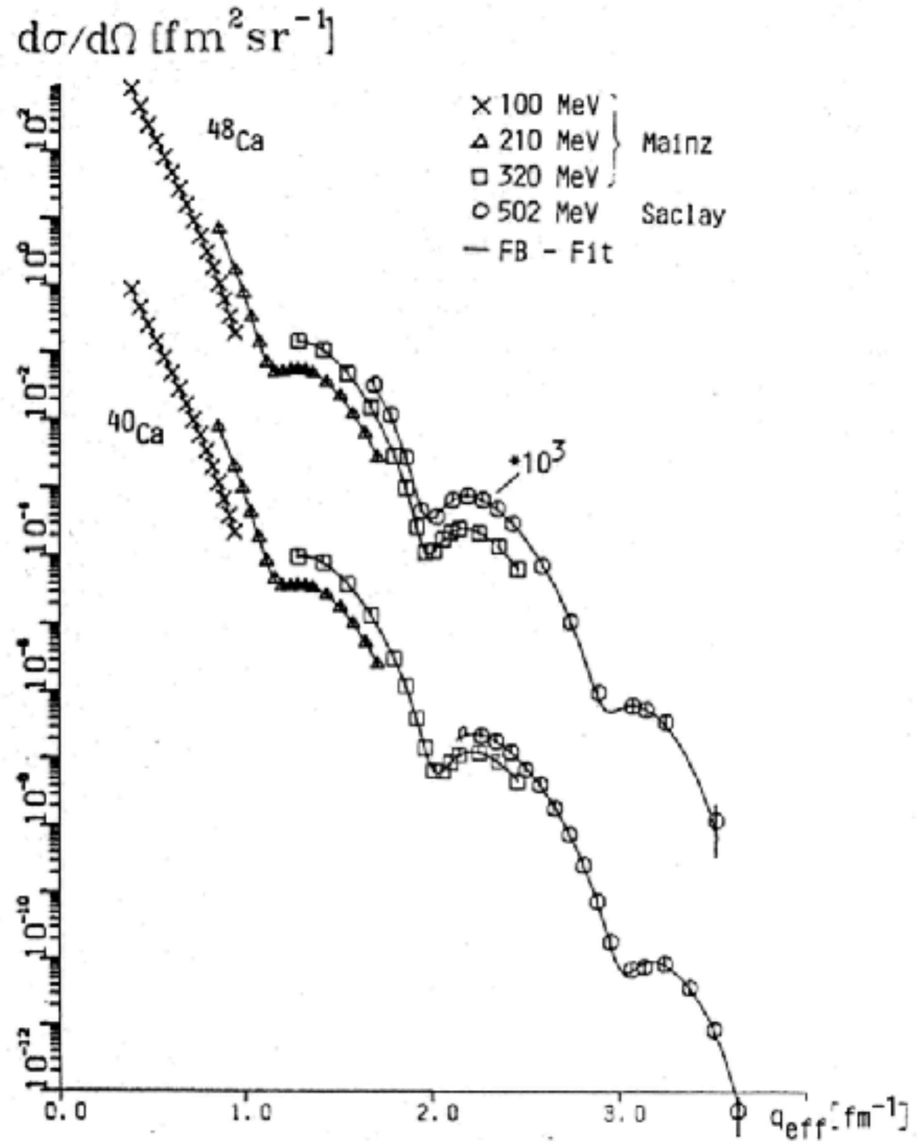

		R_p	R_n	δR
^{48}Ca	Rel.	3.378(0.005)	3.597(0.021)	0.220(0.026)
	Non.	3.372(0.009)	3.492(0.028)	0.121(0.036)
	Exp.	$R_c = 3.451(0.009)$		

H. Kurasawa, T. S, and T. Suzuki, Prog. Theor. Exp. Phys. 2021, 013D02

4th moment of the charge density

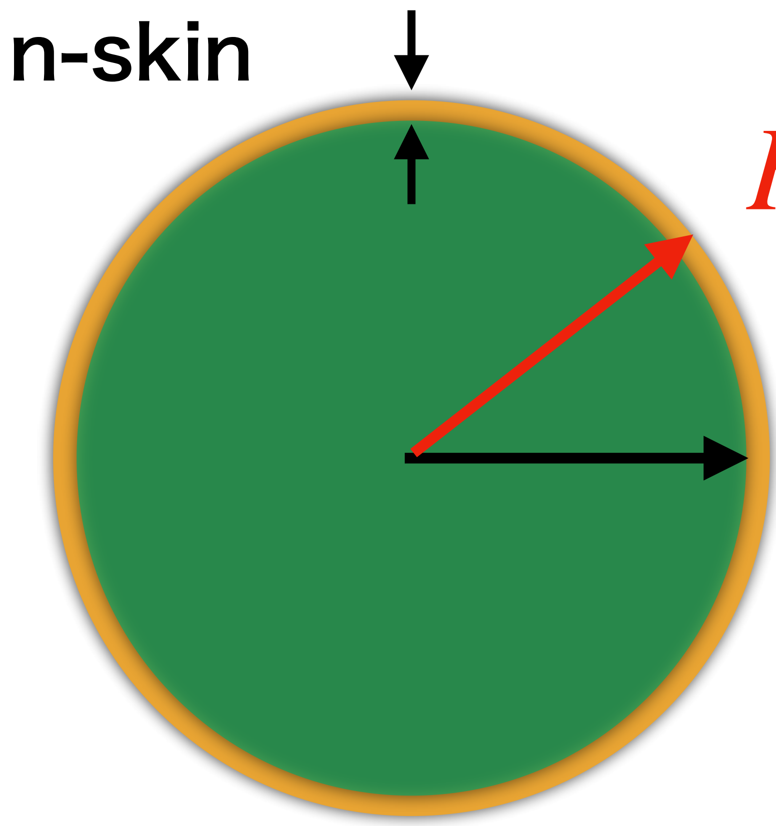

^{208}Pb

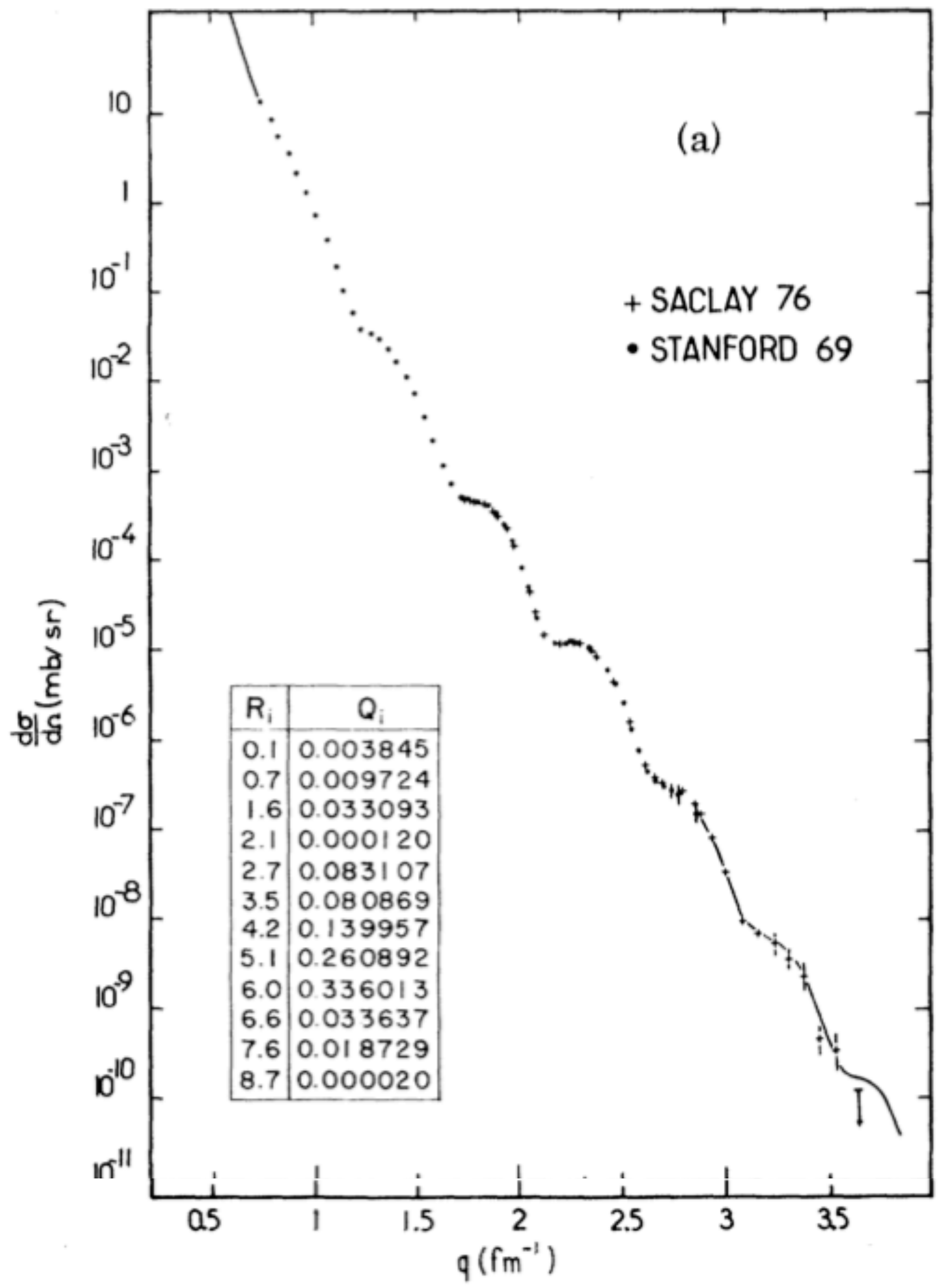

		R_p	R_n	δR
^{208}Pb	Rel.	5.454(0.013)	5.728(0.057)	0.275(0.070)
	Non.	5.447(0.014)	5.609(0.054)	0.162(0.068)
	Exp.	$R_c = 5.503(0.014)$		

JLab : PREX I,II (parity-violating e-scattering)

$$\Delta r_{np} \equiv R_n - R_p = 0.283 \pm 0.071 \text{ fm}$$

PRL 126, 172502 (2021)

^{48}Ca

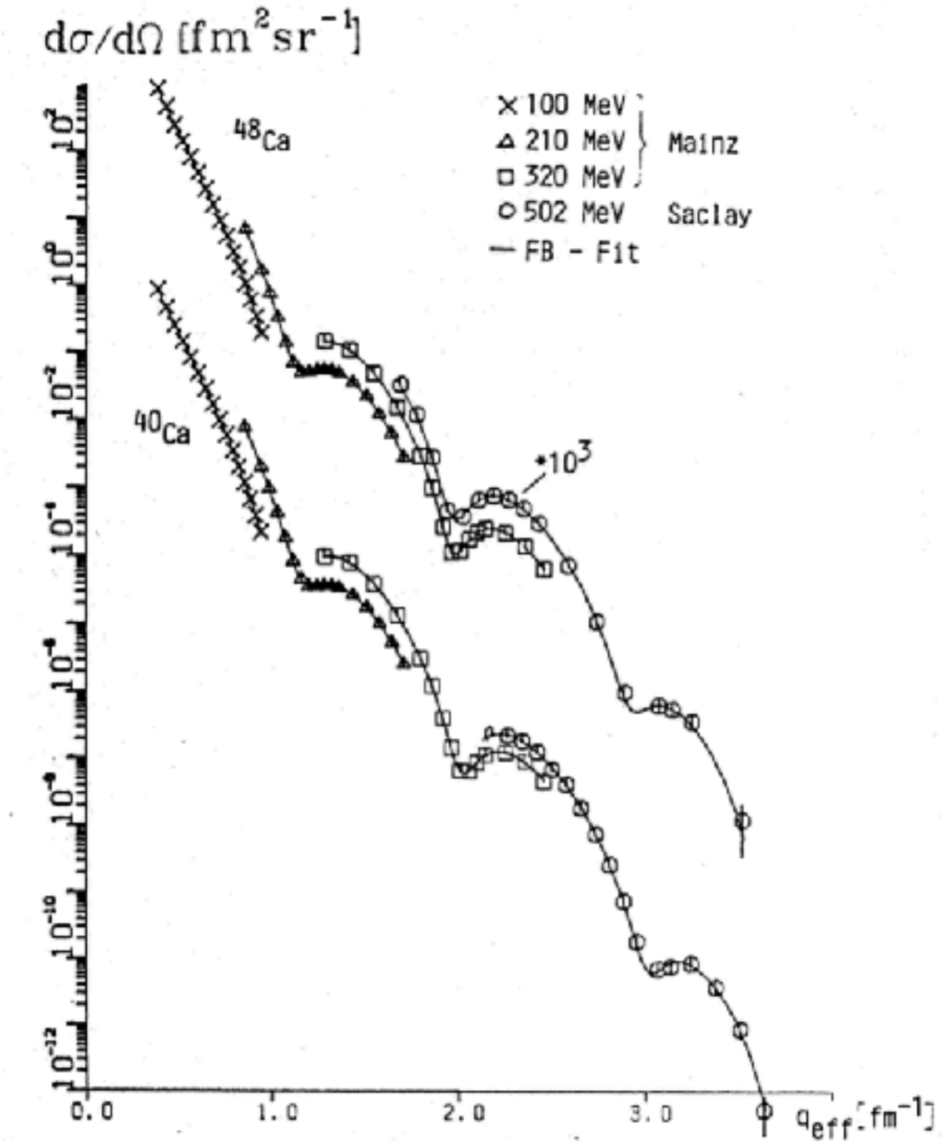

		R_p	R_n	δR
^{48}Ca	Rel.	3.378(0.005)	3.597(0.021)	0.220(0.026)
	Non.	3.372(0.009)	3.492(0.028)	0.121(0.036)
	Exp.	$R_c = 3.451(0.009)$		

JLab : CREX (parity-violating e-scattering)

$$\Delta r_{np} \equiv R_n - R_p = 0.121 \pm 0.026 \text{ fm}$$

H. Kurasawa, T. S, and T. Suzuki, Prog. Theor. Exp. Phys. 2021, 013D02

ways to access the fourth moment, $<r_c^4>$

$$< r_c^4 > = \int r^4 \rho_c(r) \, \mathrm{d}^3 r$$

ways to access the fourth moment, <r$_c^4$>

$$< r_c^4 > = \int r^4 \rho_c(r)\ \mathrm{d}^3 r$$

$$\frac{\mathrm{d}\sigma}{\mathrm{d}\Omega} = \frac{\mathrm{d}\sigma_{Mott}}{\mathrm{d}\Omega}\ |F_c(q)|^2$$

$$\Rightarrow \rho_c(r) = \int F_c(q) e^{-iqr}\ \mathrm{d}^3 q$$

ways to access the fourth moment, $<r_c^4>$

$$< r_c^4 > = \int r^4 \rho_c(r)\ \mathrm{d}^3 r$$

$$\frac{\mathrm{d}\sigma}{\mathrm{d}\Omega} = \frac{\mathrm{d}\sigma_{Mott}}{\mathrm{d}\Omega}\ |F_c(q)|^2$$

$$\Rightarrow \quad \rho_c(r) = \int F_c(q) e^{-iqr}\ \mathrm{d}^3 q$$

1) elastic scattering covering upto very high *q*

ways to access the fourth moment, $<r_c^4>$

$$< r_c^4 > = \int r^4 \rho_c(r)\, \mathrm{d}^3 r$$

$$\frac{\mathrm{d}\sigma}{\mathrm{d}\Omega} = \frac{\mathrm{d}\sigma_{Mott}}{\mathrm{d}\Omega} \, |F_c(q)|^2$$

$$\rho_c(r) = \int F_c(q) e^{-iqr}\, \mathrm{d}^3 q$$

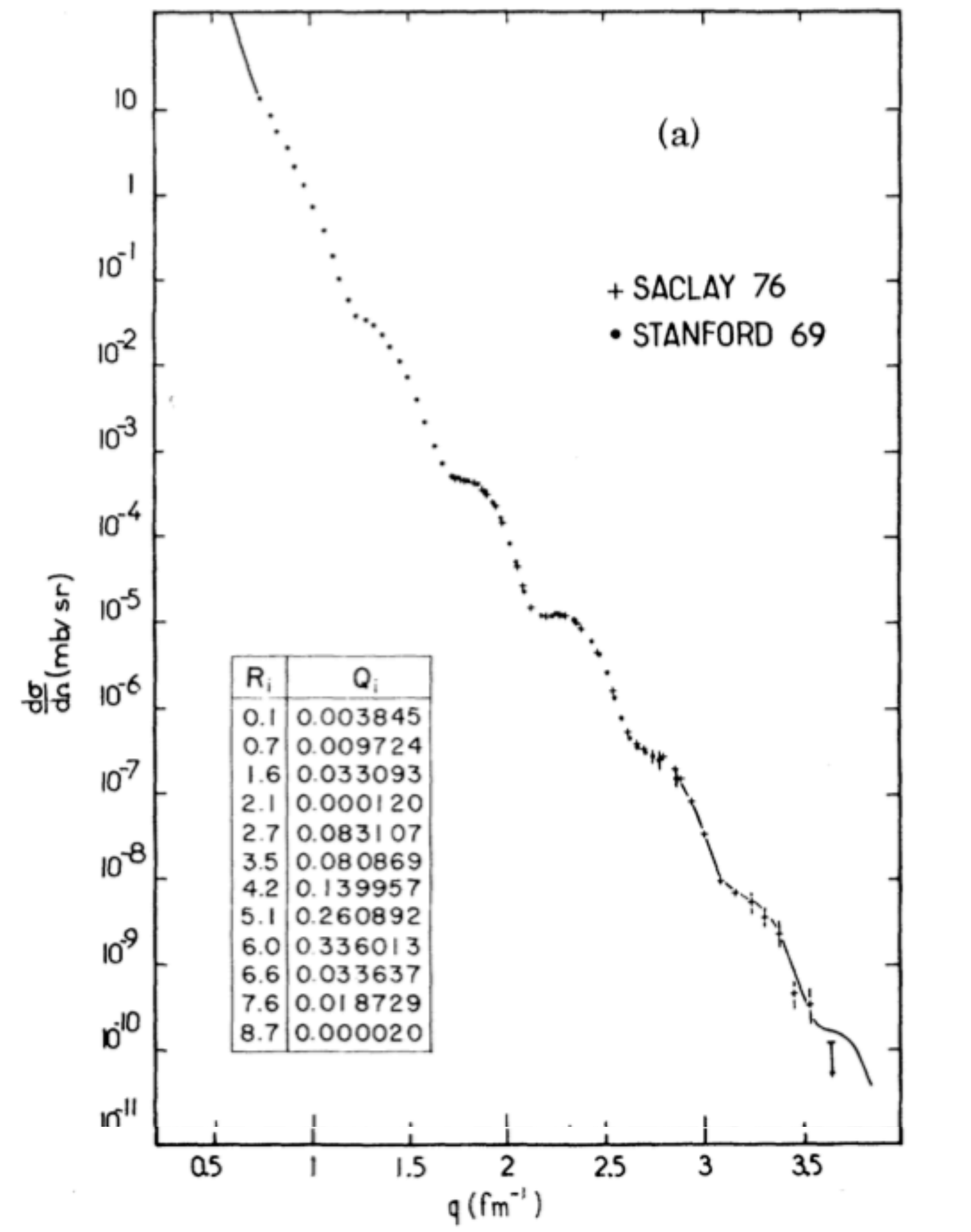

1) elastic scattering covering upto very high *q*

ways to access the fourth moment, <r_c^4>

$$< r_c^4 > = \int r^4 \rho_c(r)\, \mathrm{d}^3 r$$

$$\frac{\mathrm{d}\sigma}{\mathrm{d}\Omega} = \frac{\mathrm{d}\sigma_{Mott}}{\mathrm{d}\Omega} \,|F_c(q)|^2$$

$$\Rightarrow \quad \rho_c(r) = \int F_c(q) e^{-iqr}\, \mathrm{d}^3 q$$

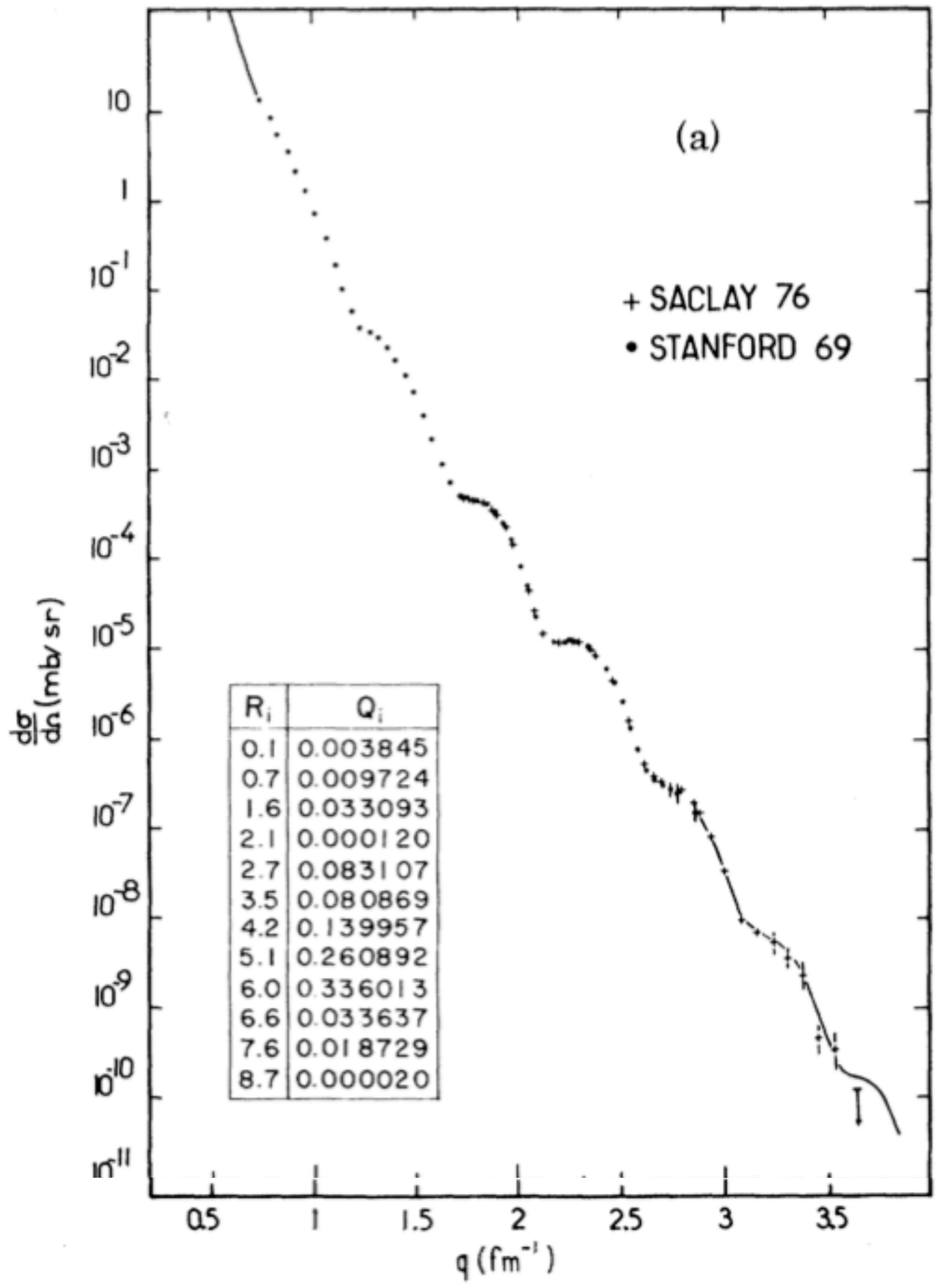

1) elastic scattering covering upto very high *q*

very high L required

=> no chance for low-L e-scatering for exotics

ways to access the fourth moment, <r_c^4>

$$< r_c^4 > = \int r^4 \rho_c(r)\, \mathrm{d}^3 r$$

$$\frac{\mathrm{d}\sigma}{\mathrm{d}\Omega} = \frac{\mathrm{d}\sigma_{Mott}}{\mathrm{d}\Omega}\, |F_c(q)|^2$$

$$\rho_c(r) = \int F_c(q) e^{-iqr}\, \mathrm{d}^3 q$$

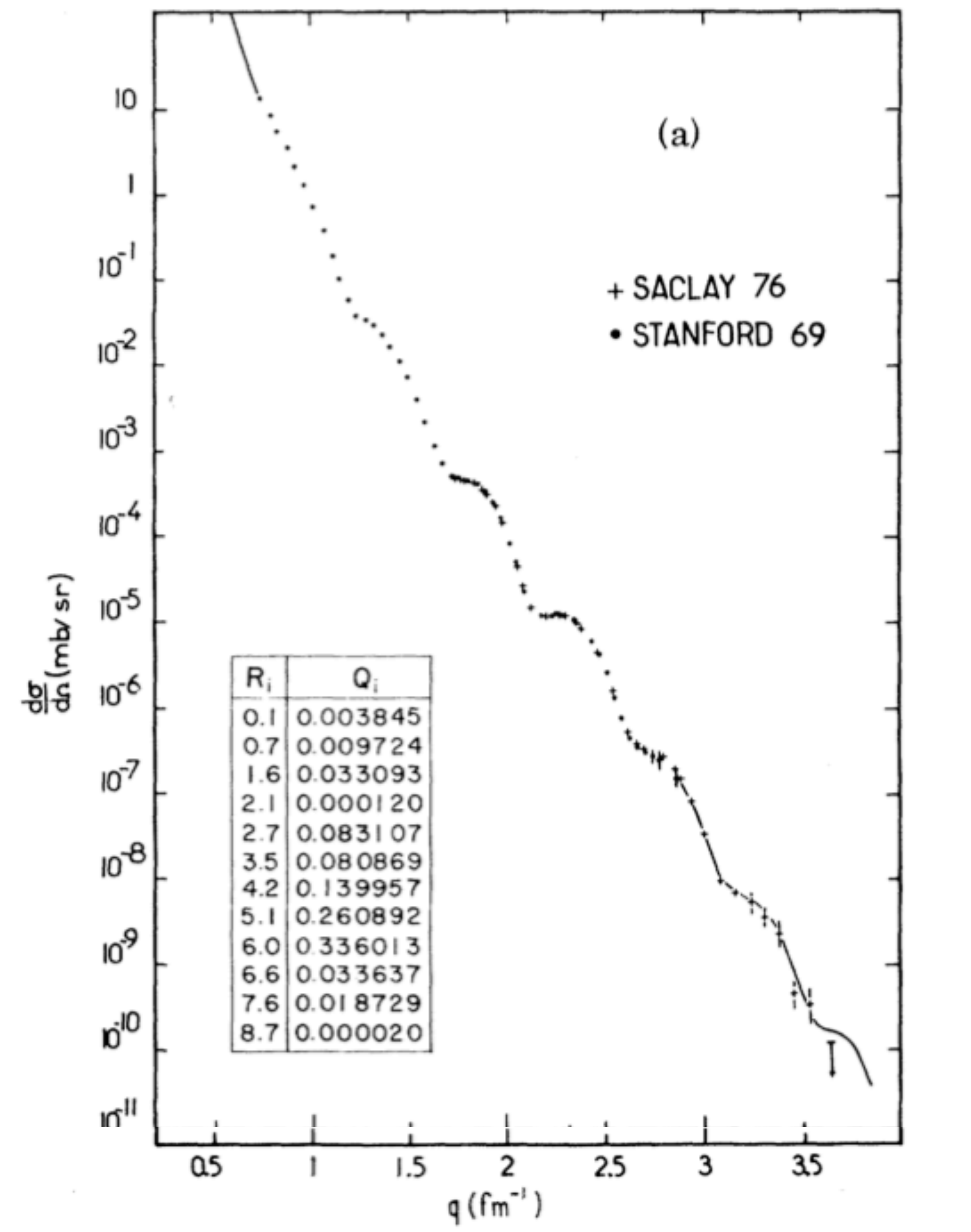

1) elastic scattering covering upto very high *q*

very high L required

=> no chance for low-L e-scatering for exotics

2) elastic scattering at very low *q*

ways to access the fourth moment, $<r_c^4>$

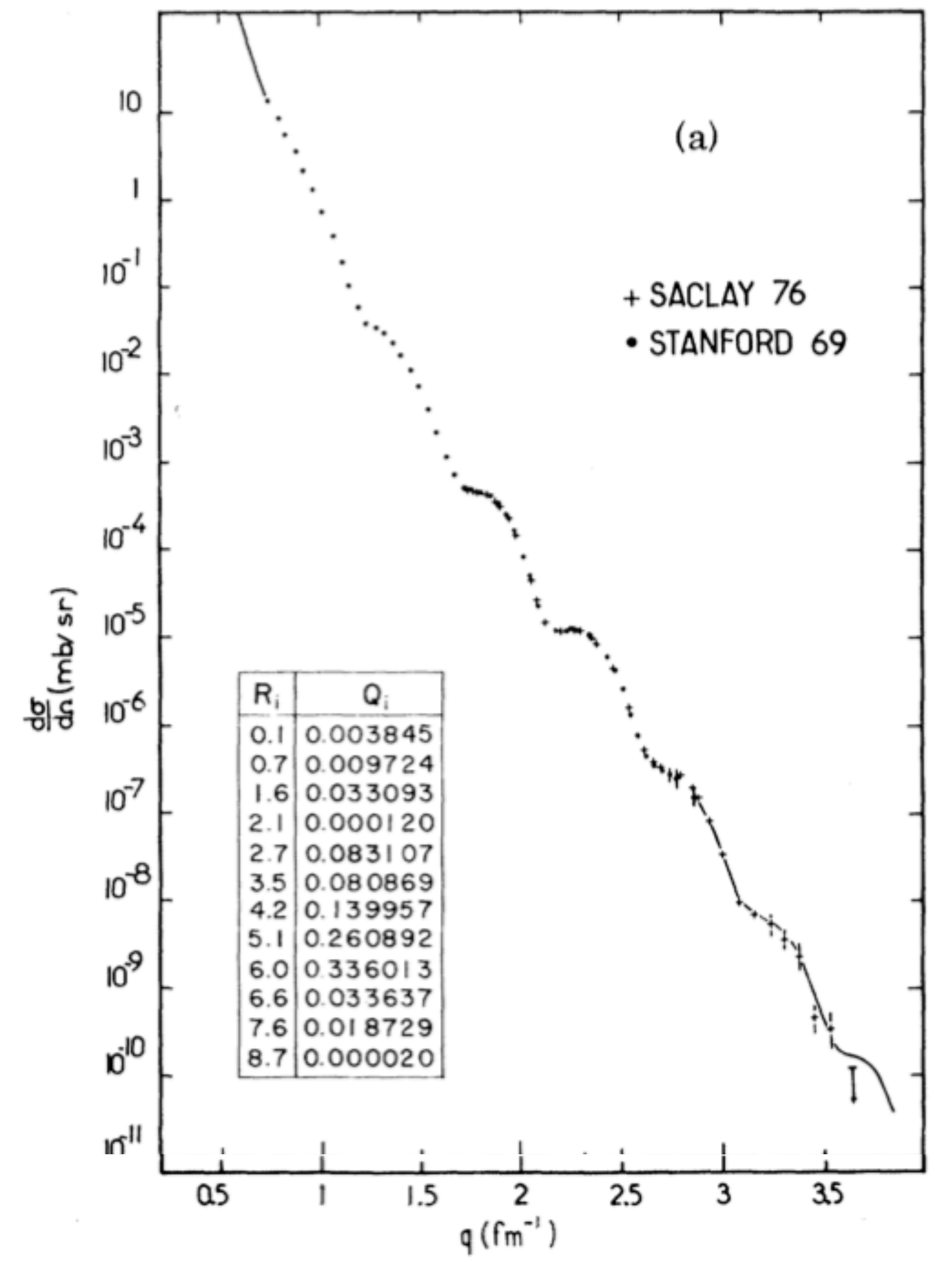

$$< r_c^4 > = \int r^4 \rho_c(r)\, \mathrm{d}^3 r$$

$$\frac{\mathrm{d}\sigma}{\mathrm{d}\Omega} = \frac{\mathrm{d}\sigma_{Mott}}{\mathrm{d}\Omega} \, |F_c(q)|^2$$

$$\Rightarrow \quad \rho_c(r) = \int F_c(q) e^{-iqr}\, \mathrm{d}^3 q$$

1) elastic scattering covering upto very high *q*

very high L required

=> no chance for low-L e-scatering for exotics

2) elastic scattering at very low *q*

$$F_c(q) \sim 1 - \frac{< r_c^2 >}{6} q^2 + \frac{< r_c^4 >}{120} q^4 + \ldots$$

ways to access the fourth moment, <r_c^4>

$$< r_c^4 > = \int r^4 \rho_c(r)\, \mathrm{d}^3 r$$

$$\frac{\mathrm{d}\sigma}{\mathrm{d}\Omega} = \frac{\mathrm{d}\sigma_{Mott}}{\mathrm{d}\Omega} \, |F_c(q)|^2$$

$$\Rightarrow \quad \rho_c(r) = \int F_c(q) e^{-iqr}\, \mathrm{d}^3 q$$

1) elastic scattering covering upto very high *q*

very high L required

=> no chance for low-L e-scatering for exotics

2) elastic scattering at very low *q*

$$F_c(q) \sim 1 - \frac{< r_c^2 >}{6} q^2 + \frac{< r_c^4 >}{120} q^4 + \ldots$$

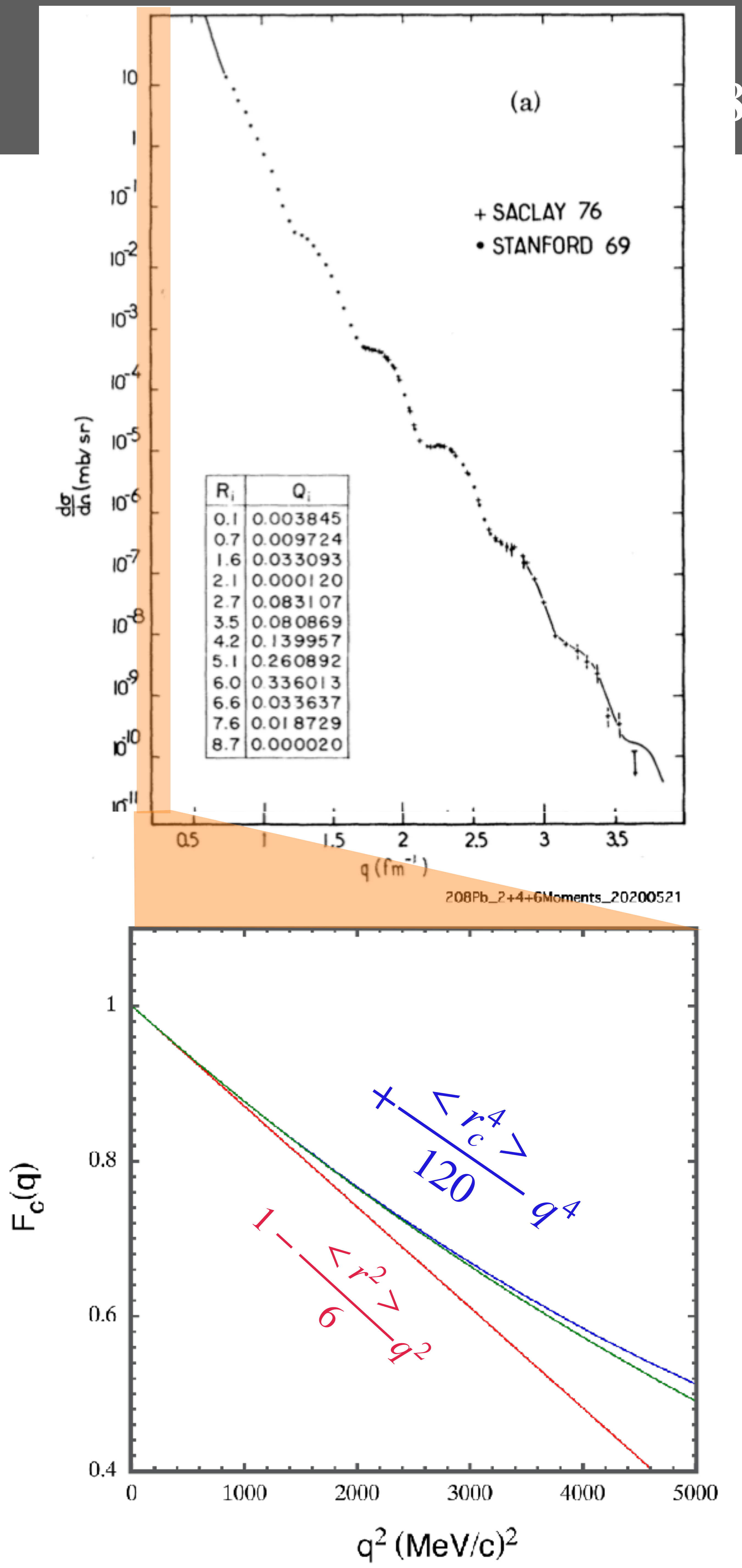

ways to access the fourth moment, $<r_c^4>$

$$< r_c^4 > = \int r^4 \rho_c(r)\, \mathrm{d}^3 r$$

$$\frac{\mathrm{d}\sigma}{\mathrm{d}\Omega} = \frac{\mathrm{d}\sigma_{Mott}}{\mathrm{d}\Omega} \, |F_c(q)|^2$$

$$\Rightarrow \quad \rho_c(r) = \int F_c(q) e^{-iqr}\, \mathrm{d}^3 q$$

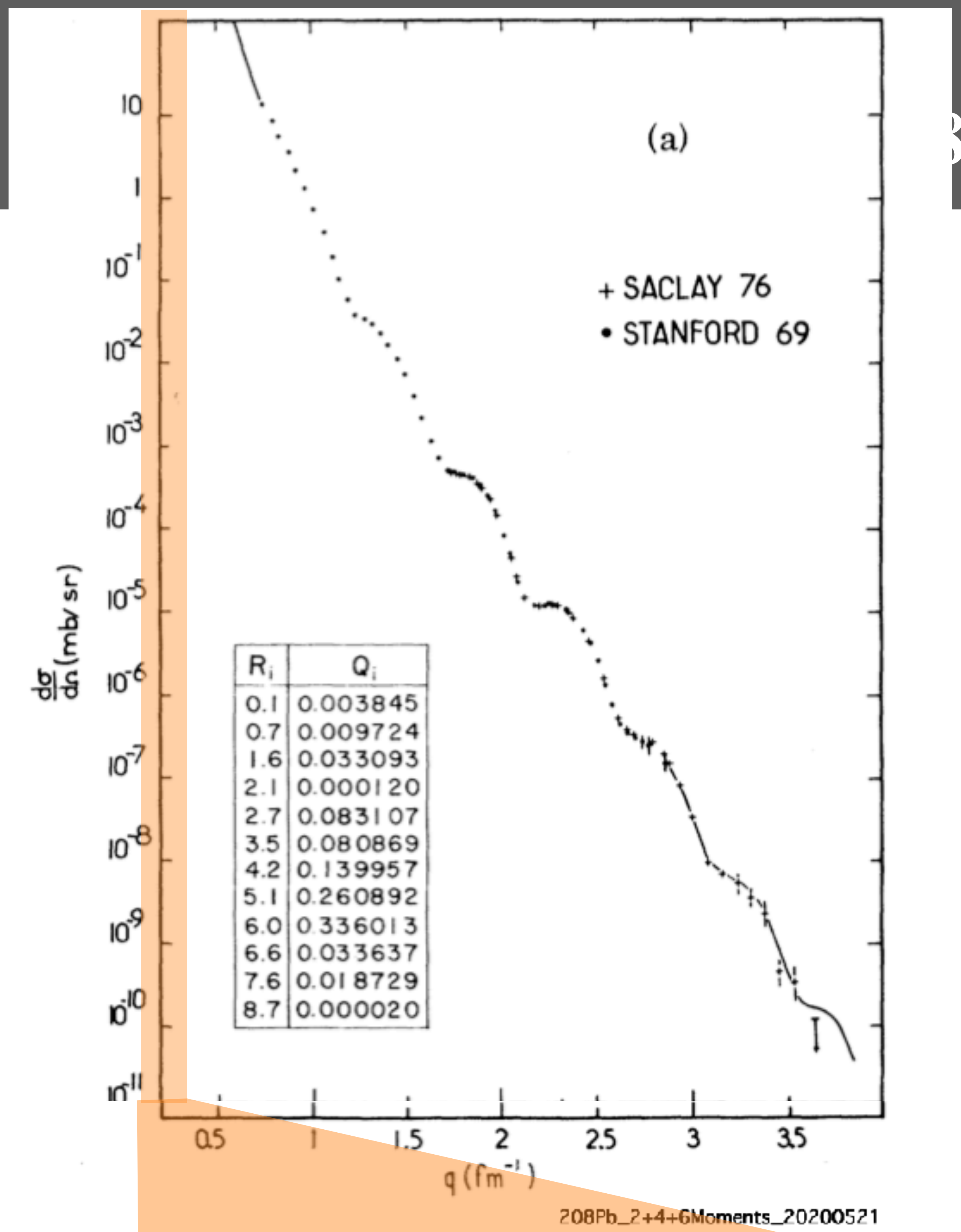

R_i	Q_i
0.1	0.003845
0.7	0.009724
1.6	0.033093
2.1	0.000120
2.7	0.083107
3.5	0.080869
4.2	0.139957
5.1	0.260892
6.0	0.336013
6.6	0.033637
7.6	0.018729
8.7	0.000020

1) elastic scattering covering upto very high *q*

very high L required

=> no chance for low-L e-scatering for exotics

2) elastic scattering at very low *q*

$$F_c(q) \sim 1 - \frac{< r_c^2 >}{6} q^2 + \frac{< r_c^4 >}{120} q^4 + \dots$$

$$\frac{\mathrm{d}\sigma_{\mathrm{Mott}}}{\mathrm{d}\Omega} \propto 1/q^4$$

=> low-L SCRIT exp. ??

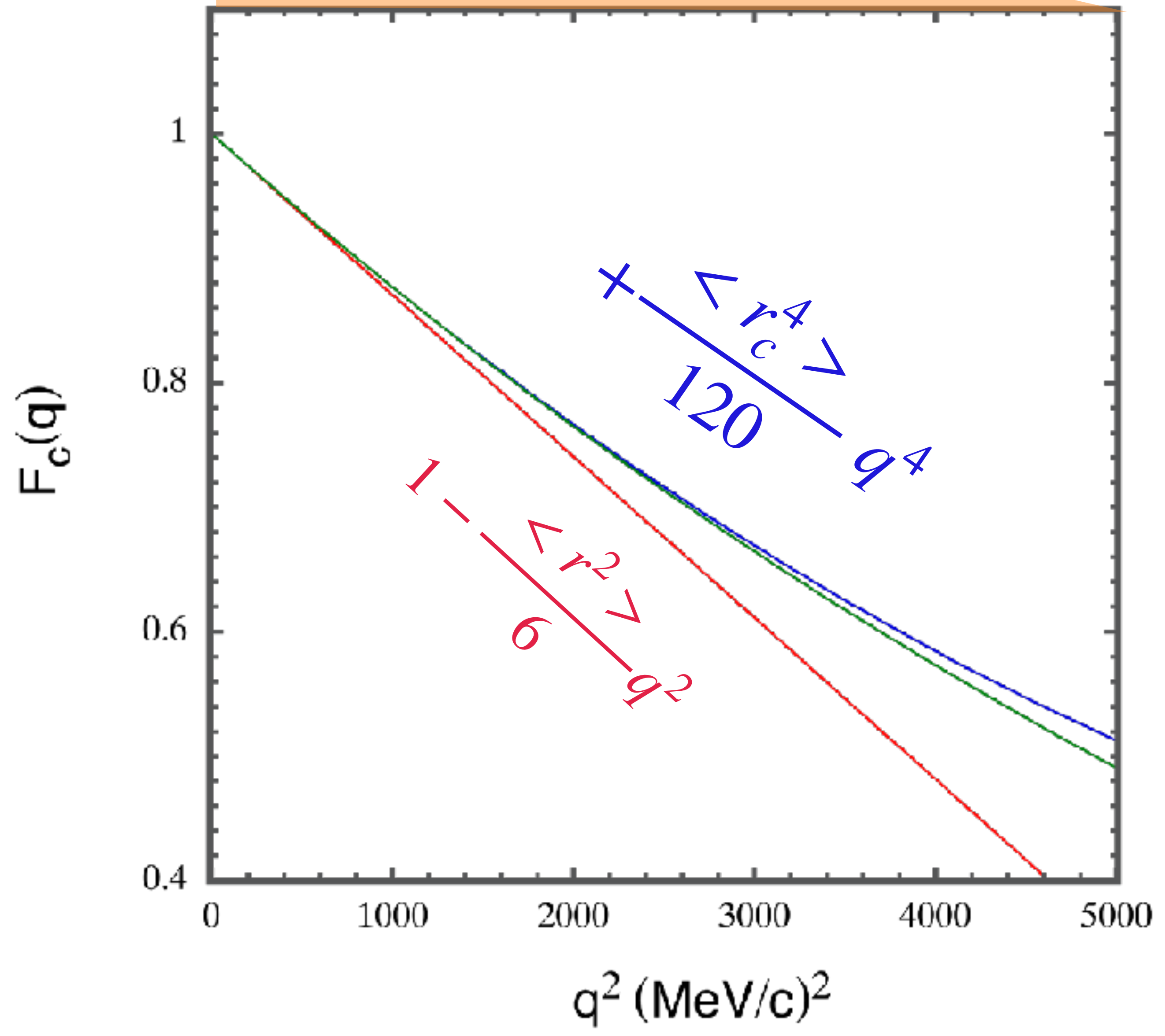

$\langle r_c^4 \rangle$ determination at extremely low-q (e,e') ?

- ^{208}Pb(e,e') at the ULQ2 beam line at Tohoku

Ee ~ 10 - 50 MeV
θ = 30 - 150°
q = 5 - 50 MeV/c

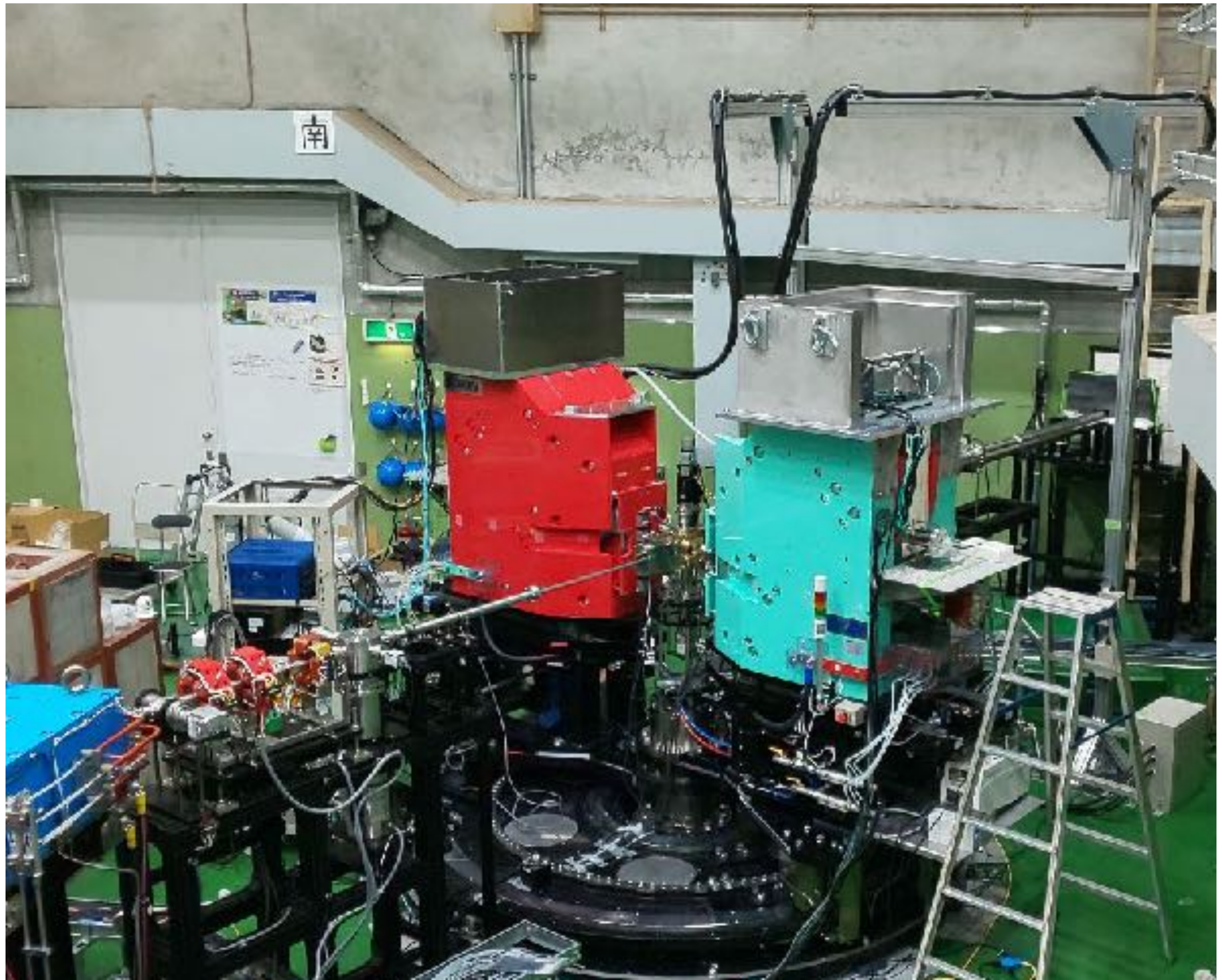

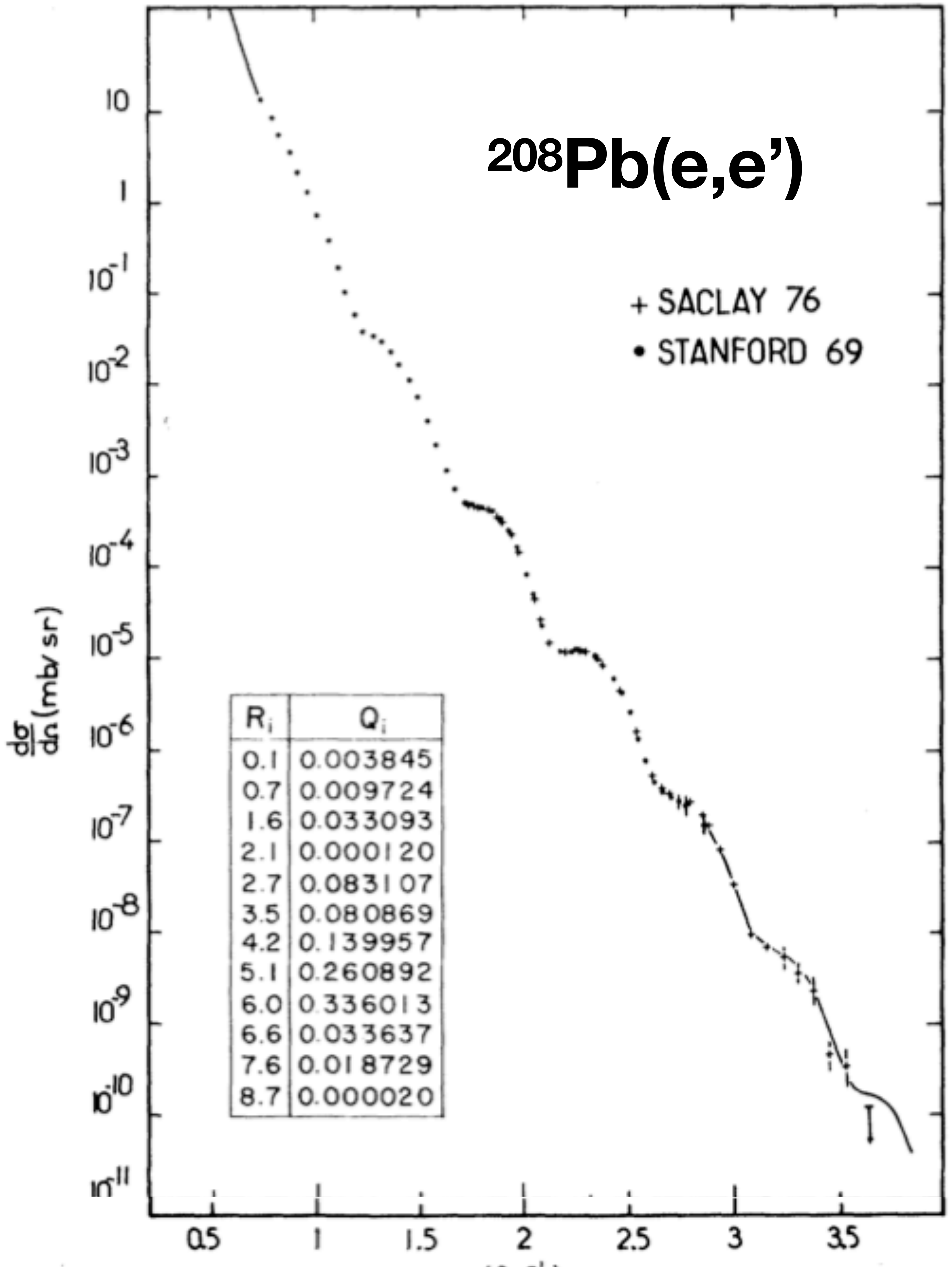

$\langle r_c^4 \rangle$ determination at extremely low-q (e,e') ?

- ^{208}Pb(e,e') at the ULQ2 beam line at Tohoku

Ee ~ 10 - 50 MeV
θ = 30 - 150°
q = 5 - 50 MeV/c

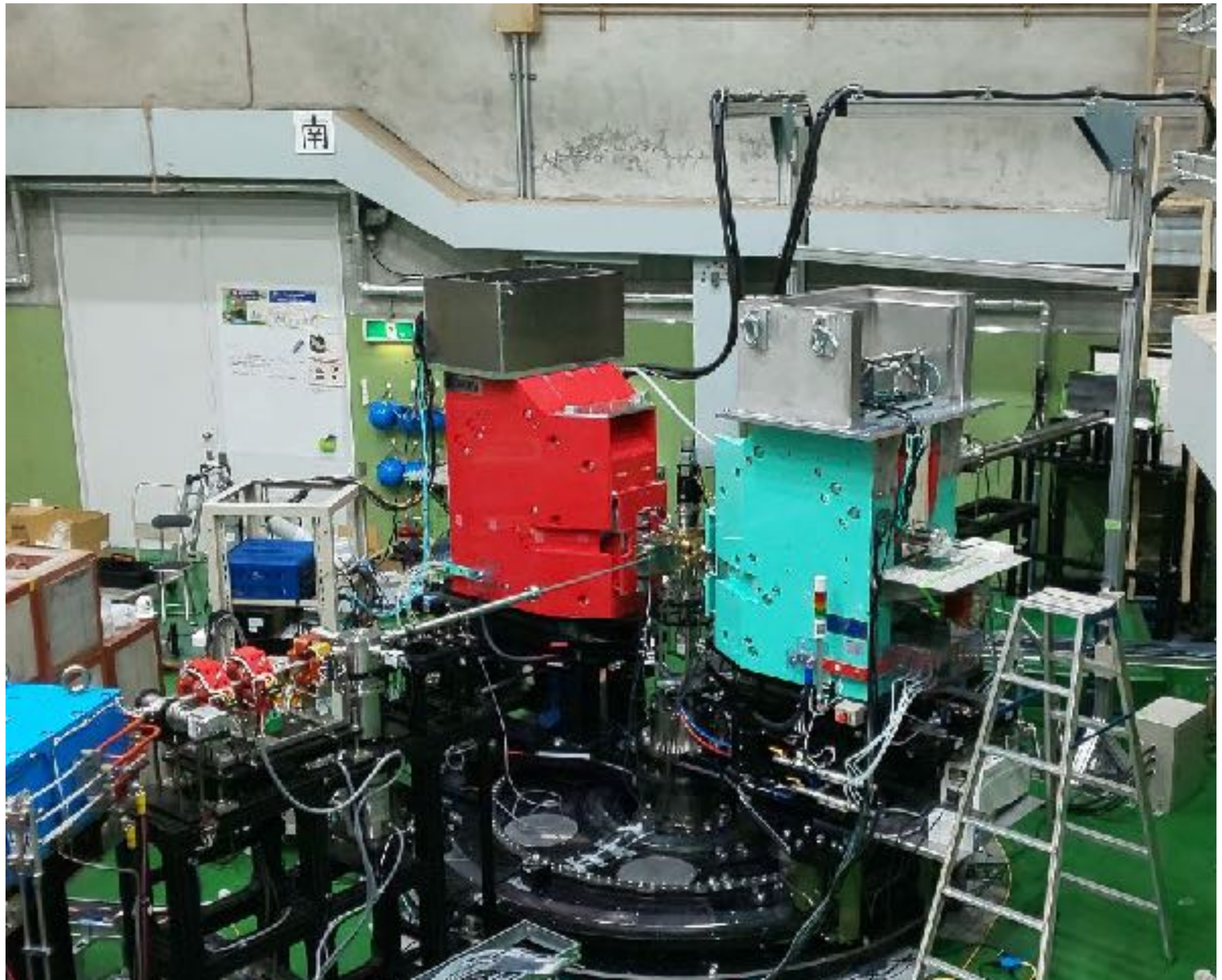

lowest-ever q region

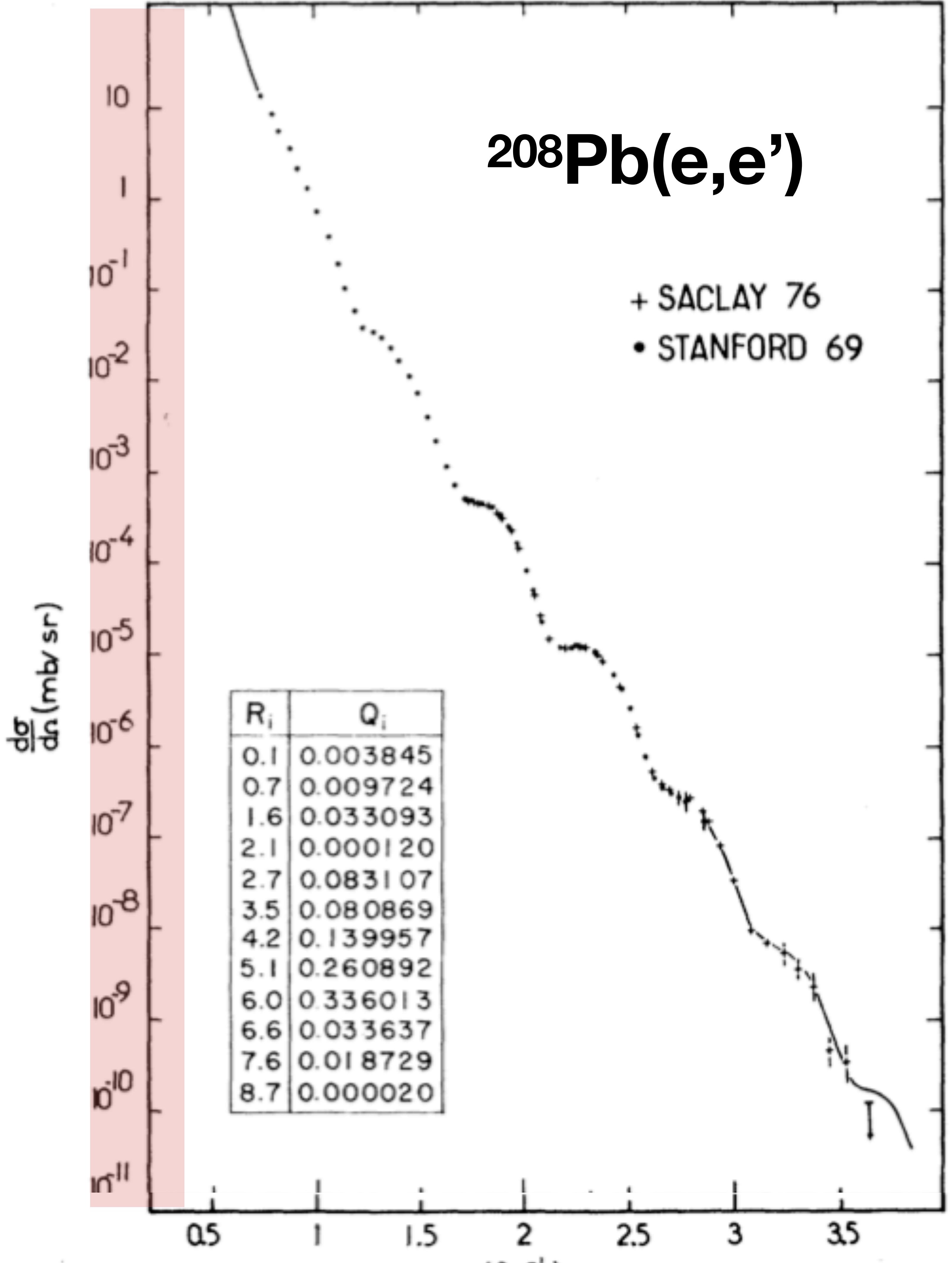

$\langle r_c^4 \rangle$ determination at extremely low-q (e,e') ?

- ^{208}Pb(e,e') at the ULQ2 beam line at Tohoku

Ee ~ 10 - 50 MeV
θ = 30 - 150°
q = 5 - 50 MeV/c

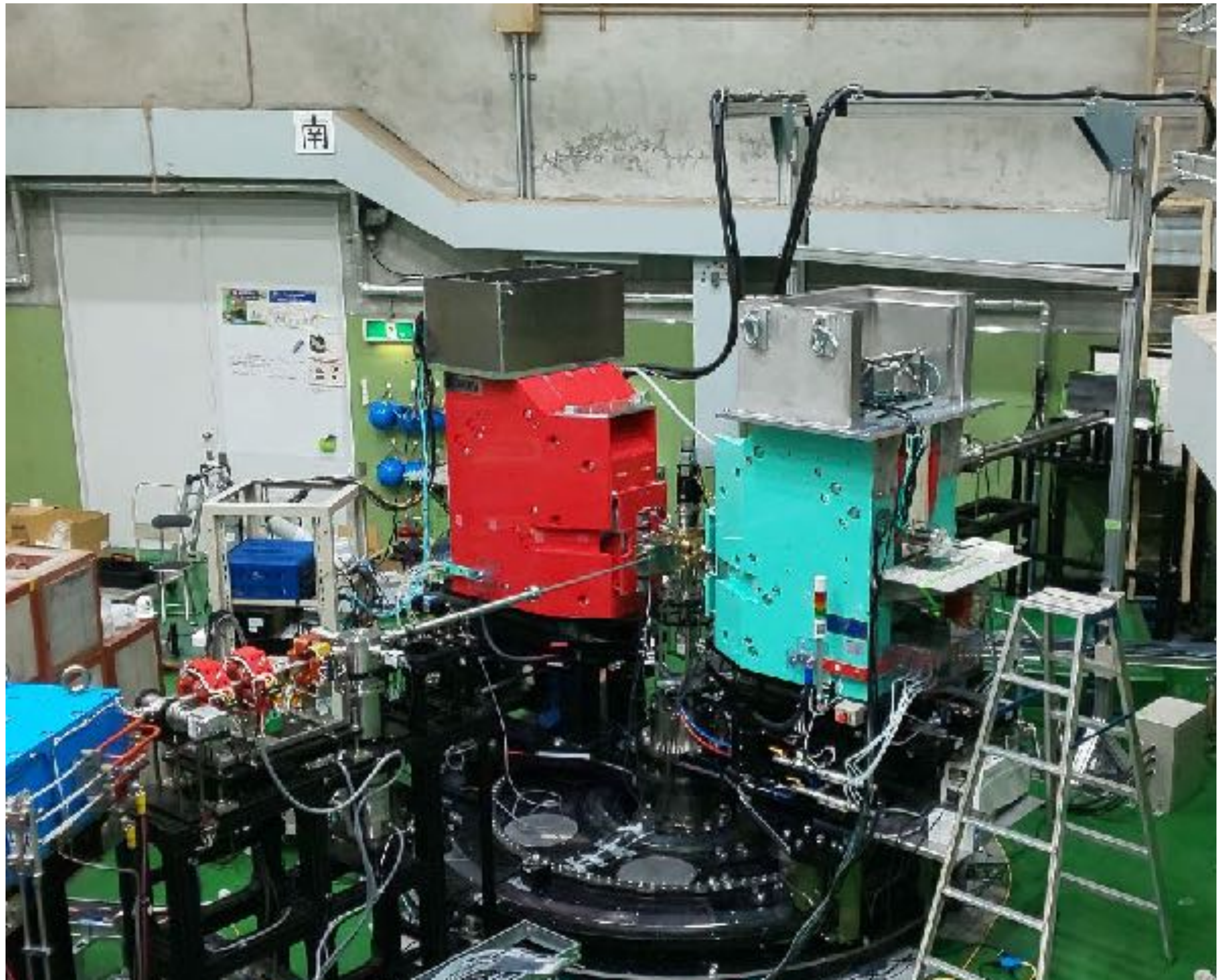

lowest-ever q region

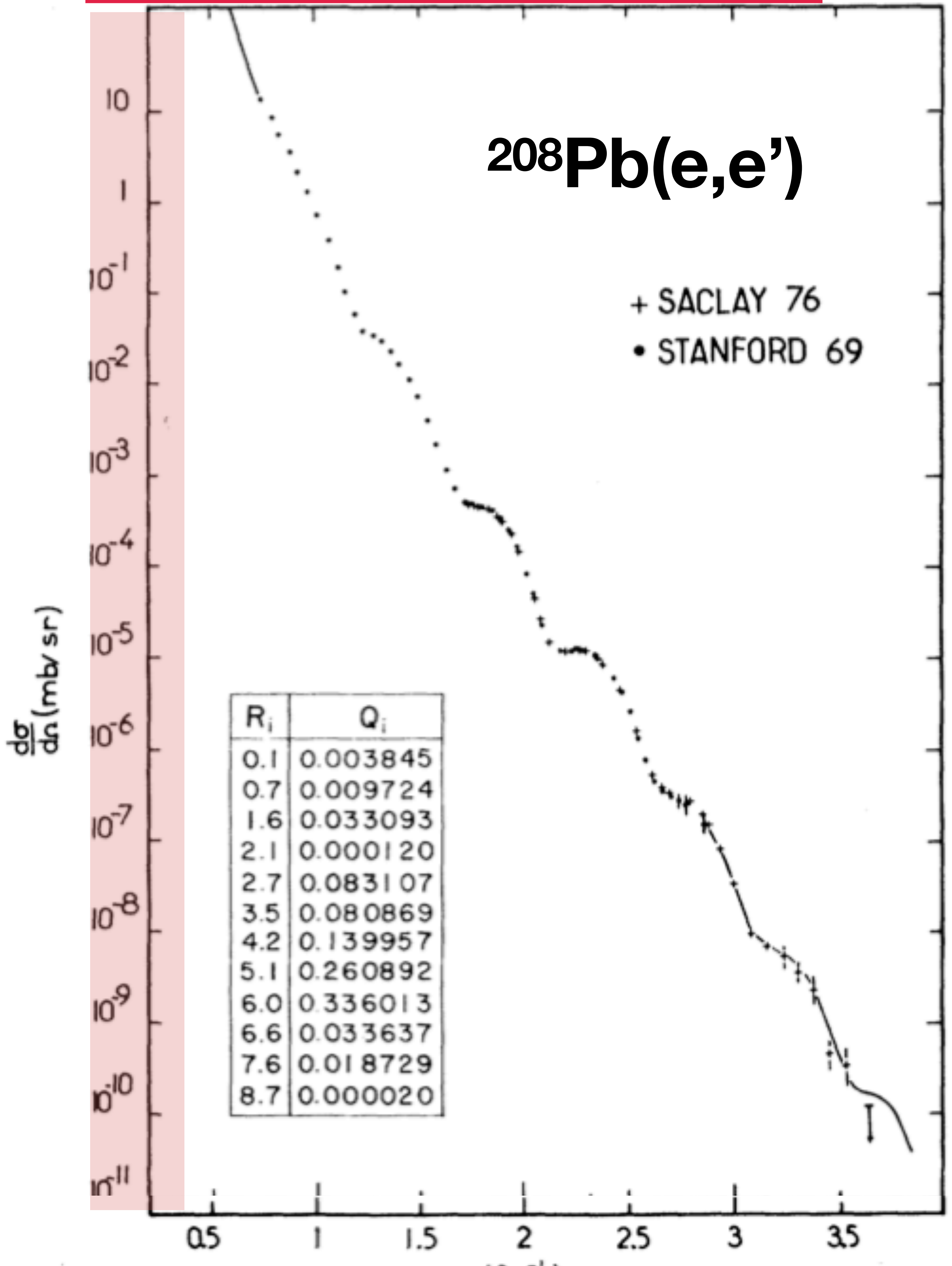

Rika Danjo

Low-energy electron-scattering facilities in Japan

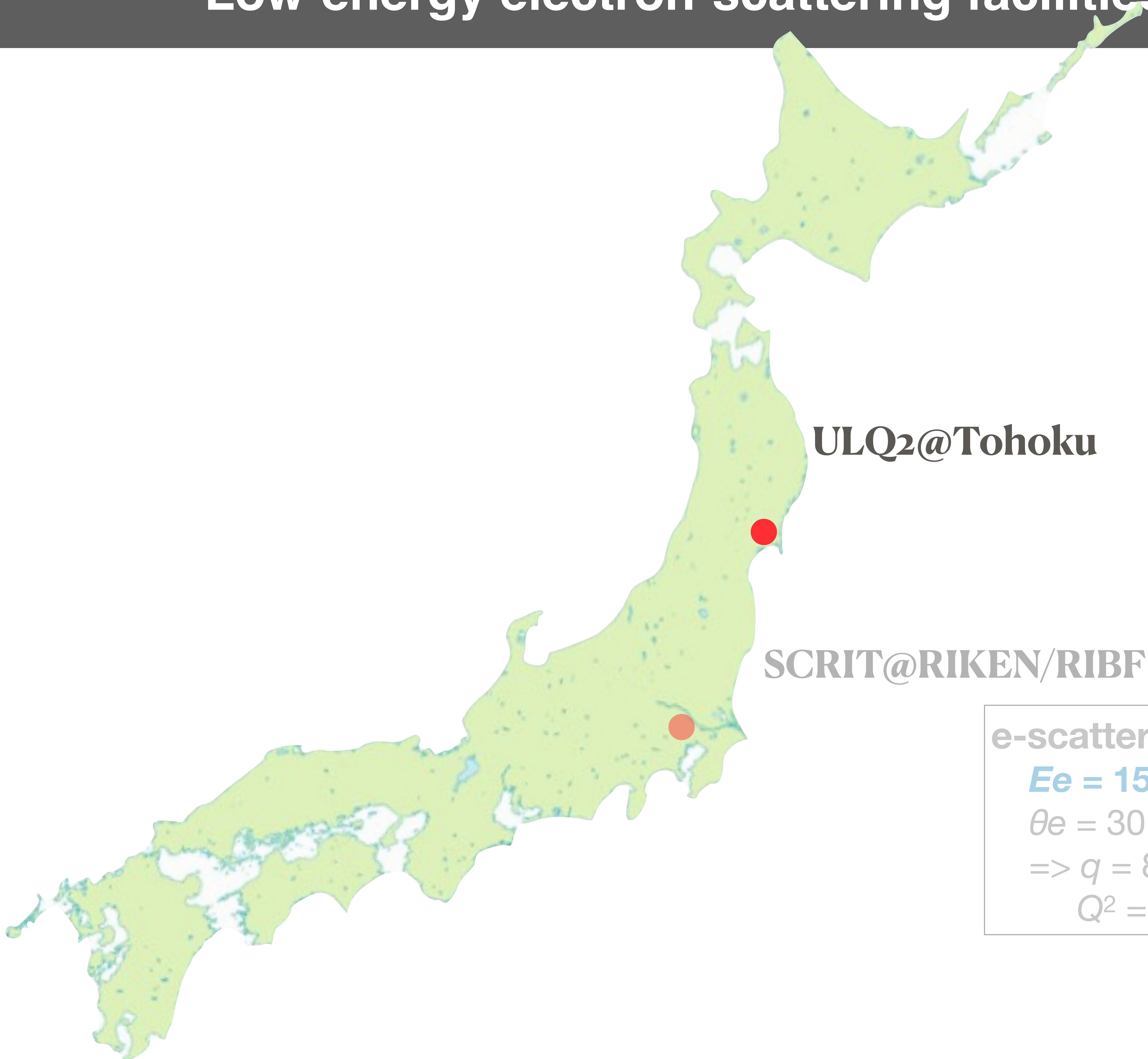

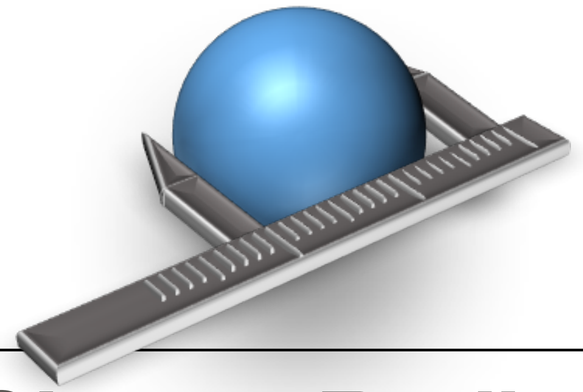

Proton Charge Radius

***Ee* = 10 - 60 MeV**

θe = 30 - 150 deg.

=> $Q^2 = 3\text{x}10^{-5} - 0.013\ (\text{GeV/c})^2$

lowest-ever Q^2 !!

e-scattering for exotic nuclei (~10^8/sec)

***Ee* = 150 - 300 MeV**

θe = 30 - 60 deg.

=> q = 80 - 300 MeV/c

$Q^2 = 0.006 - 0.09\ (\text{GeV/c})^2$

world's first !!

Proton Radius Puzzle

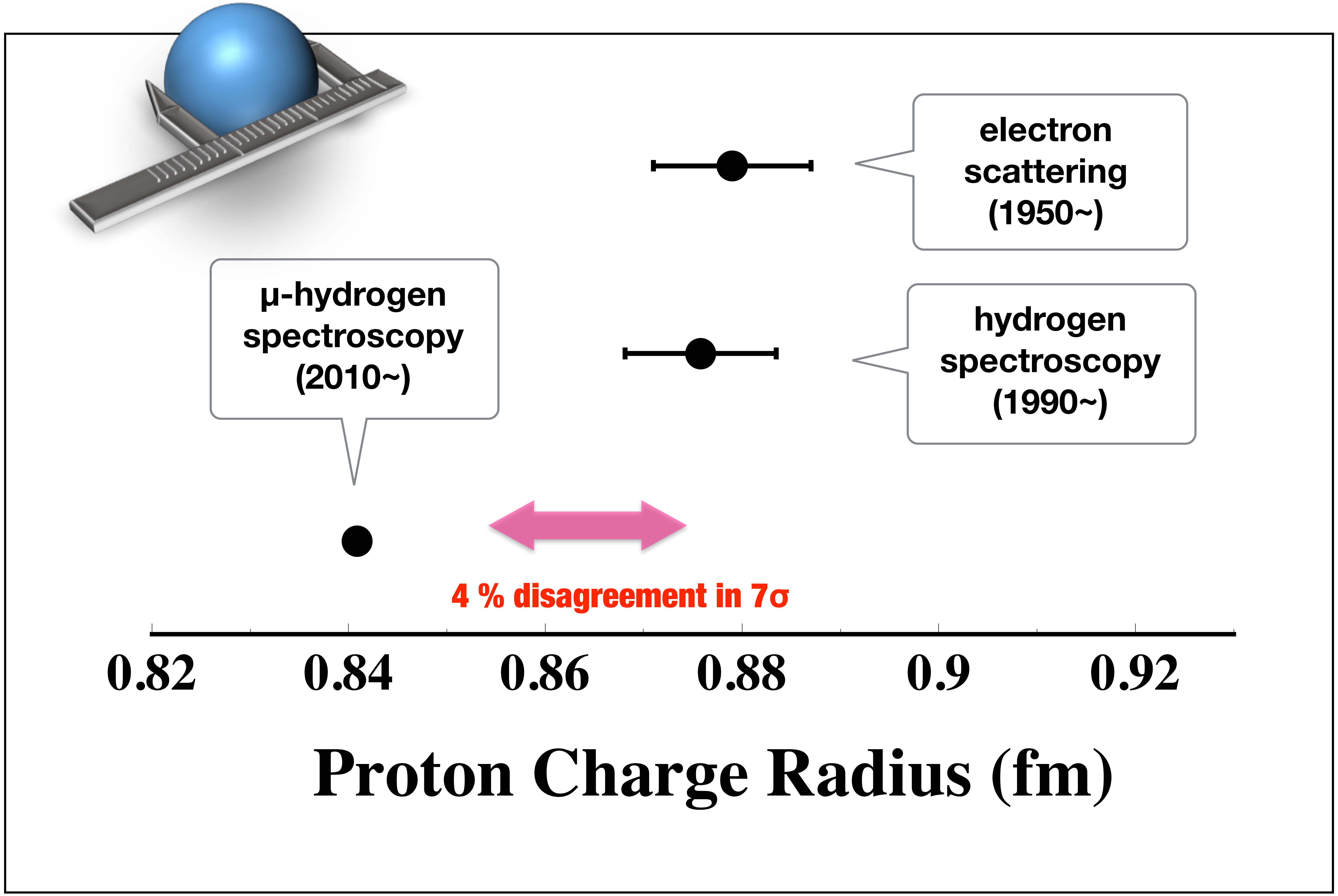

C. Carlson, Prog. Part. Nucl. Phys. 82 (2015) 59.

Proton Radius Puzzle

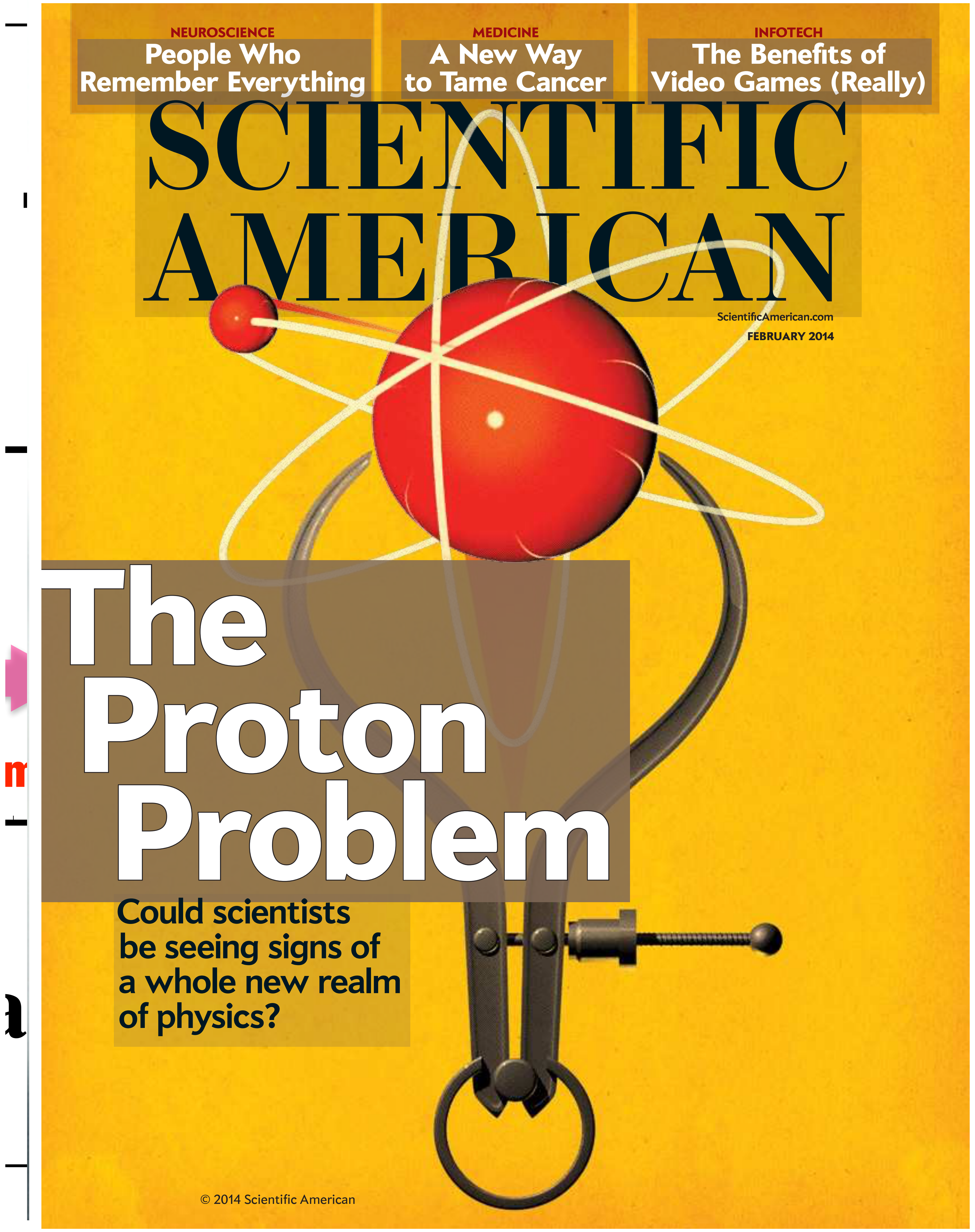

C. Carlson, Prog. Part. Nucl. Phys. 82 (2015) 59.

proton charge radius as of today

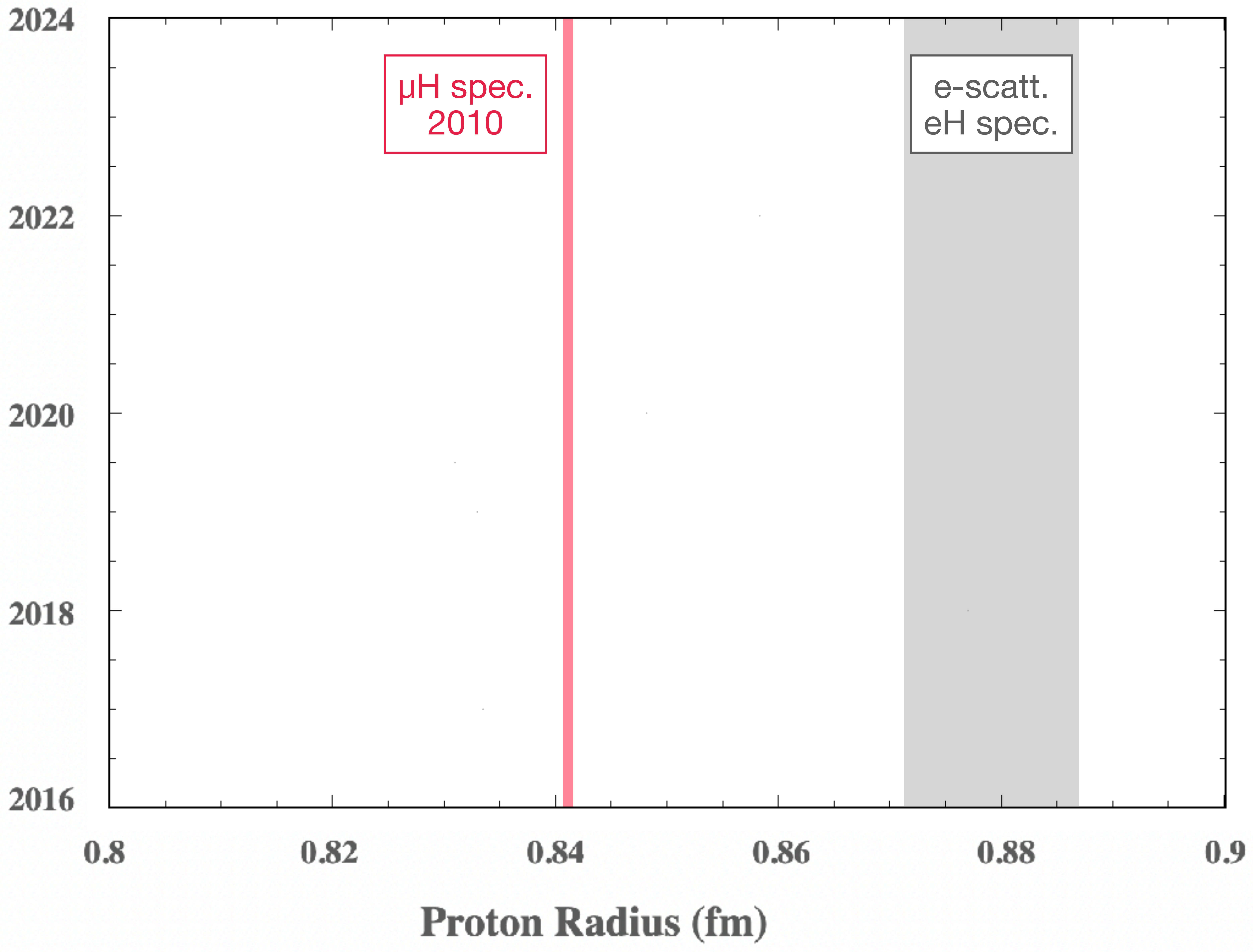

proton charge radius as of today

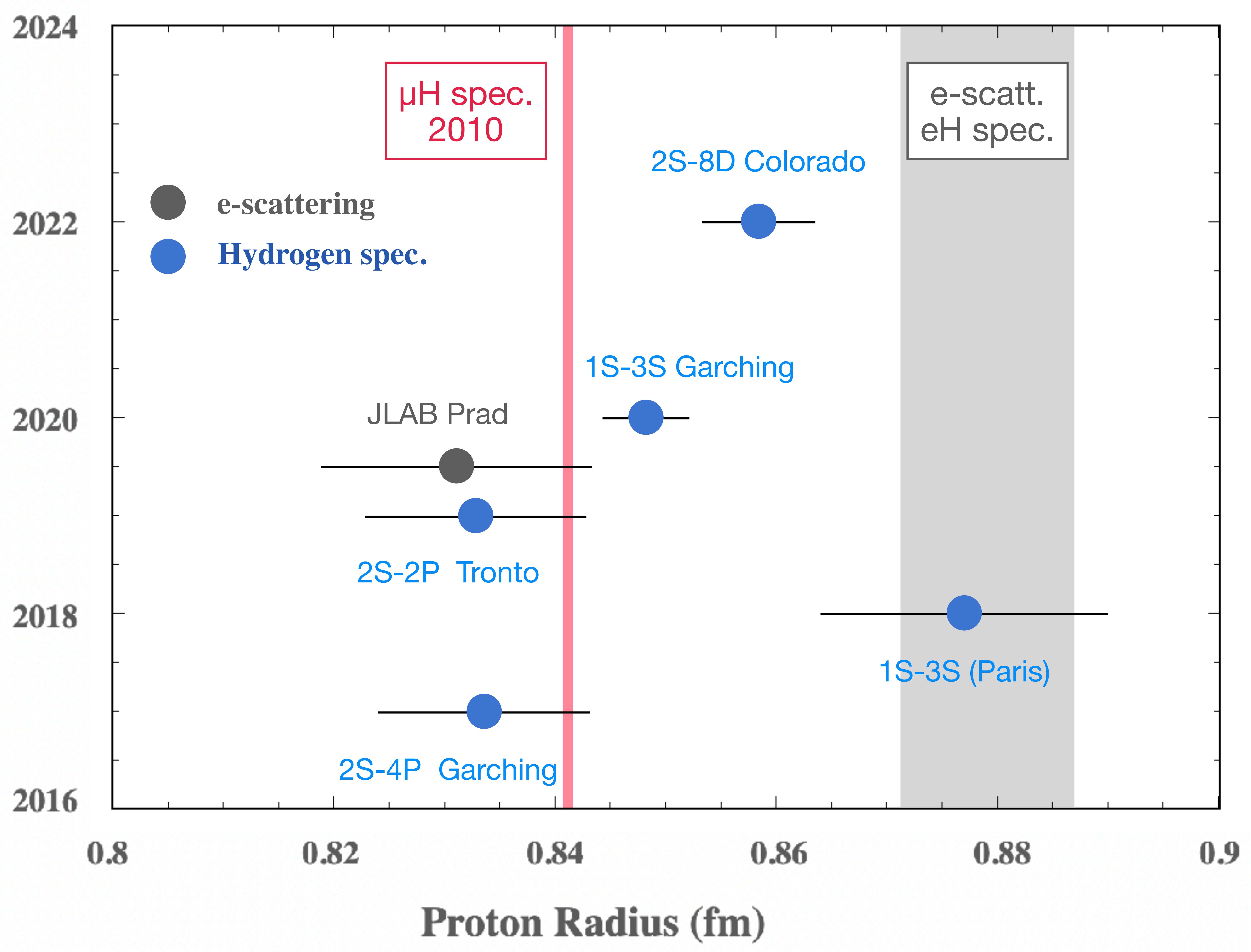

proton charge radius as of today

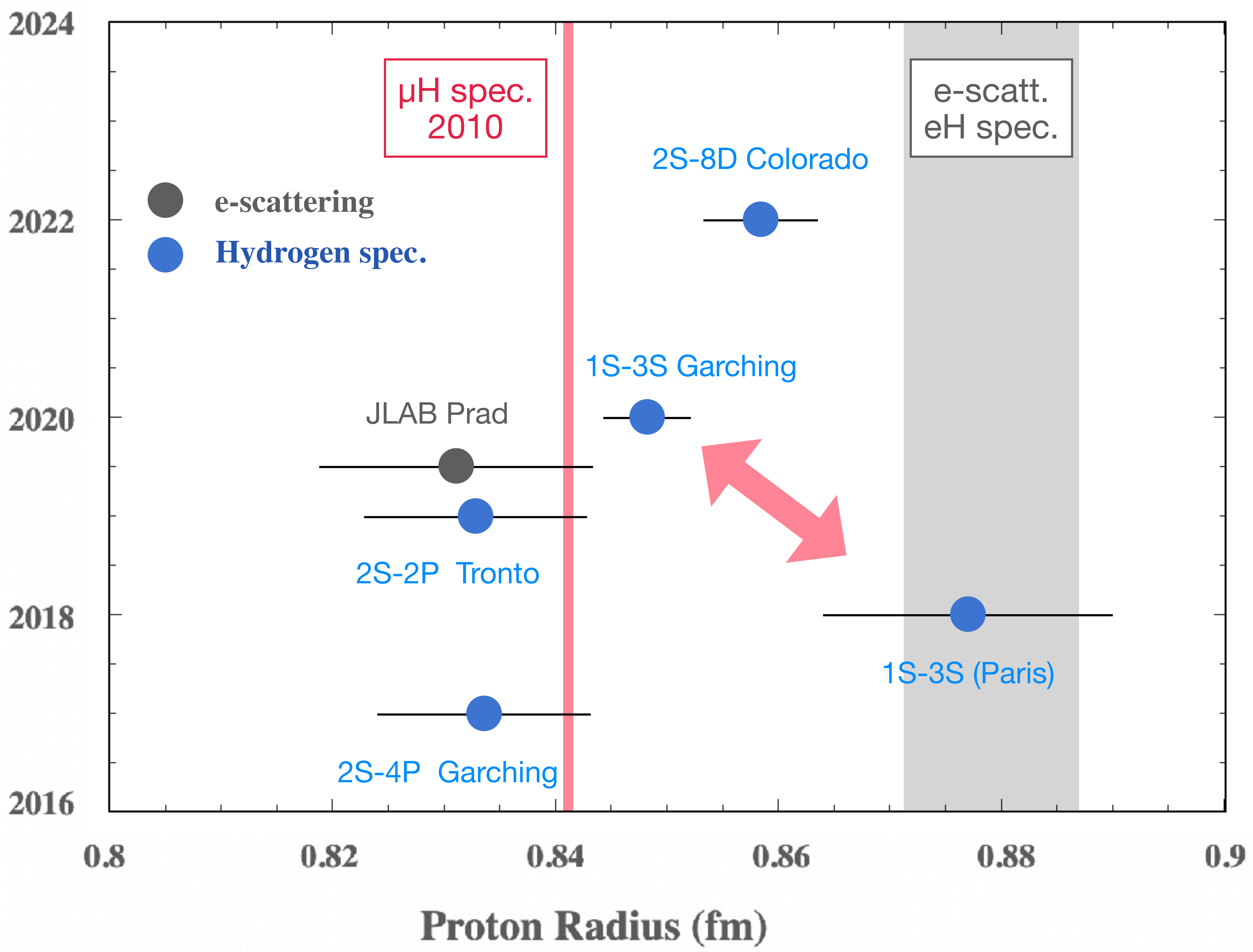

proton charge radius as of today

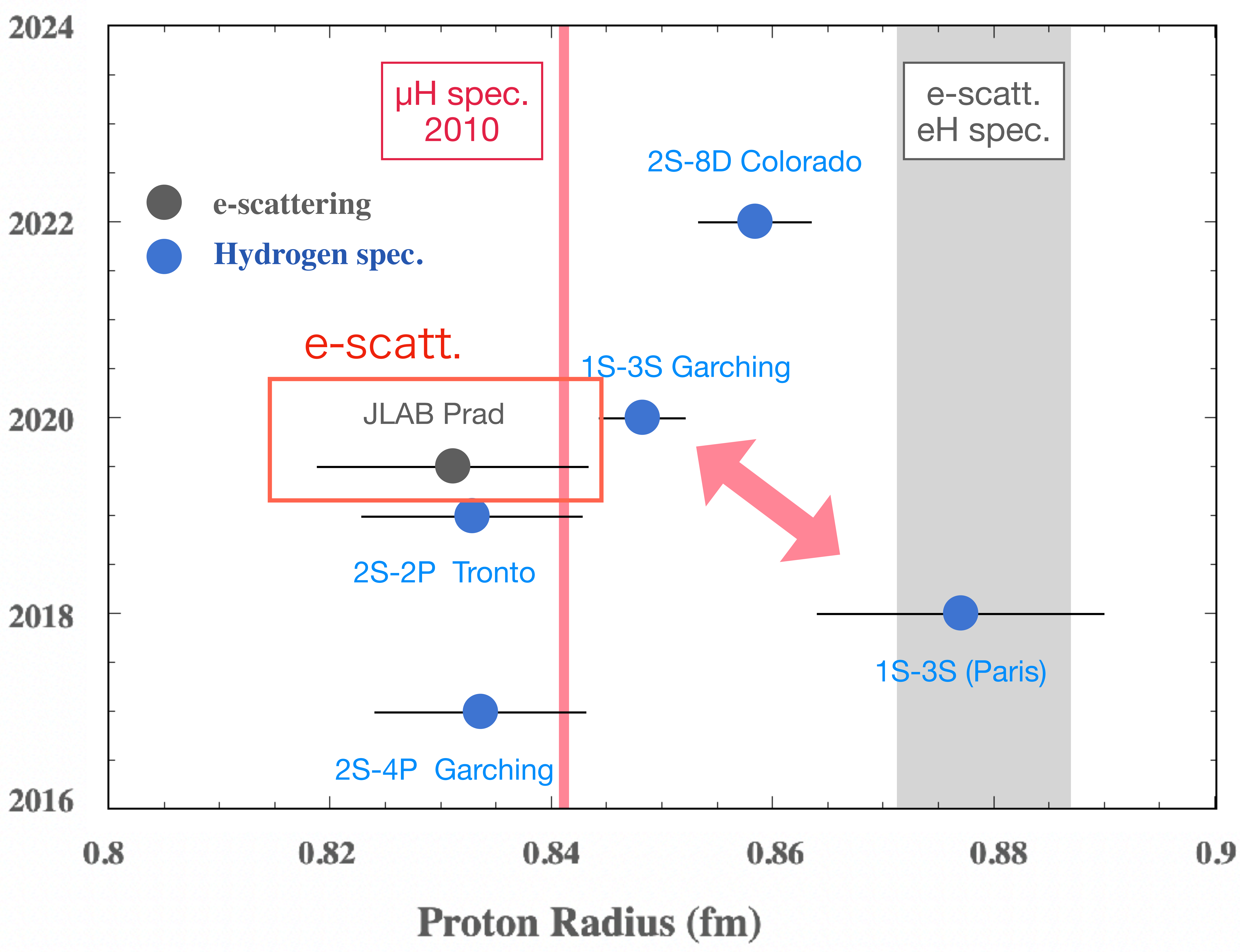

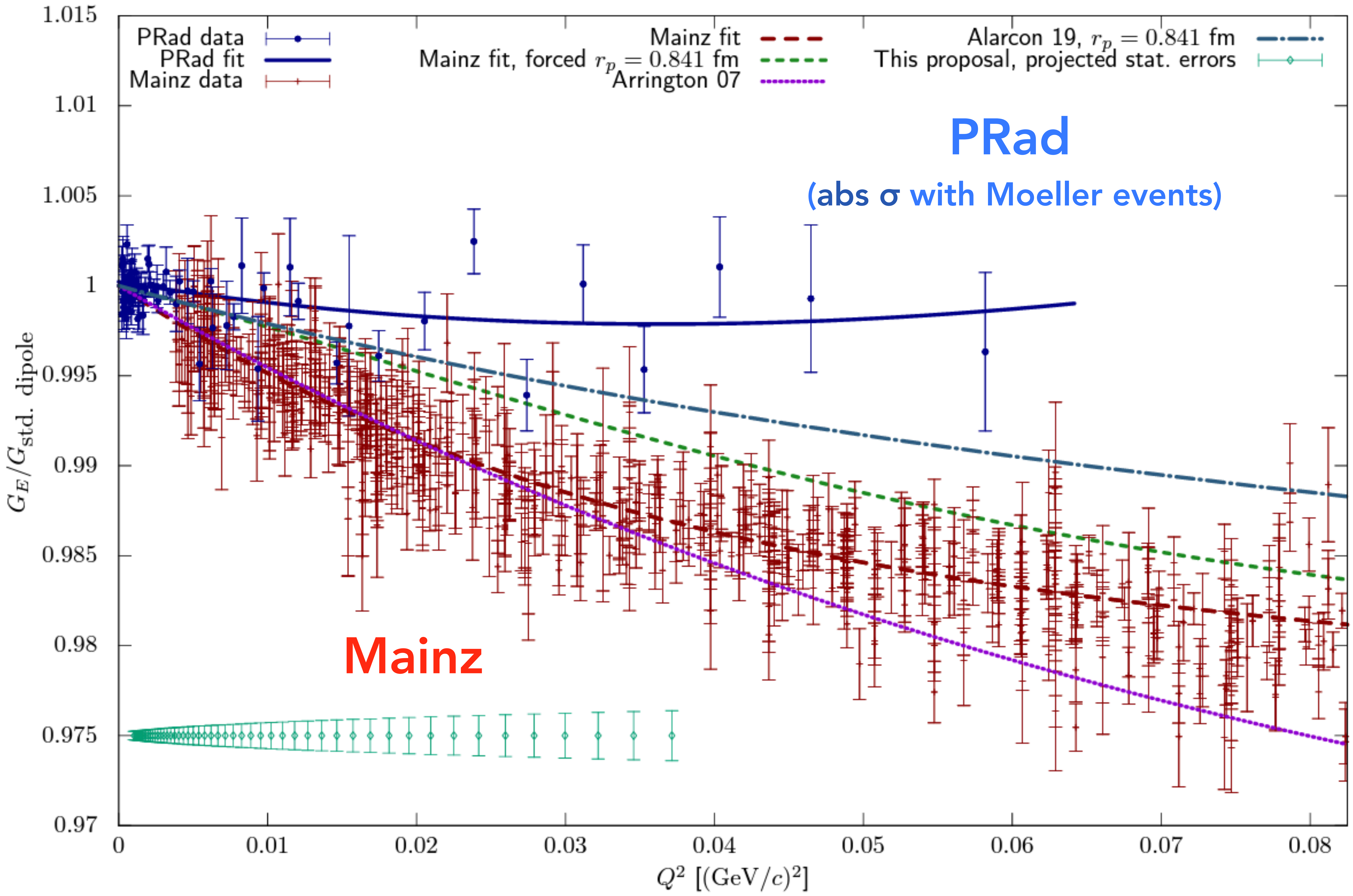
PRad data
PRad fit
Mainz data
Mainz fit
Mainz fit, forced $r_p = 0.841$ fm
Arrington 07
Alarcon 19, $r_p = 0.841$ fm
This proposal, projected stat. errors
PRad
(abs σ with Moeller events)
Mainz
$G_E/G_{\text{std. dipole}}$
Q^2 [(GeV/c)^2]
1.015
1.01
1.005
1
0.995
0.99
0.985
0.98
0.975
0.97
0
0.01
0.02
0.03
0.04
0.05
0.06
0.07
0.08

ULQ2 (Ultra-Low Q^2) at Tohoku, JAPAN since 2016~

"*least model-dependent*" proton charge radius

1) lowest-ever Q^2 by lowest-ever energy e-scattering (10-60 MeV)
2) absolute σ measurements with 10^{-3} accuracy
3) Rosenbluth-separated $G_E(Q^2)$ and $G_M(Q^2)$

possible only at Tohoku accel.

60 MeV electron linac (since 1967)

Ee = 10 - 60 MeV
$\Delta E/E = 0.6 \times 10^{-4}$
beam size ~ 0.6 mm on target
duty factor = 10^{-3}

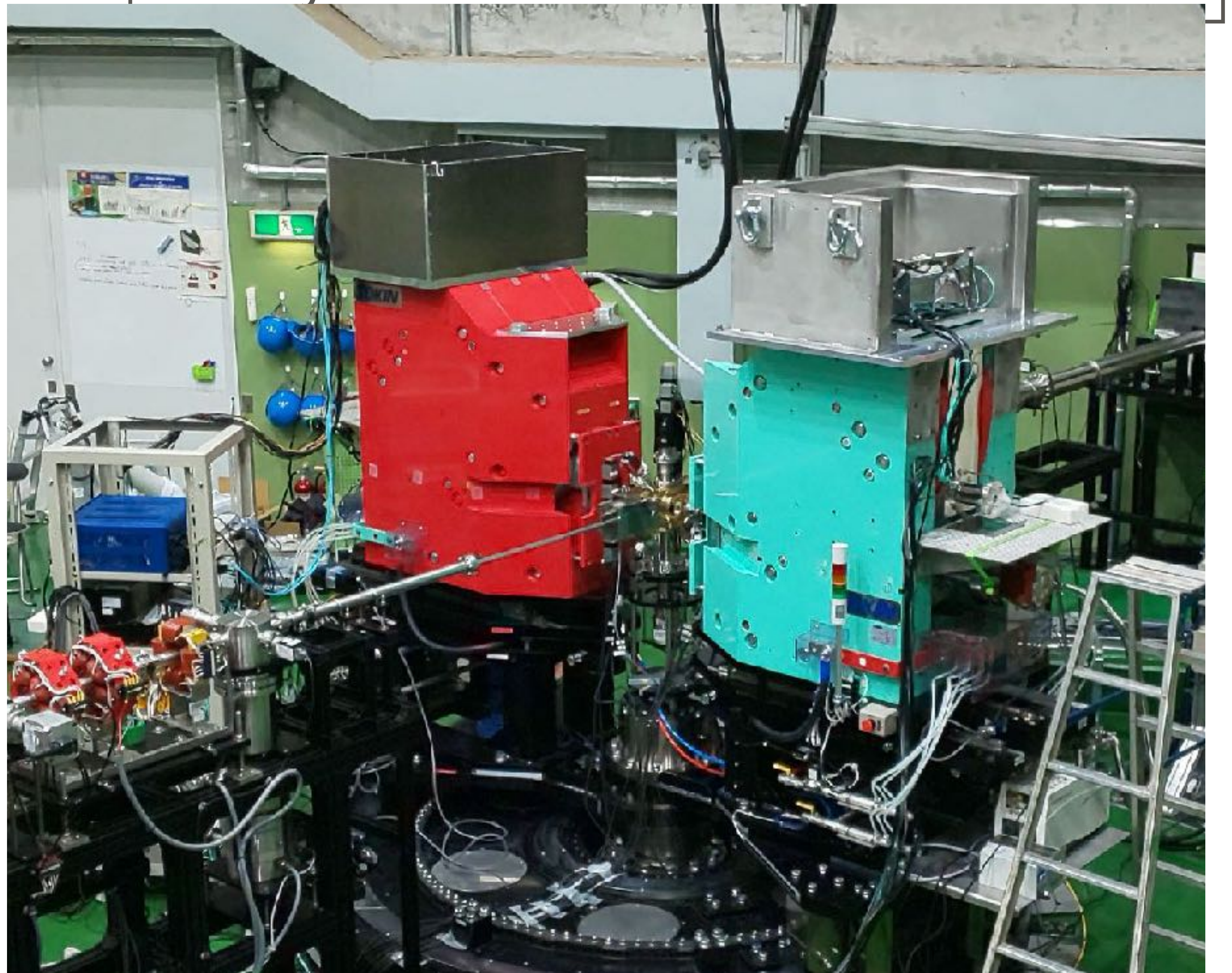

ULQ2 twin-spectrometer setup

Luminosity monitoring
$\Delta p/p = 5.6 \times 10^{-3}$
$\Delta\Omega$ = 6 mSr
θ = 30 - 150 deg.
$Q^2 = 3 \times 10^{-5}$ - 0.013 $(\mathrm{GeV}/c)^2$

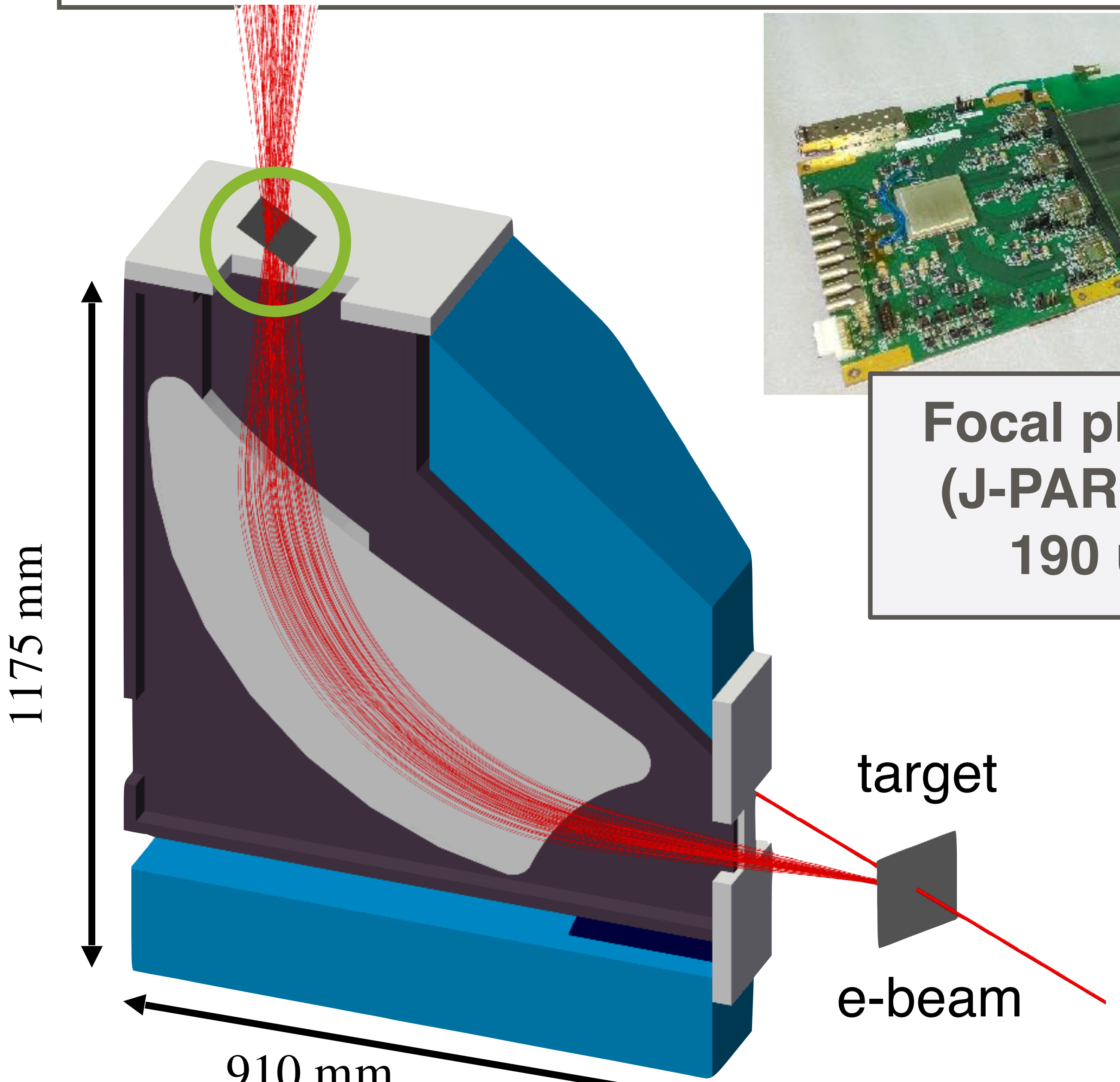

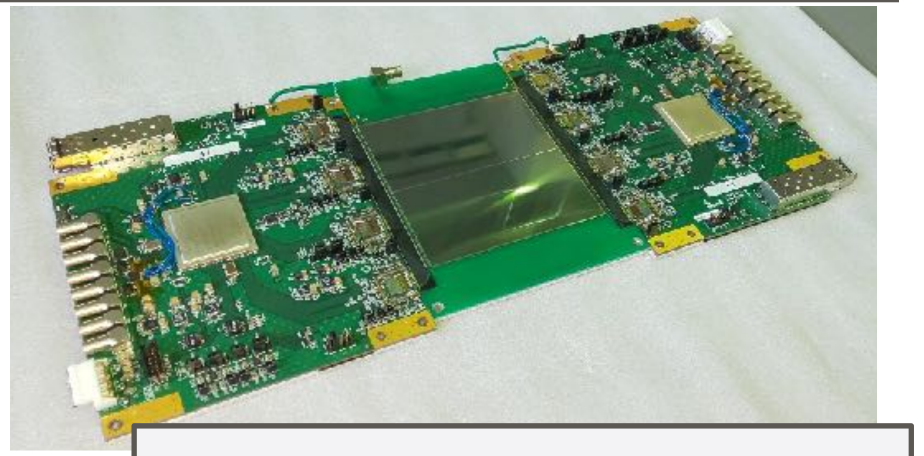

Focal plane detectors
(J-PARC g-2 + ULQ2)
190 um x 4k ch

Yuki Honda

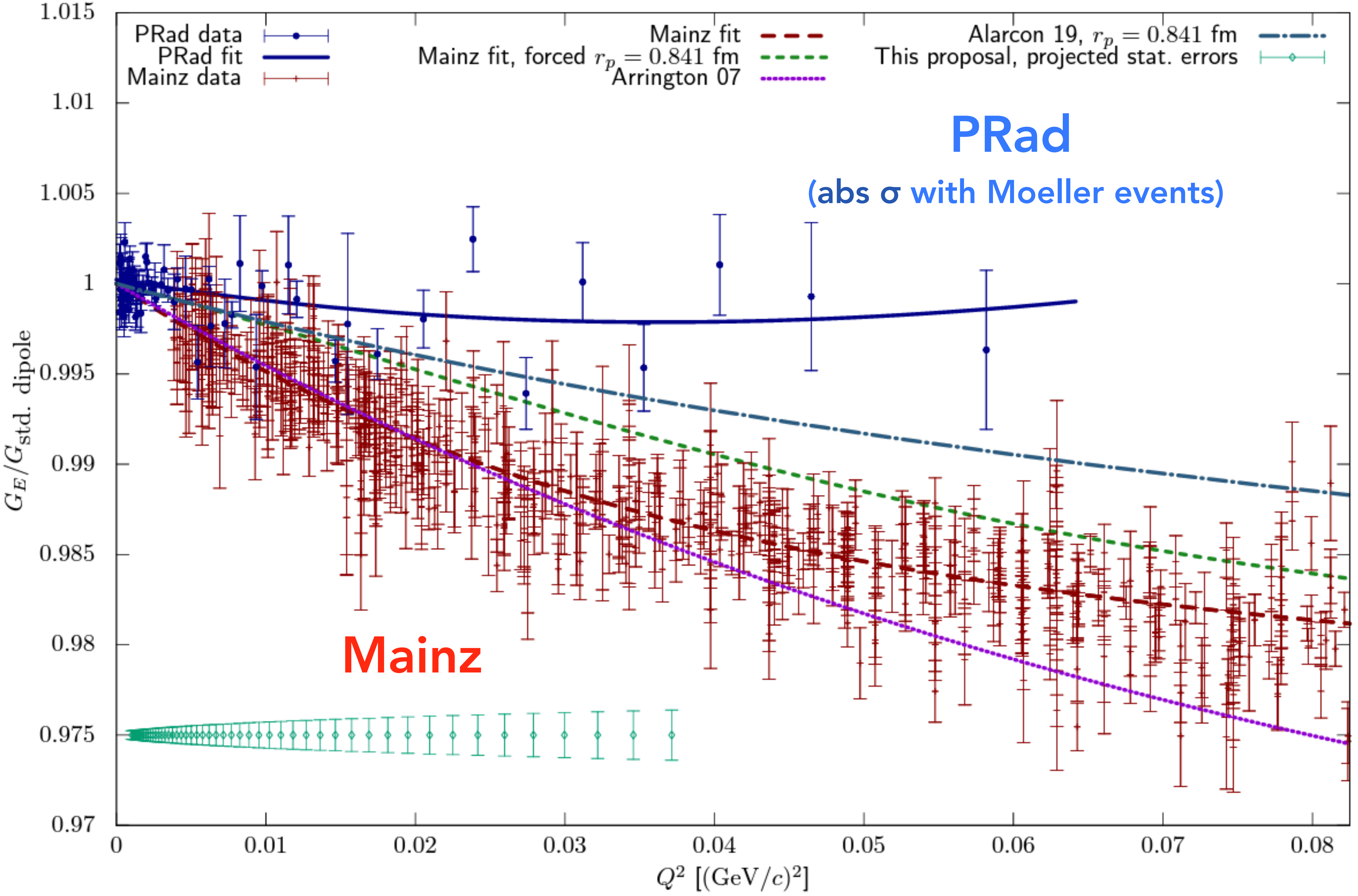

PRad data
PRad fit
Mainz data
Mainz fit
Mainz fit, forced $r_p = 0.841$ fm
Arrington 07
Alarcon 19, $r_p = 0.841$ fm
This proposal, projected stat. errors
PRad
(abs σ with Moeller events)
Mainz
$G_E/G_{\text{std. dipole}}$
Q^2 [(GeV/c)^2]
1.015
1.01
1.005
1
0.995
0.99
0.985
0.98
0.975
0.97
0
0.01
0.02
0.03
0.04
0.05
0.06
0.07
0.08

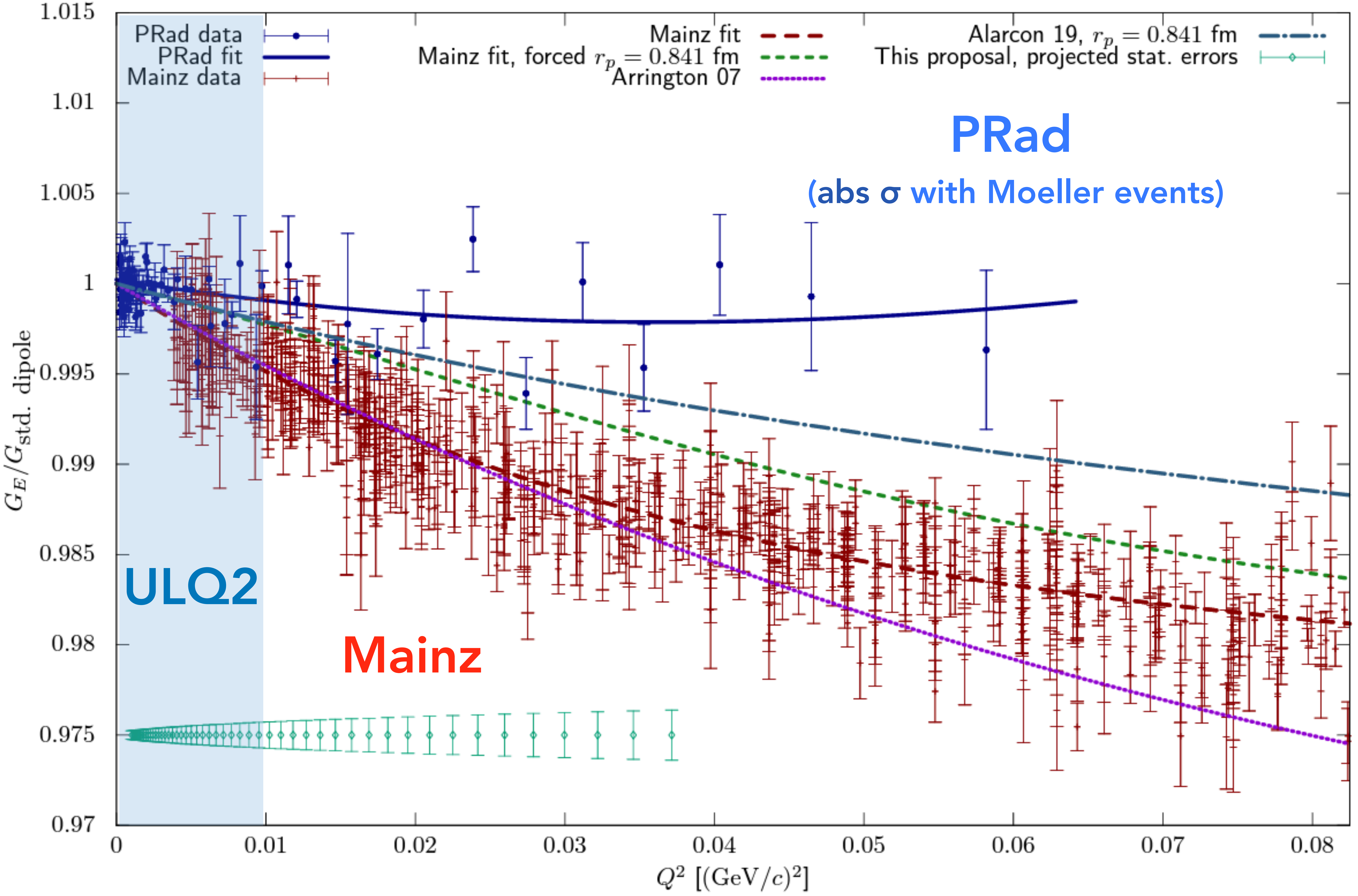
PRad data
PRad fit
Mainz data
Mainz fit
Mainz fit, forced $r_p = 0.841$ fm
Arrington 07
Alarcon 19, $r_p = 0.841$ fm
This proposal, projected stat. errors
PRad
(abs σ with Moeller events)
ULQ2
Mainz
$G_E/G_{\text{std. dipole}}$
Q^2 [(GeV/c)^2]
1.015
1.01
1.005
1
0.995
0.99
0.985
0.98
0.975
0.97
0
0.01
0.02
0.03
0.04
0.05
0.06
0.07
0.08

ULQ2 measurements for e+p and e+d

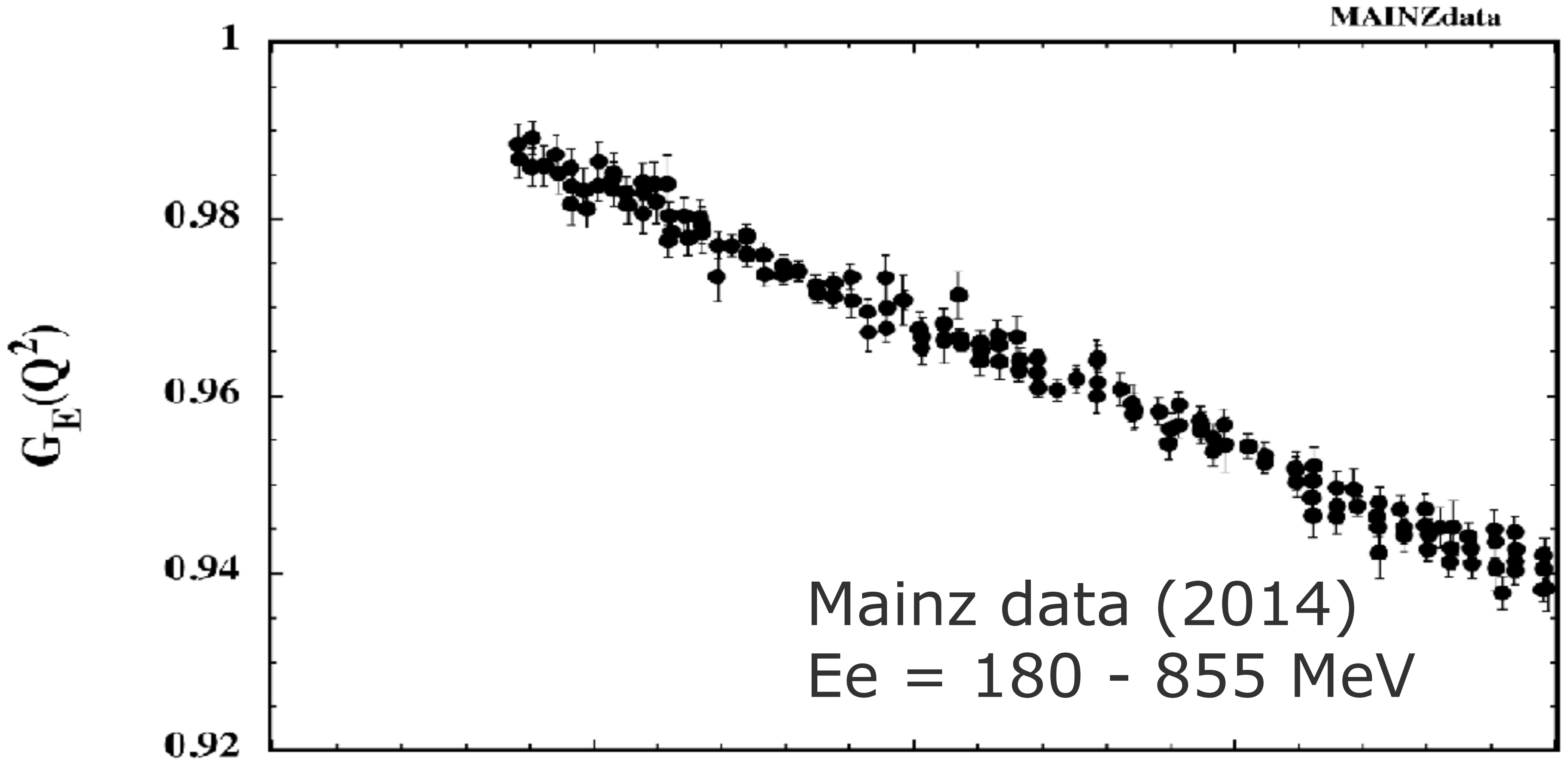

ULQ2 measurements for e+p and e+d

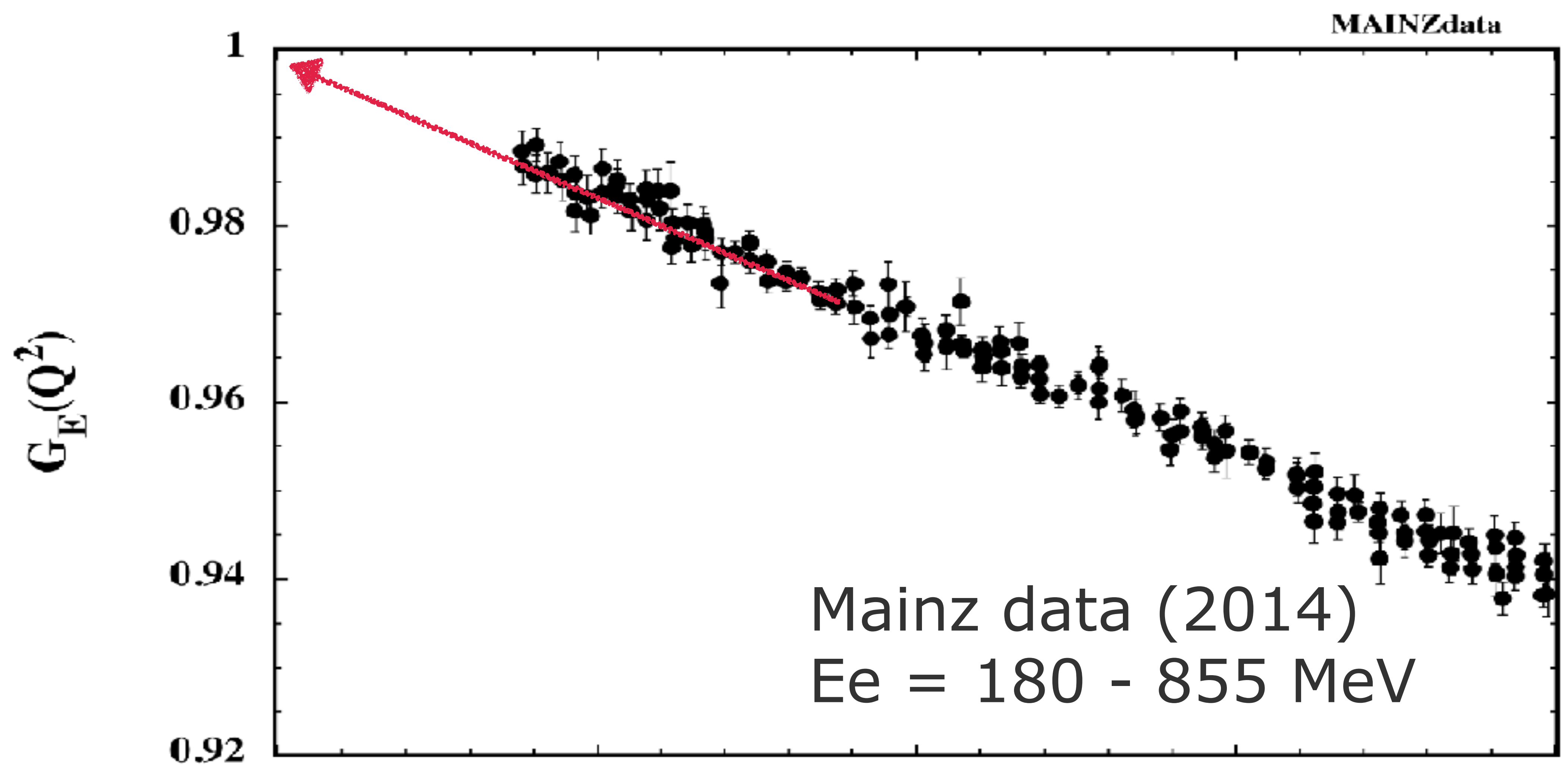

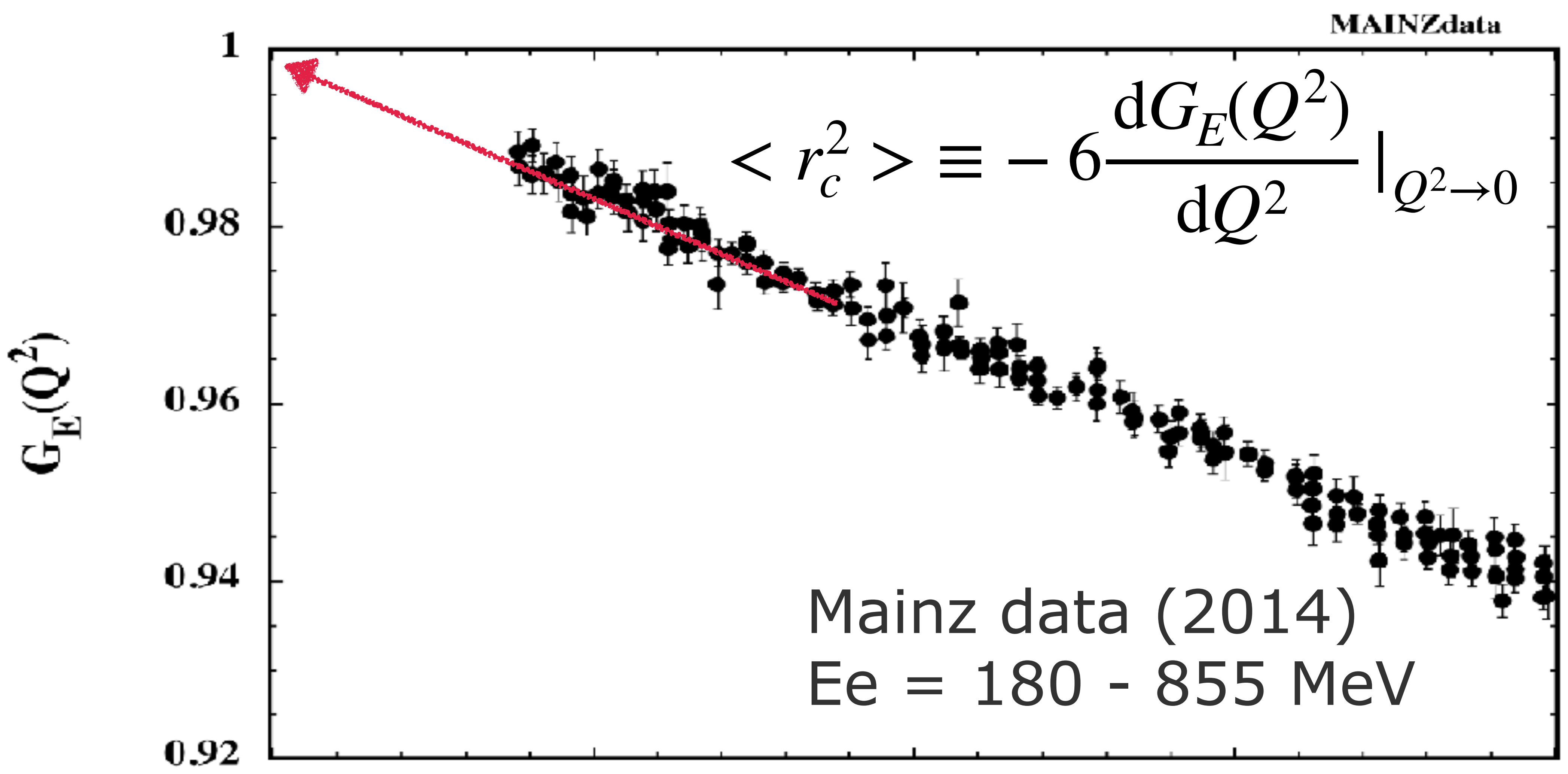
MAINZdata
$G_E(Q^2)$
1
0.98
0.96
0.94
0.92
$< r_c^2 > \equiv -6 \frac{dG_E(Q^2)}{dQ^2} |_{Q^2 \to 0}$
Mainz data (2014)
Ee = 180 - 855 MeV

ULQ2 measurements for e+p and e+d

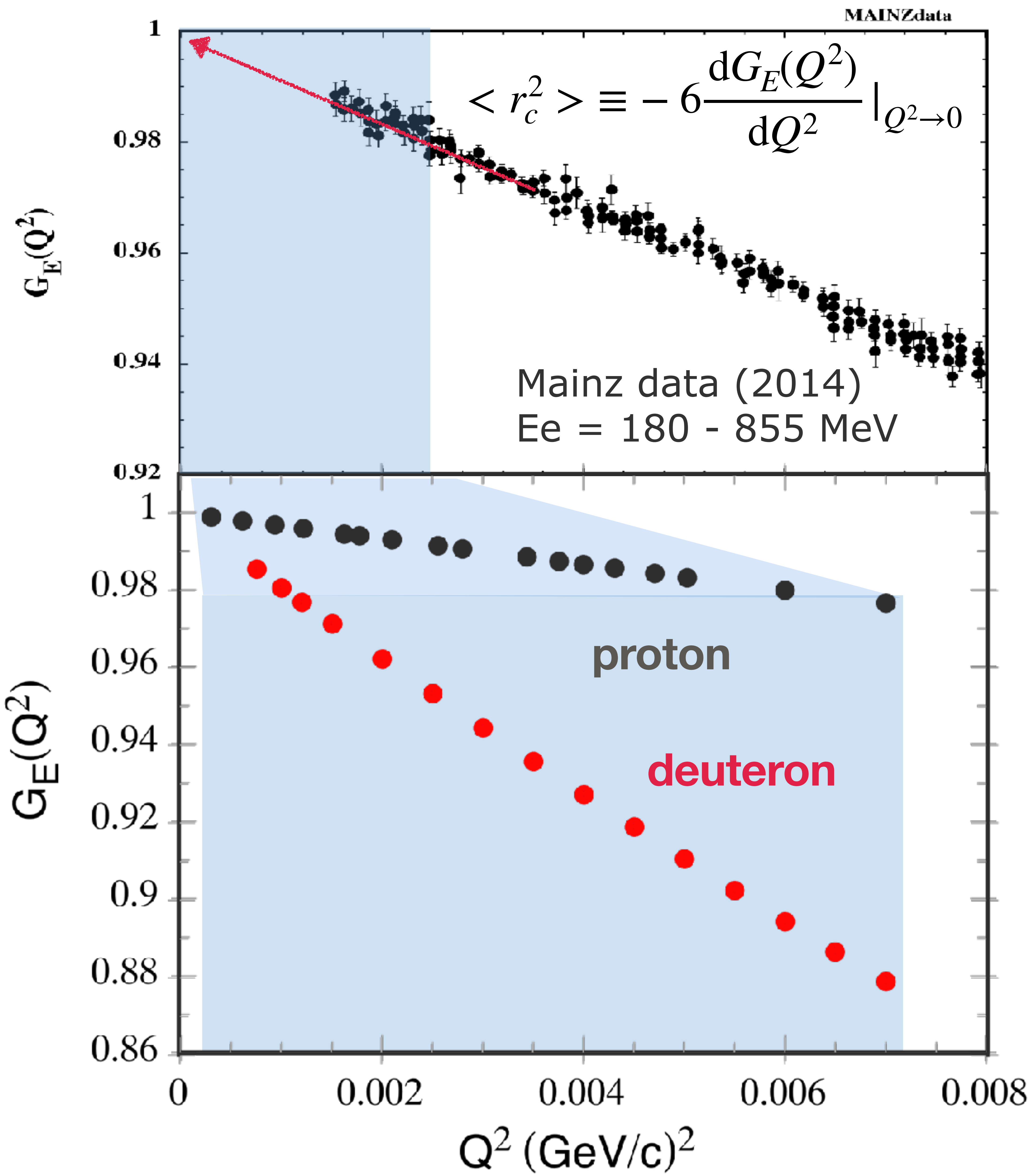

ULQ2 measurements for e+p and e+d

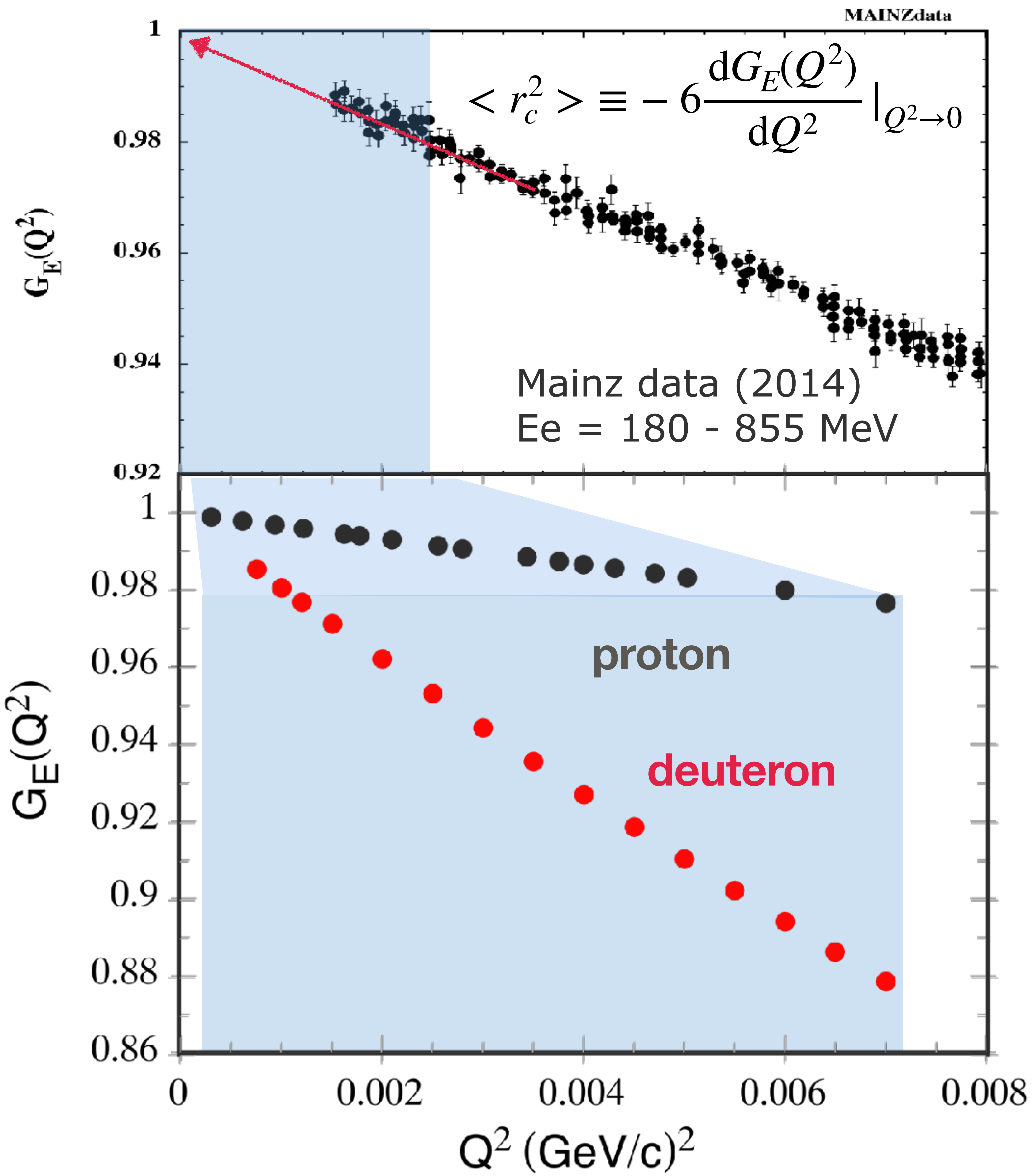

1) **proton** (Clement Legris)
   charge radius
   magnetic radius (next step)

2) **deuteron** (Taiga Goke)
   deuteron charge radius
   => neutron charge radius

ULQ2 measurements for e+p and e+d

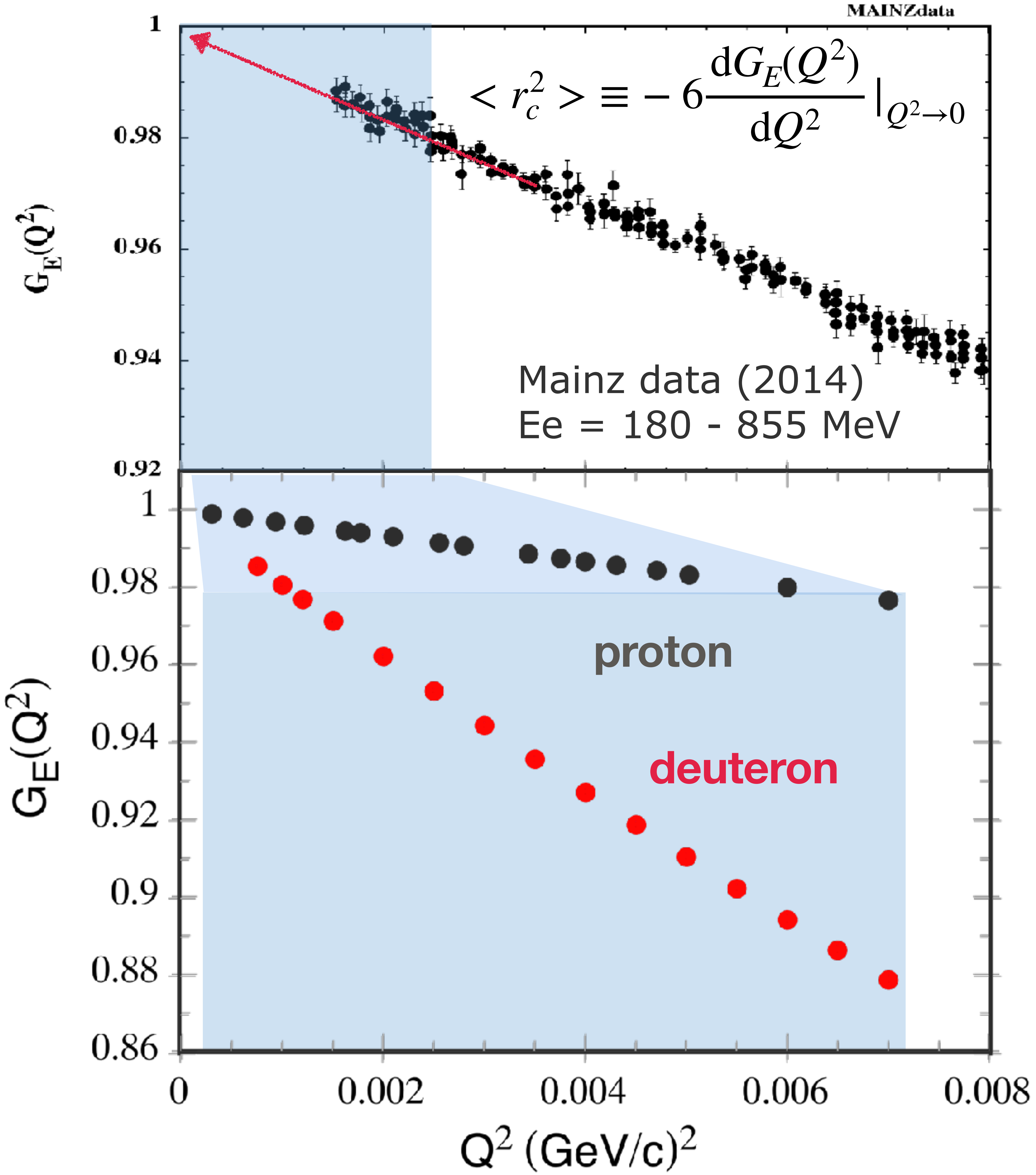

1) proton (Clement Legris)

charge radius

magnetic radius (next step)

2) deuteron (Taiga Goke)

deuteron charge radius

=> neutron charge radius

$$< r_d^2 > = < r_{str}^2 > + < r_p^2 > + < r_n^2 > + \mathrm{RC}$$

ULQ2 theory

$$< r_d^4 > = < r_{str)}^4 > + \frac{10}{3} < r_{pstr}^2 > (< r_p^2 > + < r_n^2 >) + O(4) + \mathrm{RC}$$

ULQ2 theory theory

ULQ2 measurements for e+p and e+d

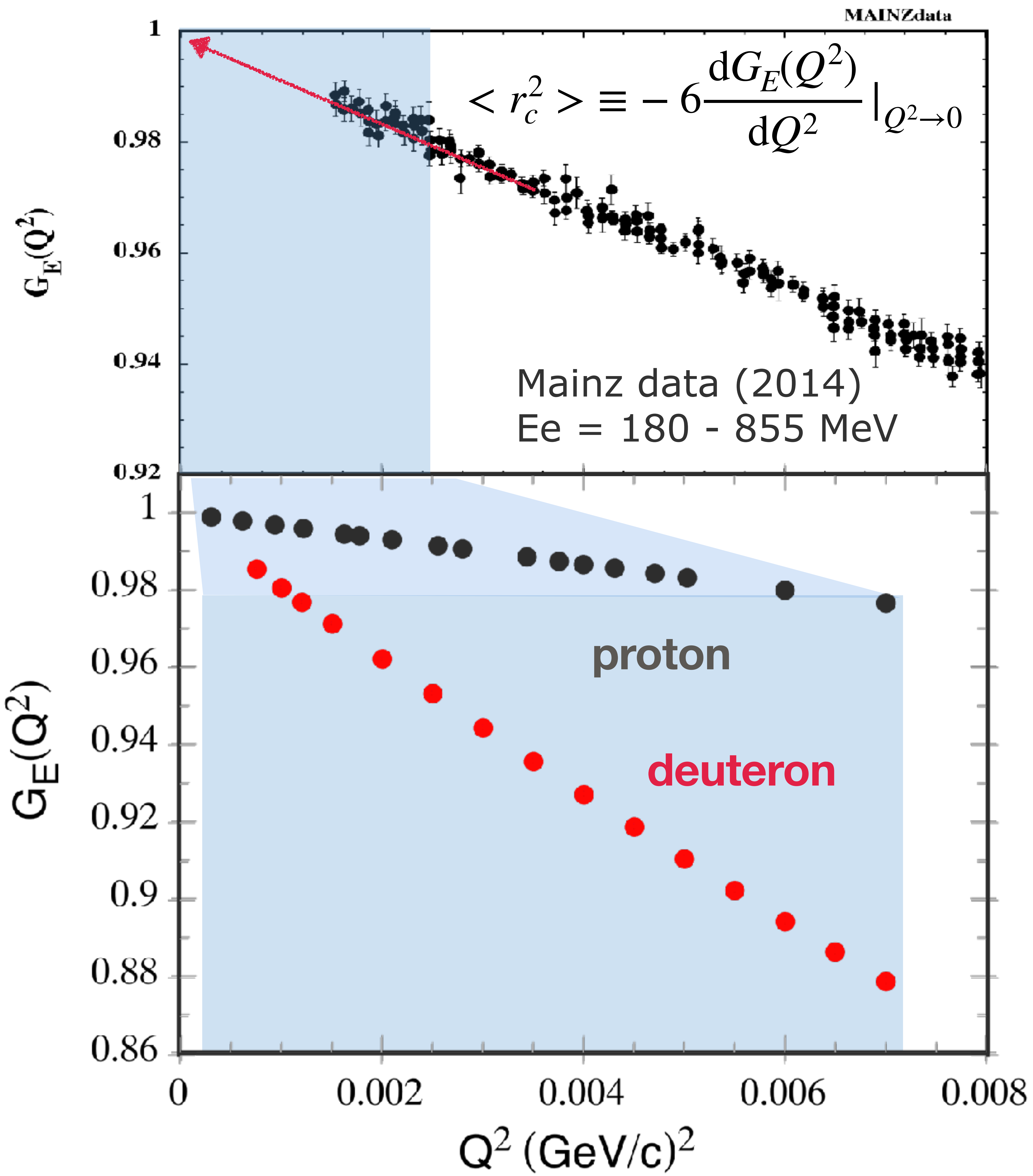

1) **proton** (Clement Legris)
 charge radius
 magnetic radius (next step)

2) **deuteron** (Taiga Goke)
 deuteron charge radius
 => neutron charge radius

$$< r_d^2 > = < r_{str}^2 > + < r_p^2 > + < r_n^2 > + \mathrm{RC}$$

ULQ2 theory

$$< r_d^4 > = < r_{str)}^4 > + \frac{10}{3} < r_{pstr}^2 > (< r_p^2 > + < r_n^2 >) + O(4) + \mathrm{RC}$$

ULQ2 theory theory

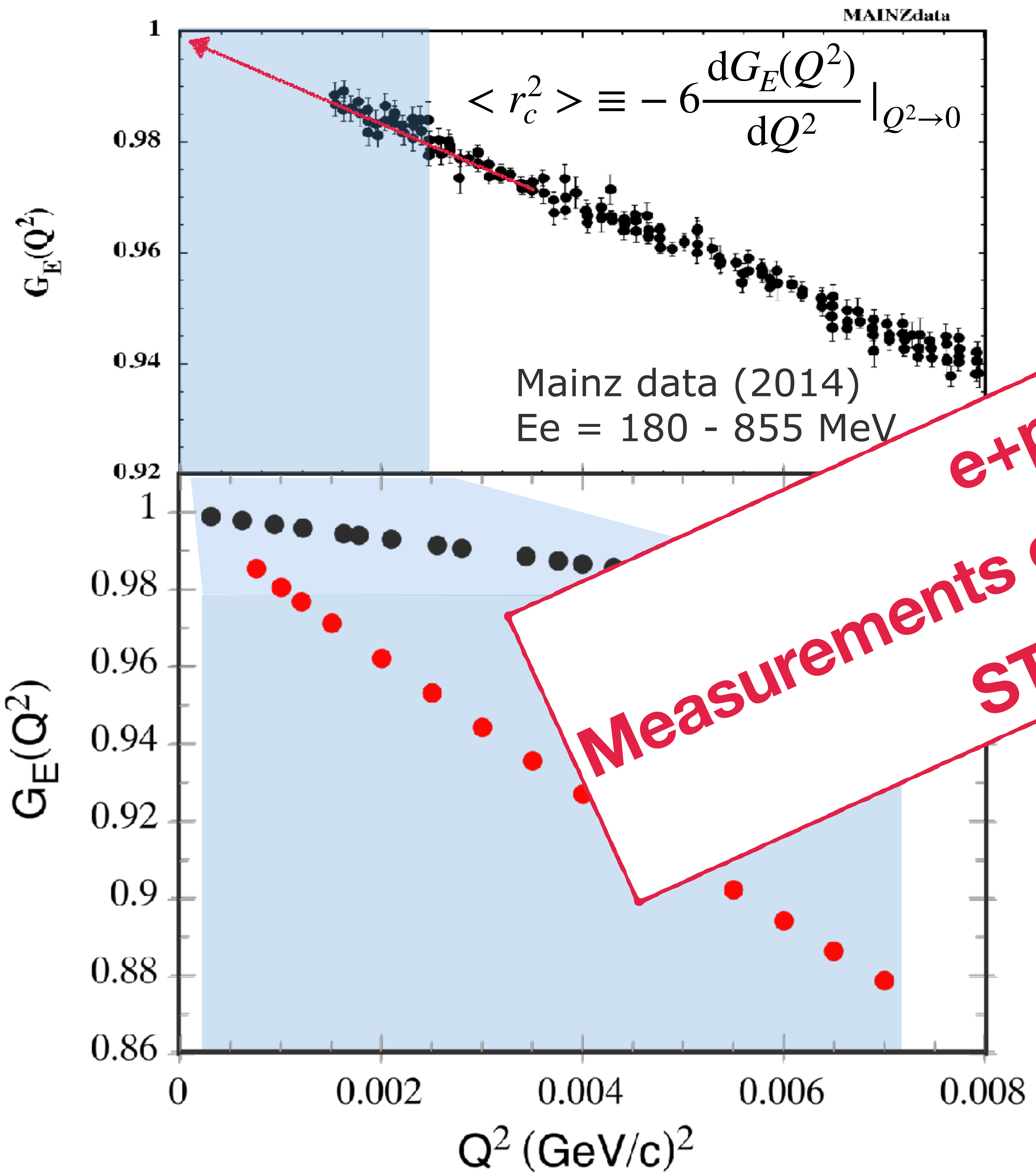

1) **proton** (Clement Legris)

charge rad

mag (next step)

Goke)

n charge radius

> neutron charge radius

e+p (e+d)

Measurements completed (Oct. 2024)

STAY TUNED!

$$< r_d^2 > = < r_{str}^2 > + < r_p^2 > + < r_n^2 > + \mathrm{RC}$$

ULQ2 theory

$$< r_d^4 > = < r_{str)}^4 > + \frac{10}{3} < r_{pstr}^2 > (< r_p^2 > + < r_n^2 >) + O(4) + \mathrm{RC}$$

ULQ2 theory theory

Neutron Charge Radius

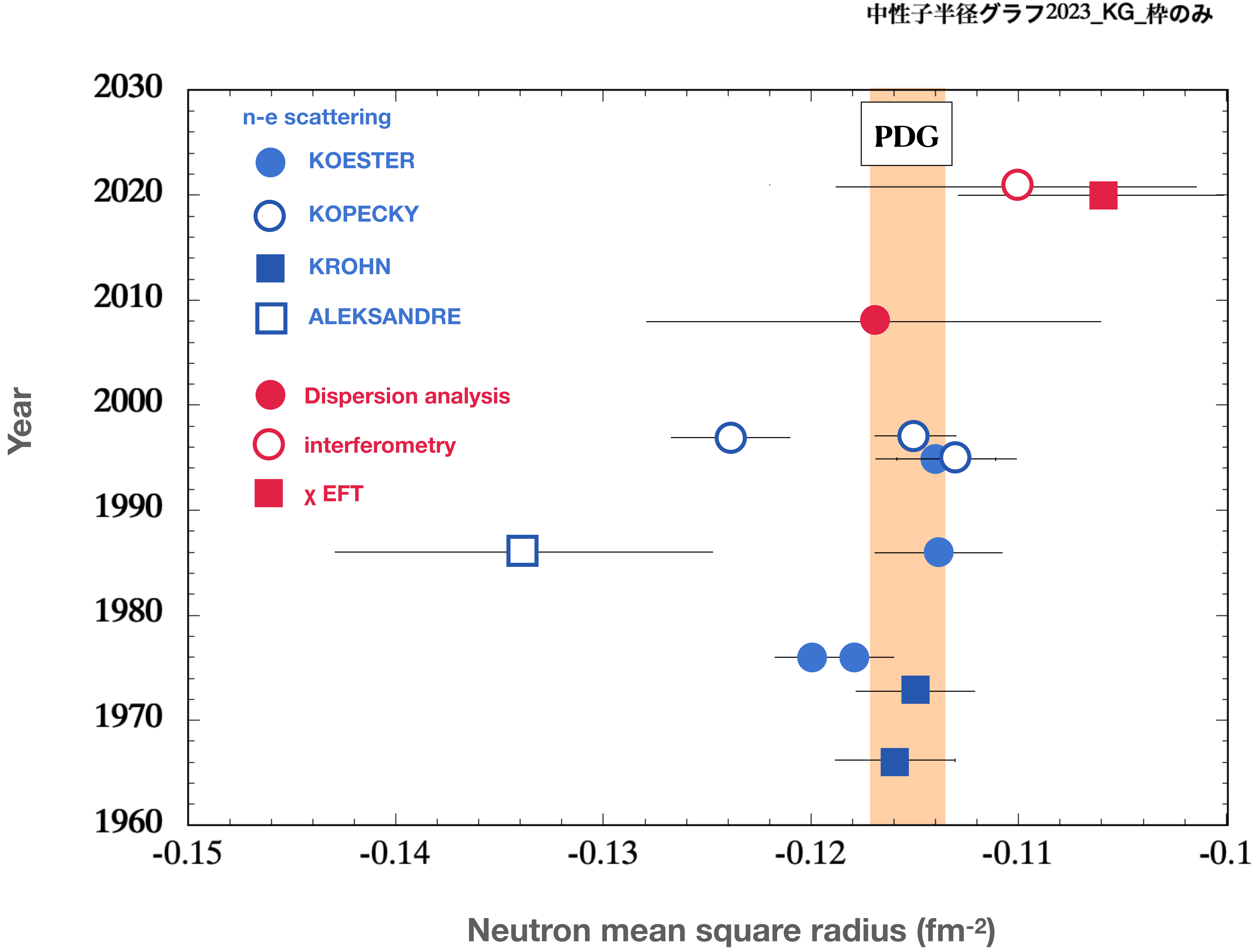

Neutron Charge Radius

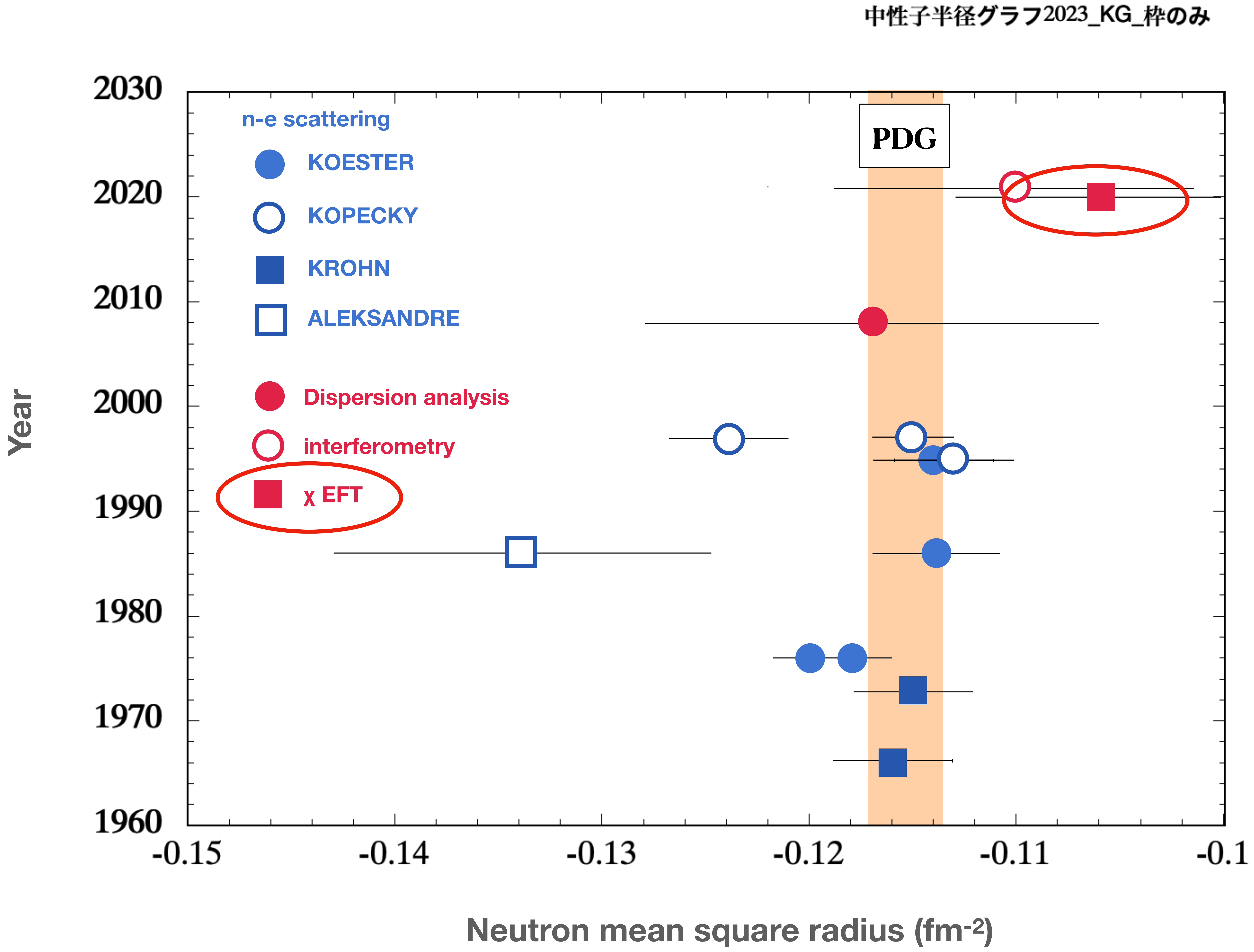

A.A. Filin et al. (Bochum G.)
Phys. Rev. Lett. 124(2020) 082501

$$< r_d^2 > = < r_{str}^2 > + < r_p^2 > + < r_n^2 > + \mathrm{RC}$$

μD exp. theory

conclusions

Low-energy e-scattering activities in Japan

- SCRIT : started operation for online-produced radioactive isotopes

  the world's first and currently only-one facility
  ISOL upgrade to 2kW is underway for ^{132}Sn(e,e')
  feasibility studies for ^{46}Ar suggested to be a proton-bubble nucleus

- ULQ2 : 1) e+p, e+D scattering

  data collection completed. data analysis underway

ongoing activities and future prospects

SCRIT

- charge form factors of exotic nuclei
- neutron-distribution radius by electron scattering

ULQ2

- ^{208}Pb n-skin thickness by low-energy electron scattering